UNIVERSITY OF CALIFORNIA

Santa Barbara

Fate, Transport & Implications of Engineered Nanomaterials in the Terrestrial Environment

A dissertation submitted in partial satisfaction of the

requirements for the degree Doctor of Philosophy

in Environmental Science and Management

by

Jon R. Conway

Committee in charge:

Professor Arturo A. Keller, Chair

Professor Patricia A. Holden

Professor Susan J. Mazer

December 2015

The dissertation of Jon R. Conway is approved.

_____

Patricia A. Holden

_____

Susan J. Mazer

_____

Arturo A. Keller, Committee Chair

August 2015

ACKNOWLEDGEMENTS

First, I would like to thank my advisor Dr. Arturo Keller for giving me the opportunity to do this research and for all of his support throughout. The patient guidance and advice I received from him as both an undergraduate researcher and a PhD student have helped me to become a better researcher, writer, and person.

I would also like to thank the other members of my thesis committee, Dr. Patricia Holden and Dr. Susan Mazer, for their invaluable comments, probing questions, and encouragement. I am especially indebted to Dr. Mazer for her generosity in sharing her lab space, equipment, and expertise, which made much of this research possible.

I am thankful to my peers Dr. Shannon Hannah, Dr. Kristen Clark, Dr. Dongxu Xhou, Dr. Adeyemi Adeleye, Yuxiong Huang, Kendra Garner, and Ty Brandt for their advice, perspectives, help, and friendship throughout this process. I am also very grateful to all of my assistants who made this work possible: Christianna Sim, Robert Burt, Kelly Carpenter, Avery Hunker, Ashley Noriega, Lily Burns, Amy Stuyvesant, and especially Arielle and Nicole Beaulieu.

Finally, I would like to express my deepest thanks to my family for their love and support, and to my fiancée, Gabriela Bernal. It is thanks to you that I started this PhD and that I finished it. This manuscript is dedicated to you.

VITA OF JON R. CONWAY
December 2015

EDUCATION

Bachelor of Science in Ecology & Evolution, University of California, Santa Barbara, June 2011

PROFESSIONAL EMPLOYMENT

2014-2015: Bren Research Blog Founding Editor, Bren School of Environmental Science & Management, University of California, Santa Barbara

2012-2013: Teaching Assistant, Bren School of Environmental Science & Management, University of California, Santa Barbara

2009-2011: Research Assistant, Bren School of Environmental Science & Management, University of California, Santa Barbara

PUBLICATIONS

Conway, J. R.; Keller, A. A., Gravity-Driven Transport of Three Engineered Nanomaterials in Unsaturated Soils and Their Effects on Soil pH and Nutrient Release. Environ. Sci. Technol. (In Review).

Conway, J. R.; Beaulieu, A. L.; Beaulieu, N. L.; Mazer, S. J.; Keller, A. A., Environmental Stresses Increase Photosynthetic Disruption by Metal Oxide Nanomaterials in a Soil-Grown Plant. ACS Nano. (In Review).

Adeleye, A. S.; **Conway, J. R.**; Garner, K.; Huang, Y.; Su, Y.; Keller, A. A., Engineered Nanomaterials for Water Treatment and Remediation: Costs, Benefits, and Applicability. Environ. Chem. Eng. (In Review).

Conway, J. R.; Adeleye, A. S.; Gardea-Torresdey, J.; Keller, A. A., Aggregation, Dissolution, and Transformation of Copper Nanoparticles in Natural Waters. Environ. Sci. Technol. 2015, 49, (5), 2749-2756.

Adeleye, A. S.; **Conway, J. R**.; Perez, T.; Rutten, P.; Keller, A. A., Influence of Extracellular Polymeric Substances on the Long-Term Fate, Dissolution, and Speciation of Copper-Based Nanoparticles. Environ. Sci. Technol. 2014, 48, (21), 12561-12568.

Conway, J. R.; Hanna, S. K.; Lenihan, H. S.; Keller, A. A., Effects and Implications of Trophic Transfer and Accumulation of CeO2 Nanoparticles in a Marine Mussel. Environ. Sci. Technol. 2014, 48, (3), 1517-1524.

AWARDS

Dean’s Fellowship for Excellence in Research, Bren School of Environmental Science & Management, University of California, Santa Barbara, 2014

ABSTRACT

Fate, Transport & Implications of Engineered Nanomaterials in the Terrestrial Environment

by

Jon R. Conway

The majority of the current production, use, and disposal of engineered nanomaterials (ENMs) occur in terrestrial environments, and consequently terrestrial ecosystems are and will increasingly be some of the largest receptors of ENMs at all stages of their life cycles. In particular, soil is predicted to be one of the major receptors of ENMs due to ENM-contaminated biosolid fertilizer and nanopesticide application to agricultural fields, runoff from landfills or ENM-bearing paints, or atmospheric deposition. Both agricultural and natural systems are at risk to ENM contamination via these release scenarios, which makes it necessary to understand the interactions between ENMs, soils, and soil organisms such as plants in order to predict their impacts in real-world scenarios.

Gravity-driven vertical transport of TiO_2, CeO_2, and $Cu(OH)_2$ engineered nanomaterials (ENMs) and their effects on soil pH and nutrient release were measured in three unsaturated soils. ENM transport was found to be highly limited in natural soils collected from farmland and grasslands, with the majority of particles being retained in the upper 0-3 cm of the soil profile, while greater transport depth was seen in a commercial

potting soil. Physical straining appeared to be the primary mechanism of retention in natural soils as ENMs immediately formed micron-scale aggregates, which was exacerbated by coating particles with Suwannee River natural organic matter (NOM).

Changes in soil pH were observed in natural soils contaminated with ENMs that were largely independent of ENM type and concentration. These changes may have been due to enhanced release of naturally present pH-altering ions (Mg^{2+}, H^{+}) in the soil, likely via substitution processes. This suggests ENMs will likely be highly retained near source zones in soil and may impact local communities sensitive to changes in pH or nutrient availability.

Few studies have investigated the influence of environmental conditions on ENM uptake and toxicity, particularly throughout the entire plant life cycle. Here, soil-grown plants (*Clarkia unguiculata*, *Raphanus sativus*, and *Triticum aestivum*) were exposed until maturity to TiO_2, CeO_2, or $Cu(OH)_2$ ENMs under different illumination intensities, in different soils, and with different nutrient levels. Fluorescence and gas exchange measurements were recorded throughout growth and tissue samples from mature plants were analyzed for metal content. ENM uptake was observed in all plant species, but was seen to vary significantly with ENM type, light intensity, nutrient levels, and soil type. Light intensity in particular was found to be important in controlling uptake, likely as a result of plants increasing or decreasing transpiration in response to light.

Significant impacts on plant transpiration, photosynthetic rate, CO_2 assimilation efficiency, water use efficiency, and other parameters related to physiological fitness were seen. The impacts were highly dependent on environmental conditions as well as ENM and soil type. Notably, many of these effects were found to be mitigated in soils with limited

ENM mobility due to decreased uptake. These results show that abiotic conditions play an important role in mediating the uptake and physiological impacts of ENMs in terrestrial plants.

TABLE OF CONTENTS

1. Introduction

1.1. Background

Nanotechnology has the potential to enhance or revolutionize many fields of study, including medicine, transportation, energy storage, personal care, construction, environmental remediation, military applications, manufacturing, and scientific research. Reflecting this broad applicability, nanotechnology has become a multi-billion dollar industry in spite of being in its infancy, and is expected to reach a global market value of over half a trillion U.S. dollars by the end of the decade.[1] With this in mind, and with nanomaterials currently used in nearly 2000 consumer products[2] and many industrial applications, concerns have naturally arisen about the health and environmental impacts of the manufacture, use, and disposal of this new and extremely varied class of materials.

A nanomaterial is defined as a material with at least one dimension in the size range of approximately 1 to 100 nm.[3] Here, the term "engineered nanomaterial" (ENM) is used to differentiate intentionally designed and manufactured nanomaterials from those produced incidentally by natural or anthropogenic processes. The extreme size of ENMs, and the high surface area to volume (SA/V) ratio that comes along with it, typically results in unique properties not found in larger scale or dissolved materials of the same composition. For example, quantum dots, nanoscale particles composed of semiconducting materials (CdS, InAs, PbSe, etc.), can utilize quantum band gap phenomena to fluoresce in a narrow range of wavelengths, which are highly dependent on their diameter.[4] Additionally, ENMs can be

extremely reactive due to their high surface area relative to their volume (a spherical particle 1 nm in diameter has a SA/V 1000 times greater than a particle 1 μm in diameter).

These novel properties are simultaneously the source of global interest in ENMs and the main issue of concern in terms of the impacts to human health and environmental safety, as regulations for a bulk or dissolved material may not be appropriate for ENMs of the same composition. Additionally, since ENMs can have radically different behavior depending on their composition, size, shape, doping agents, coatings, and/or the characteristics of the media they are present in, a predictive framework for the fate, transport, and toxicity of ENMs in a variety of environments and organisms is needed to effectively regulate ENMs throughout their life cycles.

The majority of the current production, use, and disposal of engineered nanomaterials (ENMs) occur in terrestrial environments, and consequently terrestrial ecosystems are and will increasingly be some of the largest receptors of ENMs at all stages of their life cycles.[5-8] In particular, soil is predicted to be one of the major receptors of ENMs due to ENM-contaminated biosolid fertilizer and nanopesticide application to agricultural fields, runoff from landfills or ENM-bearing paints, or atmospheric deposition.[5, 9-11] Both agricultural and natural systems are at risk to ENM contamination via these release scenarios, which makes it necessary to understand the interactions between ENMs, soils, and soil organisms such as plants in order to predict their impacts in real-world scenarios.

1.2. Research Objectives and Methods

The goal of the research presented in this thesis was to uncover some of the underlying mechanisms controlling the following processes under environmentally relevant conditions: how ENMs move through unsaturated soils, the effects ENMs have on key soil properties, the uptake and distribution of ENMs in plants, and how ENMs influence plant growth and physiology. These topics were addressed using methods approximating real-world scenarios as closely as possible while maintaining reproducibility and analytical power. The holistic approach utilized here differs fundamentally from that of many studies currently published on these subjects, which use reductionist experimental design to attempt to break down the complex ENM-soil-plant system into simplified components. Reductionist methods can be powerful in providing detailed information about well-understood systems, but when addressing systems as complex and poorly-understood as these designing experiments to closely mimic real-world scenarios can give insight into key controlling mechanisms that can then be targeted for further study. An example of this can be found in Chapter 2, which shows that the main mechanism impeding ENM transport through unsaturated natural soils is physical straining of large ENM aggregates formed via interaction with ions in the soil solution, not through electrostatic attraction or repulsion as was predicted by several studies using well-dispersed ENMs in typical saturated columns of washed quartz sand.[12-14]

As mentioned, Chapter 2 discusses tracking the movement and characteristics of three metal oxide ENMs through three soils, with ENMs being either coated with natural organic matter (NOM) or uncoated. In contrast to studies such as those cited above, which use active pumping to push ENMs through water-saturated media, ENM transport in this study was in

unsaturated soils and was driven solely by gravity. This was done in order to more closely simulate conditions likely to occur in the real world, as some of the major predicted exposure scenarios (discussed above) involve ENMs entering from the top layers of soil, which are typically unsaturated.

Chapter 3 looks at the effects ENM contamination has on several soil properties, which is a subject that is poorly represented in the literature. Metal oxide ENMs like those used in this study have characteristics that make them likely to influence soil properties in some way, such as being similar in composition to naturally-occurring clay minerals that are important in controlling nutrient retention, soil porosity, and organic content.[15, 16] Additionally, they are amphoteric, that is, capable of producing both H^+ and OH^- ions depending on their crystal structure and the composition of the media they are in and thus potentially altering soil pH. Soil pH and nutrient availability are both critically important to plants and other soil organisms and were therefore targeted in this chapter.

Chapters 4 and 5 explore two aspects of the same system: how plants grown to maturity in ENM-contaminated soils uptake and distribute ENMs throughout their tissues, and how their growth and physiological processes are affected by the presence of ENMs. Keeping with the theme of designing experiments to predict ENM behavior in real-world scenarios, aspects of the environmental conditions the plants were grown under, specifically illumination intensity and soil nutrient levels, were varied in order to mimic some of the range of conditions plants growing under real conditions would experience. This was done in a series of three experiments.

First, the model plant *Clarkia unguiculata* was grown to maturity under two illumination intensities in a potting soil with and without receiving additional fertilizer in order to

determine the effects of nutrient and light stress. Second, *C. unguiculata* was again grown to maturity under two illumination intensities, but this time in two natural soils, a grassland soil and an agricultural soil. This was done to see how these plants respond to ENM exposure in soils with different properties beyond nutrient levels. Finally, two crop plants, wheat and radishes, were grown to maturity under two illumination intensities in the grassland and agricultural soils, respectively. This was done in order to see the effects of ENM exposure on plants from different taxonomic groups that are also economically important. By varying one condition (soil or plant type) throughout this set of experiments, information can be passed from one to the next that could provide additional insight into the key factors at play.

1.3. Nanomaterials Studied

Three engineered nanomaterials were used in these experiments: TiO_2, CeO_2, and $Cu(OH)_2$. TiO_2 and CeO_2 ENMs used in this experiment are fully characterized in Keller, et al. (2010)[17] and $Cu(OH)_2$ is characterized in Adeleye, et al. (2014)[18]. A summary of relevant properties can be found in Table 1.1. TiO_2 and CeO_2 ENMs were provided by Evonik Degussa Corp. (U.S.) and Meliorum Technologies (U.S.), respectively. $Cu(OH)_2$ particles were purchased from DuPont as the commercially available agricultural biocide Kocide 3000. TiO_2 particles were semispherical with a primary particle size of 27 ± 4 nm with a crystalline structure of 82% anatase and 18% rutile. Particle size after 30 minutes of sonication in deionized water (DI) was 194 ± 7 nm. CeO_2 particles were primarily rods with dimensions of 67 ± 8 × 8 ± 1 nm with ≤10% as polyhedra of diameter 8 ± 1 nm. Crystal

structure was ceria cubic and particle size in DI after sonication for 30 minutes was 231 ± 16 nm. Kocide 3000 is composed of spherical composites on the order of 50 μm made up of irregular nano- to micro-scale $Cu(OH)_2$ embedded in a carbon-based matrix that rapidly dissolves in water to release polydisperse $Cu(OH)_2$ particles approximately 1500 ± 600 nm in diameter.

Table 1.1. ENM Properties.

Property	TiO_2	CeO_2	$Cu(OH)_2$
Primary particle diameter[a] (nm)	27±4	rods: (67± 8) × (8 ± 1) (≤10% polyhedra: 8 ± 1 nm)	100 - 1000
Hydrodynamic diameter[b] (nm)	194 ± 7	231±16	1532±580
Target metal content (wt. %)[c]	98.3	95.14	26.5±0.9
Other elements present[d]	N.M.	N.M.	C, O, Na, Al, Si, S, Zn
Phase/structure	82% anatase, 18% rutile	Cubic ceria	Orthorhombic $Cu(OH)_2$
Morphology	Semispherical	Rods (≤10% polyhedra)	Spherical/polyhedra
Moisture content (wt%)	1.97	4.01	10.84
BET surface area (m^2/g)	51.5	93.8	15.71±0.16
Isoelectric point	6.2	7.5	<3.0
Zeta potential[b] (mV)	+30.0±2.2	+32.8±1.0	-47.6±4.3
pH[b]	4.52	4.51	5.09

[a]Dry powder measured with SEM/TEM
[b]Measured at 10 mg L^{-1} in Nanopure water
[c]TiO_2 and CeO_2 purity measured with thermogravimetric analysis (TGA), $Cu(OH)_2$ purity was determined via ICP-AES
[d]Analysis was done via XRD and EDS

These ENMs were chosen because they are widely used in nanoparticulate form in a number of commercial and industrial products and have release patterns that make them relevant for studies of terrestrial ecosystems.[11, 19] For example, TiO_2 ENMs are currently one of the most common nanomaterial in production[20] and are used in a wide variety of industrial and consumer applications that will likely result in their introduction into the terrestrial environment.[9, 21-23] CeO_2 ENMs are used in several common industrial processes and as a catalyst in diesel fuel, where they are expelled in exhaust and deposited from the atmosphere onto the land surface.[11, 24, 25] Kocide 3000 is a nano-$Cu(OH)_2$ based pesticide manufactured by DuPont[26] that is specifically developed to be applied to produce and consequently will be directly or incidentally introduced into soils.

Exposure levels were chosen to cover a range of ENM concentrations that we predicted to be environmentally relevant based on previous reports of exposure modeling and detection for CeO_2 and TiO_2. CeO_2 has been predicted to be present at levels up to about 1 mg/kg in roadside soils due to atmospheric deposition,[11] and while there are no direct measurements of anthropogenic TiO_2 in soil that we are aware of, Kiser, et al. (2009)[27] found TiO_2 in wastewater treatment plant (WWTP) solids at concentrations ranging from 1-6 mg kg^{-1}, which are spread on agricultural fields for fertilizer. The $Cu(OH)_2$ ENM used here is recommended by the manufacturer for use at application rates of up to 18 g m^{-2} per season.[26]

1.4. Soils Studied

Three soils were used in this study: a commercial potting soil, a grassland soil, and a farmland soil. These soils were chosen as representatives of a high organic content soil, a soil from an undisturbed wilderness area, and an agricultural soil, respectively. Sunshine® Mix #4 potting soil was purchased from Sun Gro (USA), and was composed of peat moss, perlite, and dolomitic limestone. Grassland soil was collected from a flat, well drained grassy area at the Sedgwick Reserve in Santa Ynez, CA (N 34° 40' 33.9", W 120° 02' 07.6"), and farmland soil was collected from a fallow field at an organic farm in Carpinteria, CA (N 34° 23' 34.5", W 119° 28' 46.9"). Soil properties can be found in Table 1.2.

Table 1.2. Soil Properties.

Property	Potting Soil	Grass Soil	Farm Soil
pH	5.90 ± 0.03	5.90 ± 0.04	6.86 ± 0.02
Electrical conductivity ($\mu S\ cm^{-1}$)	474.3 ± 27.9	18.9 ± 0.6	142.1 ± 5.4
Cation exchange capacity ($meq\ 100g^{-1}$)	69.2 ± 1.2	25.8 ± 0.1	8.7 ± 0.1
Loss-on-ignition organic matter (%)	52.83 ± 0.91	3.11 ± 0.07	1.44 ± 0.04
Bulk density ($g\ cm^{-3}$)	0.086 ± 0.001	0.981 ± 0.017	1.101 ± 0.003
Sand / Silt / Clay (%)	N.A.	54.0 / 29.0 / 17.0	66.0 / 22.0 / 12.0
Saturation percent (%)	514.5 ± 48.4	43.0 ± 0.7	28.0
Water content of air-dry soil (wt. %)	26.91 ± 2.58	10.54 ± 0.02	6.23 ± 0.04
Exchangeable PO_4-P ($\mu g\ g^{-1}$)	325.5 ± 2.1	15.3 ± 0.6	51.3 ± 3.0
Exchangeable NH_4-N ($\mu g\ g^{-1}$)	10.3 ± 0.0	1.28 ± 0.04	1.69 ± 0.10
Exchangeable NO_3-N ($\mu g\ g^{-1}$)	372.3 ± 9.4	11.5 ± 0.5	51.9 ± 0.7
Exchangeable K ($\mu g\ g^{-1}$)	1398 ± 6	206 ± 1	278 ± 1
Total Ce ($\mu g\ g^{-1}$)	7.0 ± 0.7	30.3 ± 0.8	66.6 ± 0.4
Total Cu ($\mu g\ g^{-1}$)	1.2 ± 0.1	25.4 ± 0.3	30.5 ± 0.4
Total Ti ($\mu g\ g^{-1}$)	16 ± 0	1864 ± 10	1726 ± 9

Soils were air dried, sieved through a 2 mm mesh, and stored at 4°C until use. Samples of sieved soil were characterized for pH, texture, saturation percent, soluble salts, cation exchange capacity, conductivity, organic content, and exchangeable NH_4, NO_3, K, and PO_4 by the University of California, Davis Analytical Laboratory (http://anlab.ucdavis.edu/). Total Ce, Cu, and Ti concentrations of each soil were measured after digesting ~0.3 g soil samples in 10 mL 1:3 HNO_3:HCl at 200°C for 1.5 hours in a microwave digestion system (Multiwave Eco, Anton Paar) followed by analysis via inductively coupled plasma atomic emission spectroscopy (ICP-AES, iCAP 6300 Thermo Scientific, Waltham, MA). Detection limits for all elements tested were approximately 5 $\mu g\ L^{-1}$. Standard solutions and blanks were measured every 15-20 samples for quality assurance. This technique was sufficient to dissolve the soil and ≥90% of TiO_2, CeO_2, and $Cu(OH)_2$. Soil bulk density was measured following McKenzie, et al. (2004)[28] and the water content of air-dried soil was measured also following Rhoades (1982)[29].

1.5. References

1. McWilliams, A. *Nanotechnology: A Realistic Market Assessment*; BCC Research LLC: 2014.
2. Nanotechnologies, T. P. o. E. Nanotechnology Consumer Product Inventory. http://www.nanotechproject.org/cpi/products/
3. Commission, E., Commission Recommendation of 18 October 2011 on the Definition of Nanomaterial Text with Eea Relevance. In Official Journal of the European Union: 2011; pp p. 38-40.
4. Alivisatos, A. P., Semiconductor Clusters, Nanocrystals, and Quantum Dots. *Science* **1996,** *271*, (5251), 933-937.
5. Gottschalk, F.; Nowack, B., The Release of Engineered Nanomaterials to the Environment. *J. Environ. Monit.* **2011,** *13*, (5), 1145-1155.
6. Keller, A. A.; McFerran, S.; Lazareva, A.; Suh, S., Global Life Cycle Releases of Engineered Nanomaterials. *J. Nanopart. Res.* **2013,** *15*, (6).
7. Keller, A. A.; Vosti, W.; Wang, H. T.; Lazareva, A., Release of Engineered Nanomaterials from Personal Care Products Throughout Their Life Cycle. *J. Nanopart. Res.* **2014,** *16*, (7).
8. Keller, A. A.; Lazareva, A., Predicted Releases of Engineered Nanomaterials: From Global to Regional to Local. *Environ. Sci. Technol. Lett.* **2014,** *1*, (1), 65-70.
9. Kaegi, R.; Ulrich, A.; Sinnet, B.; Vonbank, R.; Wichser, A.; Zuleeg, S.; Simmler, H.; Brunner, S.; Vonmont, H.; Burkhardt, M.; Boller, M., Synthetic Tio(2) Nanoparticle Emission from Exterior Facades into the Aquatic Environment. *Environ. Pollut.* **2008,** *156*, (2), 233-239.
10. Lazareva, A.; Keller, A. A., Estimating Potential Life Cycle Releases of Engineered Nanomaterials from Wastewater Treatment Plants. *ACS Sustain. Chem. Eng.* **2014,** *2*, (7), 1656-1665.
11. Park, B.; Donaldson, K.; Duffin, R.; Tran, L.; Kelly, F.; Mudway, I.; Morin, J. P.; Guest, R.; Jenkinson, P.; Samaras, Z.; Giannouli, M.; Kouridis, H.; Martin, P., Hazard and Risk Assessment of a Nanoparticulate Cerium Oxide-Based Diesel Fuel Additive - a Case Study. *Inhal. Toxicol.* **2008,** *20*, (6), 547-566.
12. Kurlanda-Witek, H.; Ngwenya, B. T.; Butler, I. B., Transport of Bare and Capped Zinc Oxide Nanoparticles Is Dependent on Porous Medium Composition. *Journal of Contaminant Hydrology* **2014,** *162*, 17-26.
13. Lv, X. Y.; Gao, B.; Sun, Y. Y.; Shi, X. Q.; Xu, H. X.; Wu, J. C., Effects of Humic Acid and Solution Chemistry on the Retention and Transport of Cerium Dioxide Nanoparticles in Saturated Porous Media. *Water Air Soil Pollut.* **2014,** *225*, (10).
14. Ben-Moshe, T.; Dror, I.; Berkowitz, B., Transport of Metal Oxide Nanoparticles in Saturated Porous Media. *Chemosphere* **2010,** *81*, (3), 387-393.
15. Brady, N. C.; Weil, R. R., *Elements of the Nature and Properties of Soils*. 2nd ed.; Pearson Education: Upper Saddle River, New Jersey, 2003.
16. Kleber, M.; Sollins, P.; Sutton, R., A Conceptual Model of Organo-Mineral Interactions in Soils: Self-Assembly of Organic Molecular Fragments into Zonal Structures on Mineral Surfaces. *Biogeochemistry* **2007,** *85*, (1), 9-24.

17. Keller, A. A.; Wang, H. T.; Zhou, D. X.; Lenihan, H. S.; Cherr, G.; Cardinale, B. J.; Miller, R.; Ji, Z. X., Stability and Aggregation of Metal Oxide Nanoparticles in Natural Aqueous Matrices. *Environ. Sci. Technol.* **2010,** *44*, (6), 1962-1967.
18. Adeleye, A. S.; Conway, J. R.; Perez, T.; Rutten, P.; Keller, A. A., Influence of Extracellular Polymeric Substances on the Long-Term Fate, Dissolution, and Speciation of Copper-Based Nanoparticles. *Environ. Sci. Technol.* **2014,** *48*, (21), 12561-12568.
19. Musee, N., Nanotechnology Risk Assessment from a Waste Management Perspective: Are the Current Tools Adequate? *Hum. Exp. Toxicol.* **2011,** *30*, (8), 820-835.
20. Eertman, R. H. M.; Groenink, C.; Sandee, B.; Hummel, H.; Smaal, A. C., Response of the Blue Mussel Mytilus-Edulis-L Following Exposure to Pahs or Contaminated Sediment. *Mar. Environ. Res.* **1995,** *39*, (1-4), 169-173.
21. Weir, A.; Westerhoff, P.; Fabricius, L.; Hristovski, K.; von Goetz, N., Titanium Dioxide Nanoparticles in Food and Personal Care Products. *Environ. Sci. Technol.* **2012,** *46*, (4), 2242-2250.
22. Gottschalk, F.; Sonderer, T.; Scholz, R. W.; Nowack, B., Modeled Environmental Concentrations of Engineered Nanomaterials (Tio2, Zno, Ag, Cnt, Fullerenes) for Different Regions. *Environ. Sci. Technol.* **2009,** *43*, (24), 9216-9222.
23. Johnson, A. C.; Bowes, M. J.; Crossley, A.; Jarvie, H. P.; Jurkschat, K.; Jurgens, M. D.; Lawlor, A. J.; Park, B.; Rowland, P.; Spurgeon, D.; Svendsen, C.; Thompson, I. P.; Barnes, R. J.; Williams, R. J.; Xu, N., An Assessment of the Fate, Behaviour and Environmental Risk Associated with Sunscreen Tio2 Nanoparticles in Uk Field Scenarios. *Sci. Total Environ.* **2011,** *409*, (13), 2503-2510.
24. Batley, G. E.; Halliburton, B.; Kirby, J. K.; Doolette, C. L.; Navarro, D.; McLaughlin, M. J.; Veitch, C., Characterization and Ecological Risk Assessment of Nanoparticulate Ceo2 as a Diesel Fuel Catalyst. *Environ. Toxicol. Chem.* **2013,** *32*, (8), 1896-1905.
25. Dahle, J. T.; Arai, Y., Environmental Geochemistry of Cerium: Applications and Toxicology of Cerium Oxide Nanoparticles. *Int. J. Environ. Res. Public Health* **2015,** *12*, (2), 1253-1278.
26. DuPont Material Safety Data Sheet: Dupont Kocide 3000 Fungicide/Bactericide. http://www.cdms.net/LDat/mp7HK000.pdf (January 16, 2014),
27. Kiser, M. A.; Westerhoff, P.; Benn, T.; Wang, Y.; Perez-Rivera, J.; Hristovski, K., Titanium Nanomaterial Removal and Release from Wastewater Treatment Plants. *Environ. Sci. Technol.* **2009,** *43*, (17), 6757-6763.
28. McKenzie, N.; Jacquier, D.; Isbell, R.; Brown, K., *Australian Soils and Landscapes*. Csiro Publishing: Collingwood, 2004; p 1-416.
29. Rhoades, J., Soluble Salts. In *Methods of Soil Analysis: Part 2: Chemical and Microbiological Properties.*, 2nd ed.; Page, A., Ed. ASA: Madison, WI, 1982.

2. Gravity-Driven Transport of Engineered Nanomaterials in Unsaturated Soils

2.1. Introduction

ENM mobility in the subsurface is governed by several processes of varying influence, including dissolved ion and pH-induced aggregation, coating by organic and inorganic molecules, sorption to organisms and other media components, and physical straining through soil pore spaces. In particular, chemical and electrostatic interactions with soil clay particles have been implicated as key factors in the subsurface movement of raw or coated ENMs. This has been demonstrated for TiO_2[1] and uncoated, citrate-coated, and phosphate-coated CeO_2 ENMs[2] in soil and implied as the method of retention in other studies.[3, 4] Sorption can occur via electrostatic attraction between charged clay surfaces and oppositely charged ENMs[5] or chemically (for metal oxides or metals with an outer oxide layer) through a dehydration reaction similar to the binding of phosphate or iron oxides to clays.[6, 7] Sorption to organic matter[8] and organisms[9] in soil may also take place through similar mechanisms.

The specific organic compounds present in subsurface waters will also differ over geographic area with soil and vegetation type due to the presence of plant root exudates[10-12] and bacterial communities,[6] which will result in different coatings being available to ENMs in different areas. There is also the possibility of physical straining and collection at air-water-soil interfaces when flowing through porous media like soil.[13] Physical straining of high aspect ratio ENMs in soil has been demonstrated with single-walled carbon nanotubes[14]

and implicated as a primary retention mechanism for nanoscale Fe^0 (nZVI) in a sandy loam soil.[15] As aggregation caused by high ionic strength, pHs near the PZC, or coatings increases, physical straining becomes more likely, particularly in soils like Vertisols or Ultisols that are characterized by small pore sizes.

Two hypotheses were addressed in these series of experiments. The first hypothesis was that ENM transport would be limited to the upper layers of soil, but particles coated with NOM would penetrate further into the soil due to increased electrostatic repulsive forces as a result of their more negative surface charge.[16, 17] The second hypothesis was that particles would be transported further through potting soil than agricultural or grassland soils due to the greater density and clay contents of the two natural soils causing increased physical straining and electrostatic/chemical sorption.

2.2. Methods

2.2.1. ENM Preparation

Stock suspensions of CeO_2, $Cu(OH)_2$, and TiO_2 ENMs (properties shown in Table 1.1) were prepared by suspending dry ENM powders in 18.2 MΩ cm Nanopure water (Barnstead) and sonicating for 30 min in a bath sonicator (Branson 2510, Danbury, CT). Stock suspensions were sonicated for 10 min after dilution to the desired concentration and used within 24 hr. Suwannee River NOM stock solutions were prepared as described in Zhou and Keller (2010)[18]. Hydrodynamic diameter and ζ-potential of TiO_2, CeO_2, and $Cu(OH)_2$ ENMs with and without NOM were measured via dynamic light scattering (DLS,

Zetasizer Nano ZS-90, Malvern Instruments) at 20°C by preparing 10 mg L^{-1} ENM suspensions with and without the addition of 1 mg L^{-1} NOM in Nanopure water and in soil solution extracts (described below) through dilution of a 100 mg L^{-1} stock, probe sonicating for 2 sec at 20% amplitude (sufficient to disperse aggregates) with a Misonix Sonicator S-4000 (QSonica LLC, Newtown, CT).

2.2.2. ENM Transport through Unsaturated Soils

ENM transport through the three soils was tested by loosely packing 2.5 cm diameter x 16.34 cm long cylindrical plastic columns (Ray Leach Cone-tainers; Stuewe and Sons, Tangent, Oregon) with air-dried soil. Due to their different densities, 17.5 ± 0.1 g potting soil, 136 ± 1 g grass soil, or 167 ± 1 g farm soil were needed to completely fill the columns. To simulate gravity-driven transport of ENMs in suspension, 50 mL of 100 mg L^{-1} TiO_2, CeO_2, or $Cu(OH)_2$ ENM suspensions with or without the addition of 10 mg L^{-1} NOM were slowly applied to the top of the column. The resulting soil ENM concentrations were on the high end of those currently predicted for metal oxides in soil,[19] but were well within the concentrations predicted for biosolids.[19, 20] Hence, the soil ENM concentrations used in this experiment may be indicative of those found in soils repeatedly amended with biosolids.

After ENM application, columns were allowed to drain overnight, oven dried at 60°C for 72 hours, and split into 3 cm segments, ~0.3 g subsamples of which were weighed, digested, in 10 mL 1:3 HNO_3:HCl at 200°C for 1.5 hours in a microwave digestion system (Multiwave Eco, Anton Paar) followed by analysis via inductively coupled plasma atomic emission spectroscopy (ICP-AES, iCAP 6300 Thermo Scientific, Waltham, MA). This technique was sufficient to dissolve the soil and ≥90% of TiO_2, CeO_2, and $Cu(OH)_2$.

Detection limits for all elements tested were approximately 5 μg L^{-1}. Standard solutions and blanks were measured every 15-20 samples for quality assurance. Five replicate columns were prepared and analyzed for each treatment. Metal concentrations for all three ENMs are reported as ionic, although neither CeO_2 nor TiO_2 were expected to dissolve to a significant degree under the conditions used in this experiment. TiO_2 is known to be highly insoluble in water and CeO_2 is similarly insoluble at pHs similar to those found in the soils used here.[21] However, $Cu(OH)_2$ has been shown to undergo partial dissolution under acidic to neutral conditions, although at acidic pHs less dissolution occurs in media with high concentrations of dissolved organic matter.[22, 23] Based on this, dissolution of $Cu(OH)_2$ is not expected to occur to a significant degree under the conditions and time scales used in this experiment.

To measure size distribution of particles throughout the column, air-dried samples of contaminated soils were collected from the top and bottom 3 cm of columns and analyzed using environmental scanning electron microscopy (ESEM) with backscattering electron detection (BSE) and energy-dispersive X-ray spectroscopy (EDS) to confirm identification of CeO_2, $Cu(OH)_2$, or TiO_2 ENMs. Beam voltage was set at 12 kV, spot size at 6.0, water vapor pressure was kept at 2.7 Torr, and working distance averaged around 10.5 cm. These settings were chosen in order to minimize X-ray subsurface penetration for EDS analysis. Elemental hypermap data was collected over a period of 6 min per image. ImageJ image analysis software (National Institute of Health, Bethesda, Maryland, USA; available at http://rsbweb.nih.gov/ij) was used to determine particle or aggregate size.

Soil solution extracts of potting, grassland, and farm soils were prepared following Rhoades (1982)[24], although no Na_3PO_4 was added in order to avoid influencing ENM physicochemical behavior. Soil solution extracts were stored at 4°C until use.

2.2.3. Statistical Analyses

To determine the influence of the presence of NOM coating, ENM type, and soil solution extract type on ENM hydrodynamic diameter and ζ-potential 3-way ANOVA with interactions and post-hoc Tukey's tests were used. Levene's test was used to ensure homogeneity of variance. Statistical analyses were performed using the statistical software R (v. 2.11.1).

2.3. Results and Discussion

2.3.1. ENM Transport through Unsaturated Soils

Gravity-driven vertical transport of ENMs through unsaturated soil was found in general to follow the hypothesis that the majority of ENMs would be retained in the upper portion of the column, but as predicted was found to be highly dependent on soil type with increased retention occurring in the denser, less porous natural soils (Figure 2.1). However, ENMs coated with natural organic matter (NOM) did not have increased vertical transport, and in fact were retained more in potting soil. TiO_2 and CeO_2 aggregate sizes (Figure 2.2) were seen to decrease with column depth, suggesting physical straining to be the primary impediment to transport. Aggregate hydrodynamic diameters tended to be larger in soil solution extracts than Nanopure H_2O and were also generally larger with NOM-coated particles, with several exceptions (Figure 2.3).

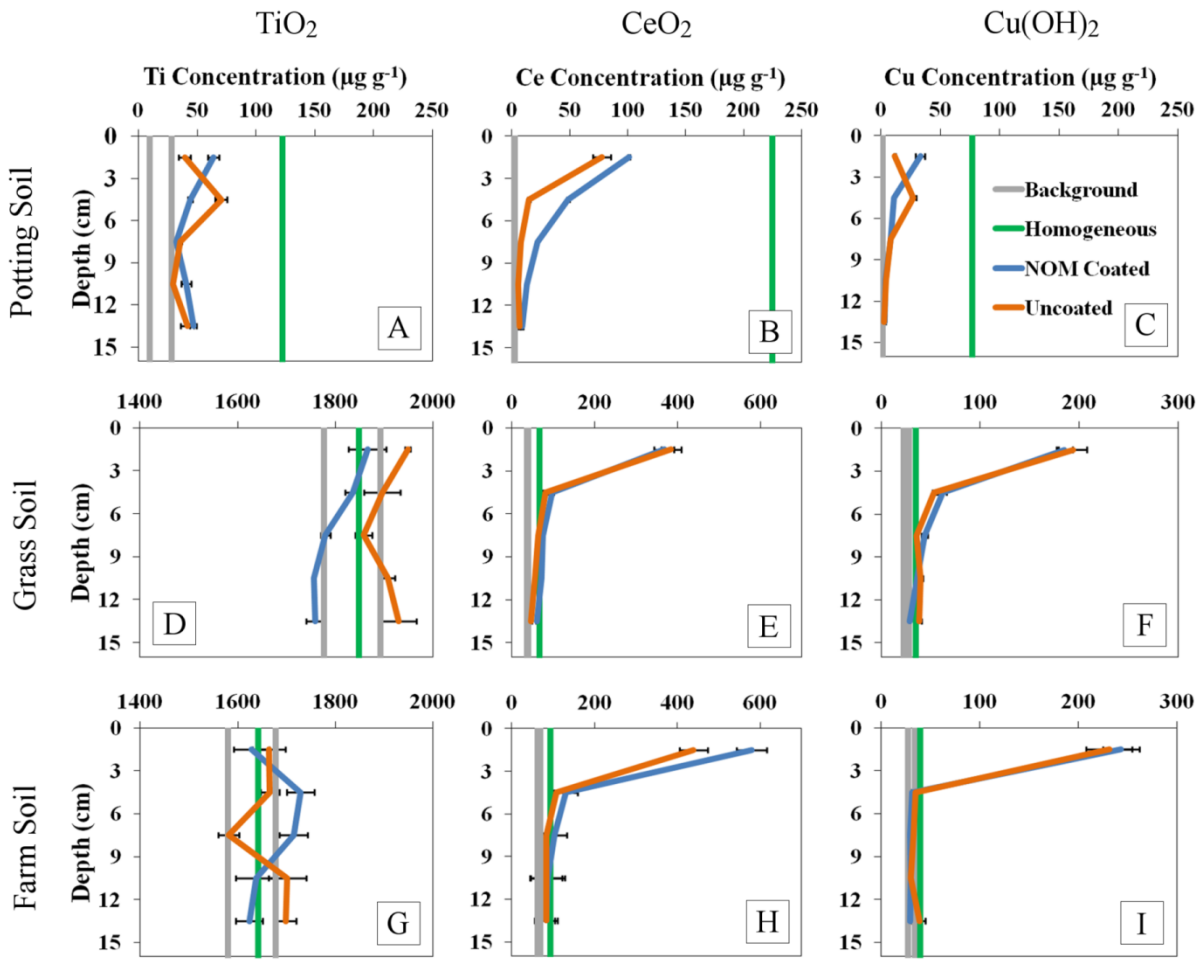

Figure 2.1. Gravity-driven transport of suspended uncoated and NOM-coated TiO_2, CeO_2, and $Cu(OH)_2$ ENMs through potting, grass, and farm soil columns. Each point represents the average concentration of a 3 cm vertical segment of a column (i.e., 0-3 cm, 3-6 cm, etc.). For reference, grey lines show the range of background concentrations of target metals present naturally in soils (mean ± 1 SD) and green lines represent hypothetical concentrations that would be found if the ENMs were mixed homogeneously throughout the entire column. Error bars are ± 1 SE. Note variable x-axis.

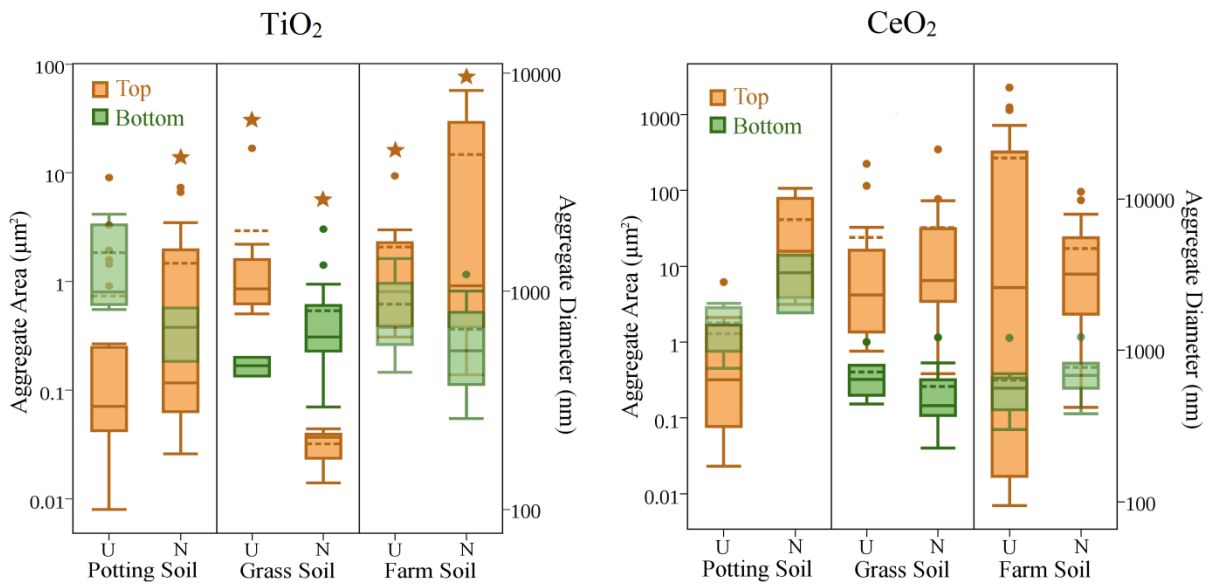

Figure 2.2. Tukey box plots of aggregate size distributions of uncoated (U) or NOM-coated (N) TiO_2 and CeO_2 ENMs in potting soil, grass soil, and farm soil measured by electron micrograph analysis. Aggregate areas (in μm^2) were estimated from micrographs and aggregate diameter (in nm) was calculated by considering aggregates as spheres in order to provide comparison to Figure 2.3. Samples taken from the upper 0-3 cm of the column are shown in orange (Top) and samples taken from the lower 12-15 cm of the column are shown in green (Bottom). Means are represented as dashed lines and outliers are shown as dots. Stars indicate samples in which large continuous surface deposits of TiO_2 were seen, which are not included in the aggregate size distributions shown here. $Cu(OH)_2$ aggregates could not be positively identified with BSE/EDS due to the low Cu content of the $Cu(OH)_2$ particles as well as the relatively low atomic mass. Note variable y-axis.

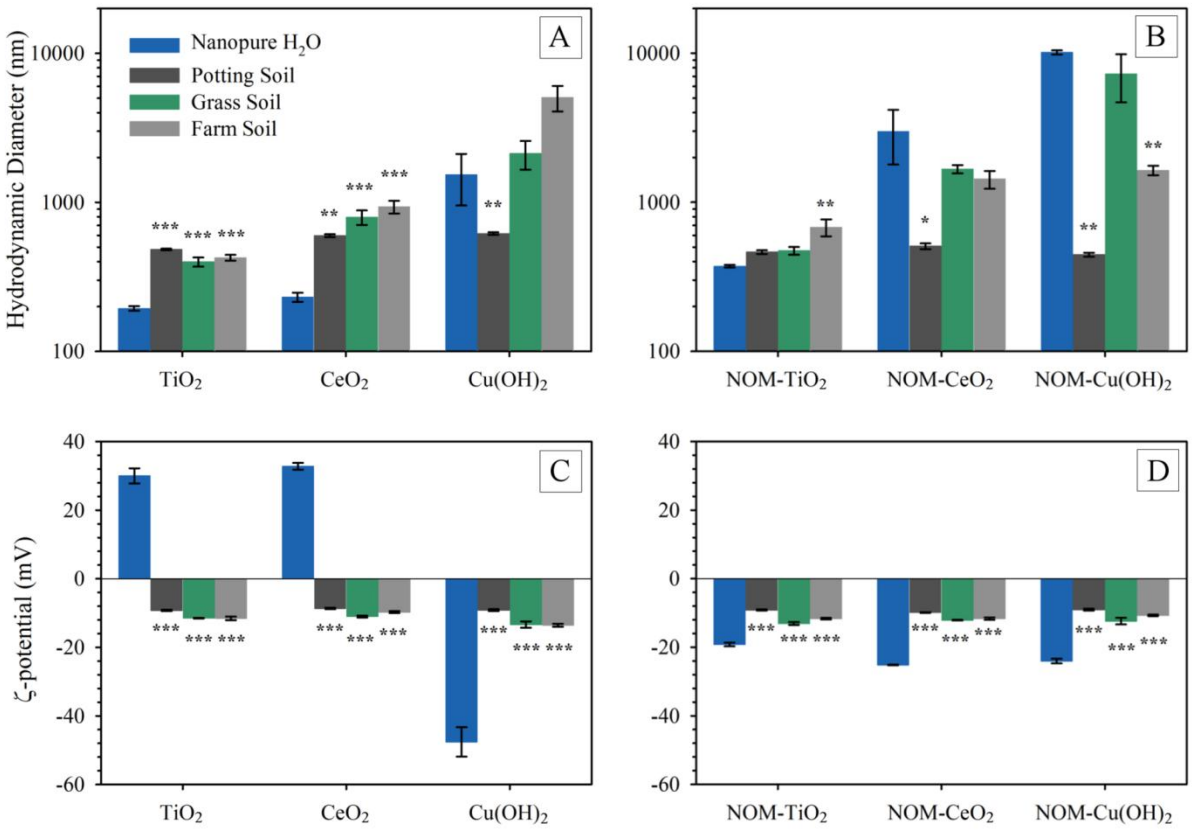

Figure 2.3. Hydrodynamic diameter (A & B) and ζ-potential (C & D) of TiO_2, CeO_2, and $Cu(OH)_2$ ENMs at a concentration of 10 mg L^{-1} with and without 1 mg L^{-1} NOM in Nanopure water or soil solution extracts from potting, grass, and farm soil. Asterisks represent significance differences between ENMs in soil solution extracts to ENMs in Nanopure water from ANOVA with post-hoc Tukey's tests. *$p < 0.05$, **$p < 0.01$, ***$p < 0.005$. Error bars are ± SE.

All three ENMs largely passed through the entire length of potting soil columns, being present in lower concentrations than the hypothetical homogeneous concentrations at all points, although there was some retention in the upper 0-6 cm that was increased with NOM-coated particles (Figs 2.1A-C). These trends can likely be explained by the primarily organic composition of the potting soil, which gave it very low density, high porosity, and high reactivity (as shown by the high CEC in Table 1.2). The low density and high porosity prevented aggregates from being physically strained, which is shown for TiO_2 and CeO_2 by

the similar aggregate sizes in the tops and bottoms of columns for both uncoated and NOM-coated particles (Figure 2.2). If physical straining was strongly influencing particle transport in potting soil it is unlikely similar aggregate sizes would be observed throughout the length of the column, but rather would result in smaller aggregates or particles penetrating through the column while larger aggregates would be retained at the surface – as was seen in the two natural soils. All three ENMs had similar hydrodynamic diameters in potting soil solution (Figs 2.3A-B), although NOM-coated aggregates were significantly smaller than uncoated aggregates (3-way ANOVA, $p < 0.0001$). ζ-potentials for all three ENMs in soil solutions from all three soils were also similar (Figs 2.3C-D), although again the presence of NOM coatings, as well as the ENM and soil types, had significant impacts on ζ-potentials (3-way ANOVA, $p < 0.05$).

Coating particles with NOM appears to increase their affinity for the organic components of the potting soil. This resulted in the increased overall retention of NOM-coated CeO_2 (Fig. 2.1B) as well as the decreased vertical transport of NOM-coated TiO_2 and $Cu(OH)_2$ (Figs. 2.1A & C). Evidence for this can be found in Figures 2.3A-B, which show that both NOM-coated and uncoated aggregates have nearly identical hydrodynamic diameters in potting soil solution extract, so the additional retention of NOM-coated aggregates is unlikely to be due to increased physical straining. This was visually confirmed in micrographs of NOM-coated TiO_2 in potting soil including Figure 2.4D, which revealed the formation of TiO_2 encrustations occurring primarily on the organic components of potting soil over the Al/Si/Na/K perlite minerals. These encrustations may have been caused in part or whole to interactions between the NOM coating and the organic matter in the potting soil. This finding is counter to several previous transport studies using TiO_2,[16]

CeO_2,[17] and ZnO[25] in quartz sand that found organic coatings decreased ENM retention by increasing electrostatic repulsion between coated aggregates and the sand grains, which further suggests interactions between the organic coating and organic soil components.

In the grassland and agricultural soils CeO_2 and $Cu(OH)_2$ shared similar transport profiles (Figure 2.1), forming large aggregates in the soil solutions (Figure 2.3) that were retained almost entirely in the upper 0-3 cm of the soil columns. However, the widely variable background concentrations of Ti in these natural soils prevented precise measurement of TiO_2 ENM distribution throughout the soil columns by ICP-AES (Figs. 2.1D & 2.1G), the majority of TiO_2 aggregates were confirmed to be retained immediately at the surface through both visual identification of white buildup on the column surfaces and through BSE/EDS analysis. As shown in Figure 2.4, both uncoated and NOM-coated TiO_2 ENMs formed large encrustations on the surfaces of all three soils with the exception of uncoated TiO_2 in potting soil. Despite having nearly identical surface charges in soil solution extracts (Fig. 2.3A), CeO_2 formed large porous sponge-like aggregates instead of the more solid encrustations seen with TiO_2. These differences in aggregate morphology may be due to differences between the primary particle shapes of these two ENMs, with TiO_2 being nanospheres and CeO_2 being nanorods. Afrooz, et al. (2013)[26] found that spherical Au ENMs had higher attachment efficiencies and deposition rates than rod-like Au ENMs identical in composition, which they attributed to differences in electrosteric and physical packing characteristics. Similarly, Zhou, et al. (2013)[27] found the critical coagulation concentration (CCC) of TiO_2 nanospheres was directly related to particle diameter while the CCC of TiO_2 nanrods was better explained by particle surface area, which they postulated was a consequence of differences in exposed crystal faces. It has also

been shown that metal oxide nanospheres and nanorods interact differently with NOM,[27, 28] which may also be a factor in explaining the differences in aggregate morphology seen here.

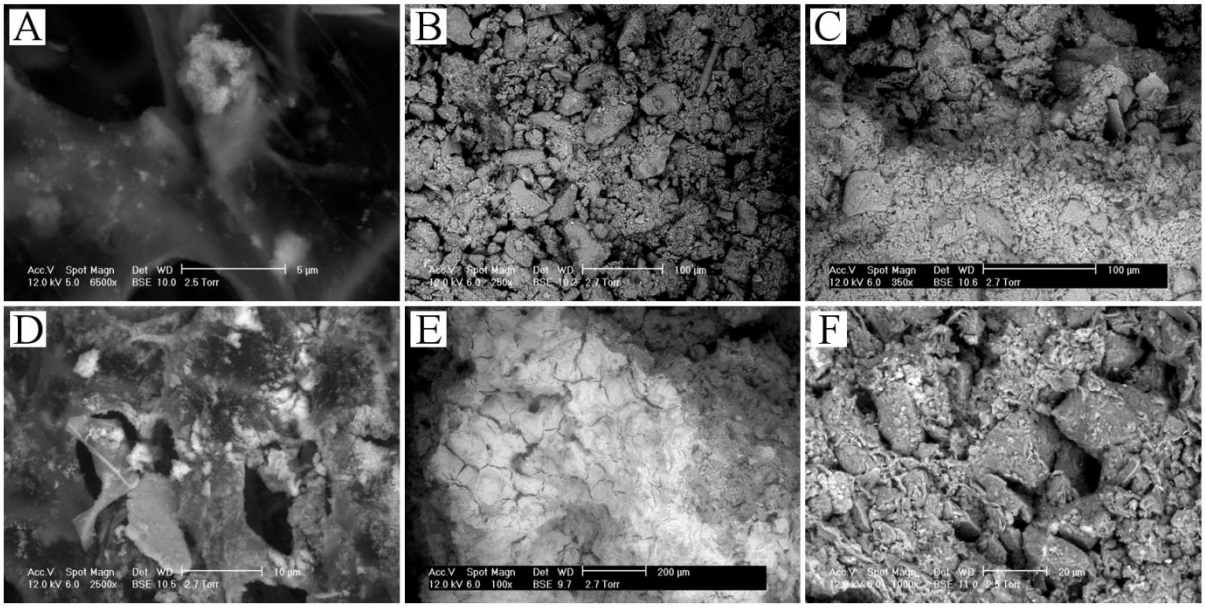

Figure 2.4. Surface encrustations (lighter areas) of uncoated (top row) and NOM-coated (bottom row) TiO_2 in potting soil (A & D), grass soil (B & E), and farm soil (C & F). Micrographs were taken of partially hydrated samples (2.7 torr) from the upper 0-3 cm of columns using ESEM with BSE. Large continuous deposits were not found with uncoated TiO_2 in potting soil (A) or grass soil (B). Scale varies between images. EDS element maps of Ti for these images can be found in Figure 2.5.

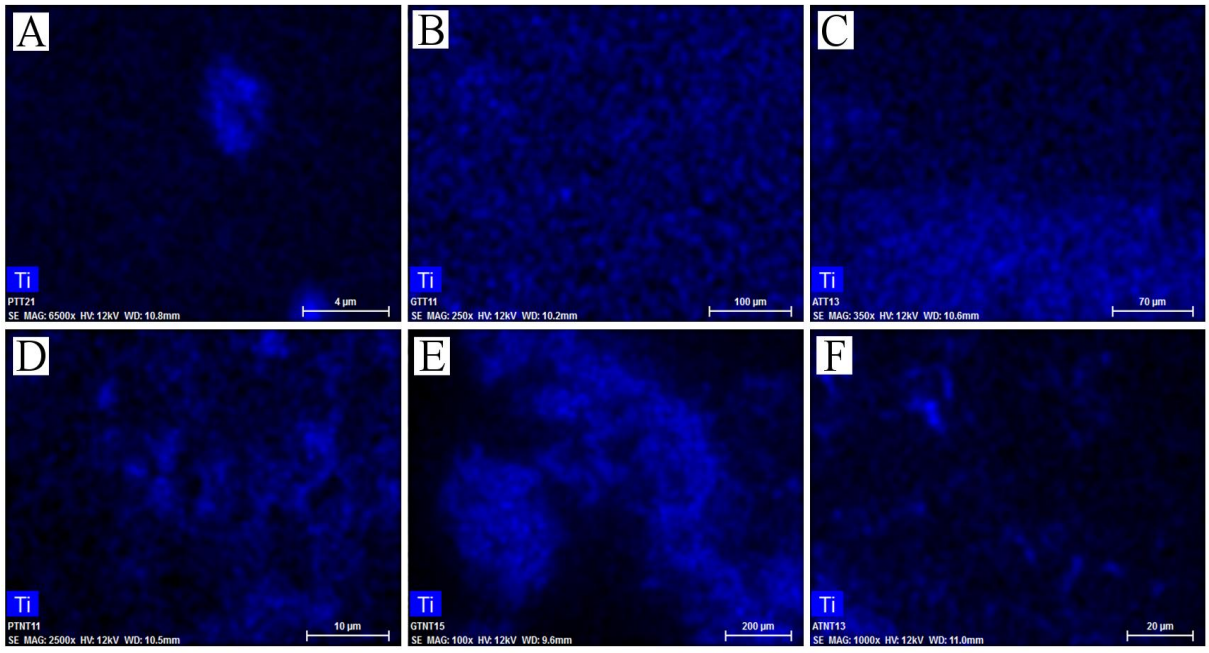

Figure 2.5. EDS element maps of Ti from micrographs shown in Figure 2.4.

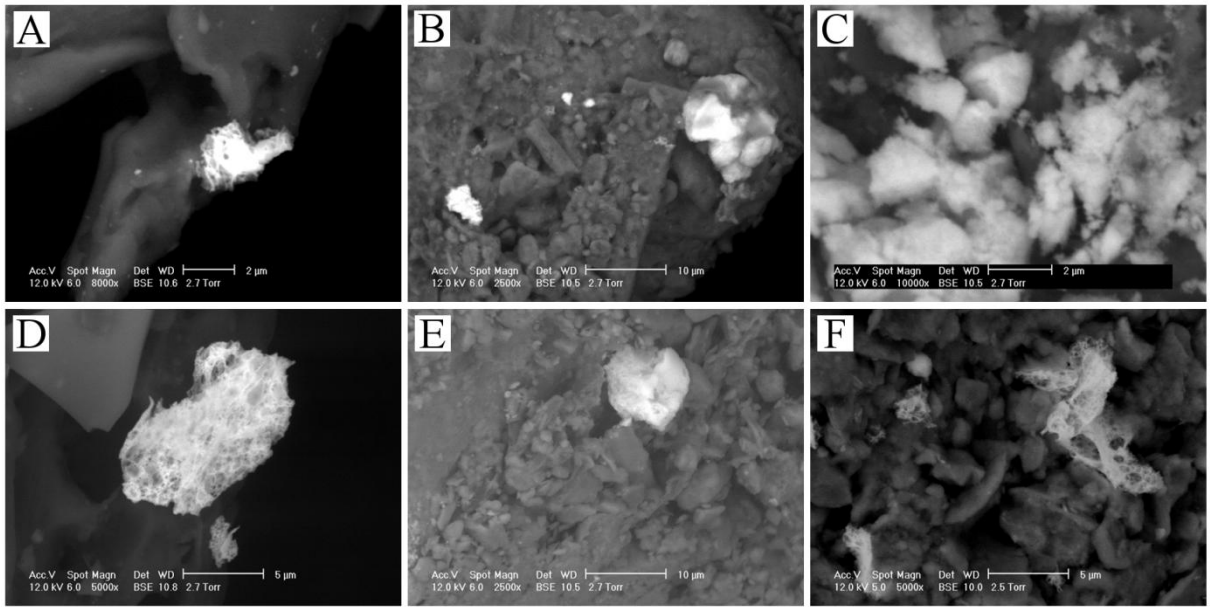

Figure 2.6. Aggregates of uncoated (top row) and NOM-coated (bottom row) CeO_2 in potting soil (A & D), grass soil (B & E), and farm soil (C & F). Micrographs were taken of partially hydrated samples (2.7 torr) from the upper 0-3 cm of columns using ESEM with BSE. Scale varies between images. EDS element maps of Ce for these images can be found in Figure 2.7.

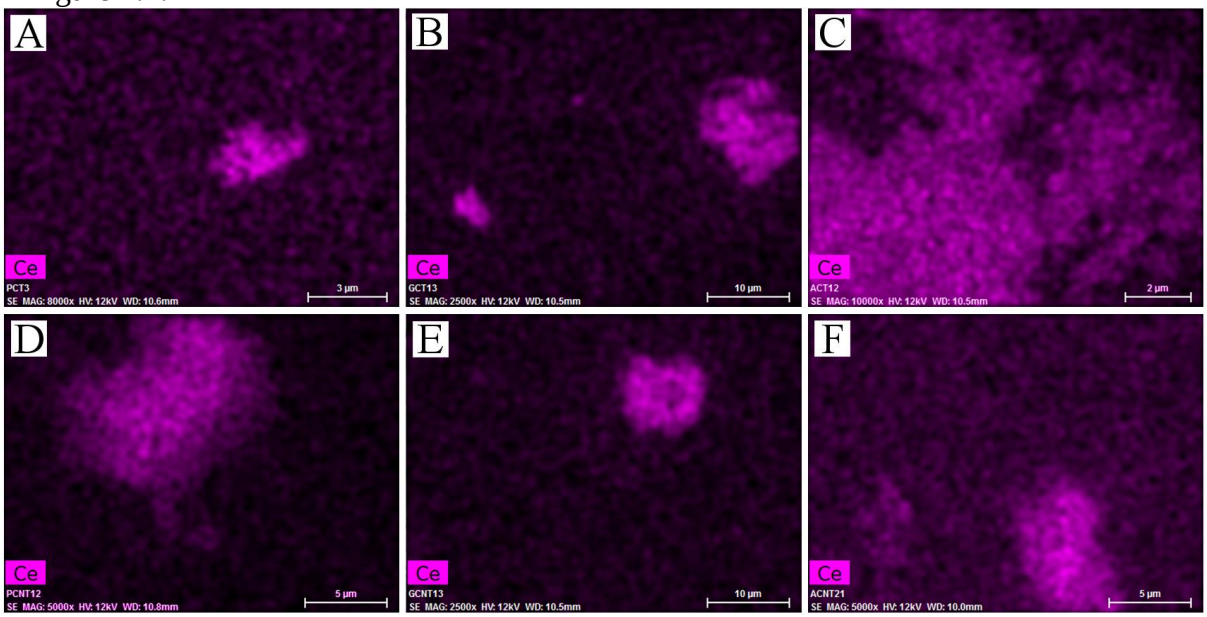

Figure 2.7. EDS element maps of Ce from micrographs shown in Figure 2.6.

Although no $Cu(OH)_2$ aggregates or particles could be identified by ESEM-BSE/EDS due to the low atomic weight of Cu and low Cu content of the $Cu(OH)_2$ particles, it is likely size exclusion and physical straining were also the primary mechanisms of retention as $Cu(OH)_2$ ENMs displayed similar transport profiles to CeO_2. This hypothesis is supported by Figure 2.3, which shows that $Cu(OH)_2$ aggregate sizes in soil solutions are equal to or larger than TiO_2 or CeO_2. Despite the low to moderate solubility of $Cu(OH)_2$ ENMs, [22, 23] it is not likely significant dissolution occurred in these transport experiments given that both uncoated and NOM-coated $Cu(OH)_2$ had nearly identical transport profiles to the relatively insoluble CeO_2.[29]

2.4. Conclusions

These results suggest that these and other ENMs similar in size and/or aggregation tendencies will primarily be retained in the immediate area of contamination and may potentially accumulate to high concentrations that may adversely affect local organisms. Additionally, since these ENMs appear to be able to pass relatively unimpeded through potting soil, which approximates the organic (O) horizon present in some soils, there may be accumulation of ENMs at the boundary between the O horizon and the underlying mineral horizon.

Metal oxide ENMs such as those used in this study are well known to be toxic to a variety of terrestrial organisms,[29-31] but real-world metal oxide ENM soil concentrations are currently predicted to be fairly low, from $\leq$10 to $\leq$0.001 mg kg^{-1}.[32] However, the results of

this study suggest that localized hotspots of highly contaminated soil may be more common than large areas of more diffuse concentrations. While this limits the range of areas that may be affected by ENM release, the impact to local communities of organisms may be more severe. These results also justify for some scenarios the use of ENM concentrations higher than those currently predicted in toxicity tests for soil organisms.

2.5. References

1. Fang, J.; Shan, X. Q.; Wen, B.; Lin, J. M.; Owens, G., Stability of Titania Nanoparticles in Soil Suspensions and Transport in Saturated Homogeneous Soil Columns. *Environ. Pollut.* **2009,** *157*, (4), 1101-1109.
2. Cornelis, G.; Ryan, B.; McLaughlin, M. J.; Kirby, J. K.; Beak, D.; Chittleborough, D., Solubility and Batch Retention of Ceo2 Nanoparticles in Soils. *Environ. Sci. Technol.* **2011,** *45*, (7), 2777-2782.
3. Collins, D.; Luxton, T.; Kumar, N.; Shah, S.; Walker, V. K.; Shah, V., Assessing the Impact of Copper and Zinc Oxide Nanoparticles on Soil: A Field Study. *PLoS One* **2012,** *7*, (8).
4. Wang, Y. G.; Li, Y. S.; Kim, H.; Walker, S. L.; Abriola, L. M.; Pennell, K. D., Transport and Retention of Fullerene Nanoparticles in Natural Soils. *J. Environ. Qual.* **2010,** *39*, (6), 1925-1933.
5. Zhou, D. X.; Abdel-Fattah, A. I.; Keller, A. A., Clay Particles Destabilize Engineered Nanoparticles in Aqueous Environments. *Environ. Sci. Technol.* **2012,** *46*, (14), 7520-7526.
6. Horst, A. M.; Neal, A. C.; Mielke, R. E.; Sislian, P. R.; Suh, W. H.; Maedler, L.; Stucky, G. D.; Holden, P. A., Dispersion of Tio2 Nanoparticle Agglomerates by Pseudomonas Aeruginosa. *Appl. Environ. Microbiol.* **2010,** *76*, (21), 7292-7298.
7. Hofstetter, T. B.; Schwarzenbach, R. P.; Haderlein, S. B., Reactivity of Fe(Ii) Species Associated with Clay Minerals. *Environ. Sci. Technol.* **2003,** *37*, (3), 519-528.
8. Duester, L.; Prasse, C.; Vogel, J. V.; Vink, J. P. M.; Schaumann, G. E., Translocation of Sb and Ti in an Undisturbed Floodplain Soil after Application of Sb2o3 and Tio2 Nanoparticles to the Surface. *J. Environ. Monit.* **2011,** *13*, (5), 1204-1211.
9. Mudunkotuwa, I. A.; Grassian, V. H., Citric Acid Adsorption on Tio2 Nanoparticles in Aqueous Suspensions at Acidic and Circumneutral Ph: Surface Coverage, Surface Speciation, and Its Impact on Nanoparticle-Nanoparticle Interactions. *Journal of the American Chemical Society* **2010,** *132*, (42), 14986-14994.
10. Cesco, S.; Mimmo, T.; Tonon, G.; Tomasi, N.; Pinton, R.; Terzano, R.; Neumann, G.; Weisskopf, L.; Renella, G.; Landi, L.; Nannipieri, P., Plant-Borne Flavonoids Released into the Rhizosphere: Impact on Soil Bio-Activities Related to Plant Nutrition. A Review. *Biology and Fertility of Soils* **2012,** *48*, (2), 123-149.
11. Cesco, S.; Neumann, G.; Tomasi, N.; Pinton, R.; Weisskopf, L., Release of Plant-Borne Flavonoids into the Rhizosphere and Their Role in Plant Nutrition. *Plant Soil* **2010,** *329*, (1-2), 1-25.
12. Dunphy Guzman, K. A.; Finnegan, M. P.; Banfield, J. F., Influence of Surface Potential on Aggregation and Transport of Titania Nanoparticles. *Environ. Sci. Technol.* **2006,** *40*, (24), 7688-7693.
13. Keller, A. A.; Auset, M., A Review of Visualization Techniques of Biocolloid Transport Processes at the Pore Scale under Saturated and Unsaturated Conditions. *Adv. Water Resour.* **2007,** *30*, (6-7), 1392-1407.

14. Jaisi, D. P.; Elimelech, M., Single-Walled Carbon Nanotubes Exhibit Limited Transport in Soil Columns. *Environ. Sci. Technol.* **2009,** *43*, (24), 9161-9166.
15. Basnet, M.; Di Tommaso, C.; Ghoshal, S.; Tufenkji, N., Reduced Transport Potential of a Palladium-Doped Zero Valent Iron Nanoparticle in a Water Saturated Loamy Sand. *Water Res.* **2015,** *68*, 354-363.
16. Ben-Moshe, T.; Dror, I.; Berkowitz, B., Transport of Metal Oxide Nanoparticles in Saturated Porous Media. *Chemosphere* **2010,** *81*, (3), 387-393.
17. Lv, X. Y.; Gao, B.; Sun, Y. Y.; Shi, X. Q.; Xu, H. X.; Wu, J. C., Effects of Humic Acid and Solution Chemistry on the Retention and Transport of Cerium Dioxide Nanoparticles in Saturated Porous Media. *Water Air Soil Pollut.* **2014,** *225*, (10).
18. Zhou, D.; Keller, A. A., Role of Morphology in the Aggregation Kinetics of Zno Nanoparticles. *Water Res.* **2010,** *44*, (9), 2948-2956.
19. Gottschalk, F.; Sun, T. Y.; Nowack, B., Environmental Concentrations of Engineered Nanomaterials: Review of Modeling and Analytical Studies. *Environ. Pollut.* **2013,** *181*, 287-300.
20. Lazareva, A.; Keller, A. A., Estimating Potential Life Cycle Releases of Engineered Nanomaterials from Wastewater Treatment Plants. *ACS Sustain. Chem. Eng.* **2014,** *2*, (7), 1656-1665.
21. Collin, B.; Auffan, M.; Johnson, A. C.; Kaur, I.; Keller, A. A.; Lazareva, A.; Lead, J. R.; Ma, X. M.; Merrifield, R. C.; Svendsen, C.; White, J. C.; Unrine, J. M., Environmental Release, Fate and Ecotoxicological Effects of Manufactured Ceria Nanomaterials. *Environ.-Sci. Nano* **2014,** *1*, (6), 533-548.
22. Adeleye, A. S.; Conway, J. R.; Perez, T.; Rutten, P.; Keller, A. A., Influence of Extracellular Polymeric Substances on the Long-Term Fate, Dissolution, and Speciation of Copper-Based Nanoparticles. *Environ. Sci. Technol.* **2014,** *48*, (21), 12561-12568.
23. Conway, J. R.; Adeleye, A. S.; Gardea-Torresdey, J.; Keller, A. A., Aggregation, Dissolution, and Transformation of Copper Nanoparticles in Natural Waters. *Environ. Sci. Technol.* **2015,** *49*, (5), 2749-2756.
24. Rhoades, J., Soluble Salts. In *Methods of Soil Analysis: Part 2: Chemical and Microbiological Properties.*, 2nd ed.; Page, A., Ed. ASA: Madison, WI, 1982.
25. Kurlanda-Witek, H.; Ngwenya, B. T.; Butler, I. B., Transport of Bare and Capped Zinc Oxide Nanoparticles Is Dependent on Porous Medium Composition. *Journal of Contaminant Hydrology* **2014,** *162*, 17-26.
26. Afrooz, A.; Sivalapalan, S. T.; Murphy, C. J.; Hussain, S. M.; Schlager, J. J.; Saleh, N. B., Spheres Vs. Rods: The Shape of Gold Nanoparticles Influences Aggregation and Deposition Behavior. *Chemosphere* **2013,** *91*, (1), 93-98.
27. Zhou, D. X.; Ji, Z. X.; Jiang, X. M.; Dunphy, D. R.; Brinker, J.; Keller, A. A., Influence of Material Properties on Tio2 Nanoparticle Agglomeration. *PLoS One* **2013,** *8*, (11).
28. Zhou, D. X.; Keller, A. A., Role of Morphology in the Aggregation Kinetics of Zno Nanoparticles. *Water Res.* **2010,** *44*, (9), 2948-2956.
29. Dahle, J. T.; Arai, Y., Environmental Geochemistry of Cerium: Applications and Toxicology of Cerium Oxide Nanoparticles. *Int. J. Environ. Res. Public Health* **2015,** *12*, (2), 1253-1278.
30. Menard, A.; Drobne, D.; Jemec, A., Ecotoxicity of Nanosized Tio2. Review of in Vivo Data. *Environ. Pollut.* **2011,** *159*, (3), 677-684.

31. Kwak, J. I.; An, Y. J., Ecotoxicological Effects of Nanomaterials on Earthworms: A Review. *Hum. Ecol. Risk Assess.* **2015,** *21*, (6), 1566-1575.
32. Holden, P. A.; Klaessig, F.; Turco, R. F.; Priester, J. H.; Rico, C. M.; Avila-Arias, H.; Mortimer, M.; Pacpaco, K.; Gardea-Torresdey, J. L., Evaluation of Exposure Concentrations Used in Assessing Manufactured Nanomaterial Environmental Hazards: Are They Relevant? *Environ. Sci. Technol.* **2014,** *48*, (18), 10541-10551.

3. Effects of Engineered Nanomaterials on Soil pH and Nutrient Release

3.1. Introduction

Little research has been done on the effects of ENM exposure on soil properties. In one of the only available studies available on this subject, Ben-Moshe, et al. (2013)[1] observed that CuO and Fe_3O_4 ENMs did not change the total organic content or macroscopic properties of two types of soil but altered the humic substances in the soils. The authors also observed an effect on the soil microbial community, which has been reported in other studies (e.g., [2-4]), but did not attempt to link changes in important soil properties with these effects. VandeVoort, et al. (2014)[5] found that silver ENMs could limit denitrification processes in soil, but that the effects were dependent on ENM concentration and coating. While previous studies in this area suggest that the effects of ENMs on soil properties are somewhat limited, there may be additional impacts not considered in these studies.

For example, metal oxide surfaces are amphoteric, capable of producing both protons (H^+) and hydroxide ions (OH^-), but tend to be predominantly acidic in nature.[6] Due to this metal oxide ENMs may be able to alter the pH of soil pore water and consequently the overall pH of the soil. pH has been called one of the "master variables" for soil systems[7] because it controls a number of critical physical and chemical properties, and if ENMs are able to alter soil pH when present above certain concentrations they may pose a hazard to

organisms that rely on the soil for habitat or sustenance. However, soils are typically well-buffered, and may be able to withstand ENM accumulation without changing pH.

Additionally, ENMs will likely aggregate as a result of the high ion content of soil solutions, thus decreasing total surface area and, potentially, proton/hydroxide production. Additionally, metal oxide ENMs bear many similarities to naturally occurring nano-scale poorly crystalline metal oxide minerals known as short-range order (SRO) minerals. SRO minerals have been shown to influence nutrient availability in natural soils via sorptive processes,[8] and metal oxide ENMs may also demonstrate this effect. In particular, metal oxides are well known for their ability to covalently adsorb phosphate ions (PO_4^{3-})[6, 9] and, depending on the strength of this interaction, may prevent organisms from accessing this important nutrient.

Two hypotheses were addressed in these series of experiments. First, I hypothesized that none of the soils would experience a significant change in pH after spiking with ENMs due to the presence of buffering compounds (such as dolomitic lime) in the soils. Second, I hypothesized that these ENMs would sorb soil nutrients, including phosphate, and reduce their mobility in the soil.

3.2. Methods

3.2.1 ENM Preparation

CeO_2, $Cu(OH)_2$, and TiO_2 ENM stock suspensions were prepared by suspending dry ENM powders in 18.2 MΩ cm Nanopure water (Barnstead) and sonicating for 30 min in a bath sonicator (Branson 2510, Danbury, CT). Stock suspensions were sonicated for 10 min after dilution to the desired concentration and used within 24 hr. Suwannee River NOM stock solutions were prepared as described in Zhou and Keller (2010)[10].

3.2.2. ENM Impacts on Soil Properties

The effect of ENM contamination on soil pH were tested over a range of ENM concentrations by adding potting, grass, or farm soil with 0, 0.1, 1, 10, and 100 μg g^{-1} TiO_2, CeO_2, or $Cu(OH)_2$ ENMs with and without the addition of 10% NOM. Soil aliquots were then air dried and mixed with Nanopure water to make a 20% (by mass) soil paste from which the pH was measured. All treatments were performed in triplicate.

Changes in soil ion release due to the presence of ENMs was tested by mixing aliquots of potting, grass, or farm soil with 100 μg g^{-1} TiO_2, CeO_2, or $Cu(OH)_2$ ENMs as suspensions, centrifuging at 8000 x g for 10 min, and analyzing the supernatant for ion concentrations. NO_3^- was measured via colorimetric methods (Hach) and Al, Ca, Fe, K, Mg, Na, P, and S were measured via ICP-AES after acidification to 10% HNO_3. The influence of the three ENMs on the bioavailability and mobility of P was investigated further by contaminating agricultural, grassland, or potting soil samples with 100 μg g^{-1} ENMs and testing P content in three fractions: water extractable P, bioavailable P, and immobile (soil

bound) P. Soil aliquots were first mixed with water for 1 min, centrifuged at 8000 x g for 10 min, then the supernatant was removed and acidified to 10% HNO_3. The same soil aliquots were then mixed with Bray extract[11] for 1 min, centrifuged at 8000 x g for 10 min, then the supernatant was removed and acidified to 10% HNO_3. The soil aliquots were then acid digested in 1:3 HNO_3:HCl at 200°C for 1.5 hours in a microwave digestion system, and all samples were analyzed for P content via ICP-AES.

Soil solution extracts of potting, grassland, and farm soils were prepared following Rhoades (1982)[12], although no Na_3PO_4 was added in order to avoid influencing ENM physicochemical behavior. Soil solution extracts were stored at 4°C until use.

3.2.3. Statistical Analyses

To determine the effects of ENM contamination on the release of ions from soils, separate Dunnett's tests were used for each ion type using Nanopure-only groups as controls. Levene's test was used to ensure homogeneity of variance. Statistical analyses were performed using Microsoft Excel 2007 and the statistical software R (v. 2.11.1).

3.3. Results and Discussion

3.3.1. ENM Impacts on Soil Properties

Despite varying ENM concentrations over four orders of magnitude, changes in soil pH due to ENM contamination were largely independent of both ENM type and concentration (Figure 3.1). Contrary to the first hypothesis, changes in soil pH due to ENM contamination

did occur, but they were found to be highly dependent on soil type. All three ENMs increased grass soil pH (Fig. 3.1C), decreased farm soil pH (Fig. 3.1E), and had no effect on potting soil pH (Fig. 3.1A). Additionally, the presence of NOM had no effect on the influence of ENMs on soil pH except in the case of farm soil, where a slight buffering effect was seen (Fig. 3.1F). As nearly all changes in soil pH were independent of ENM concentration it is unlikely these ENMs directly influenced soil pH through the production of H^+/OH^- due to their amphoteric properties. One possible alternate explanation is that the ENMs increased the release of ions that act as buffering or pH-altering agents, such as Al^{3+}, Ca^{2+}, H^+, K^+, Mg^{2+}, Na^+, and OH^-, by replacing them on the mineral surfaces of the soil matrix. Since there is a limited pool of ions available for desorption in a unit of soil, changes in ion release due to ENM sorption would be relatively independent of ENM concentration beyond the point at which total sorption/desorption occurs.

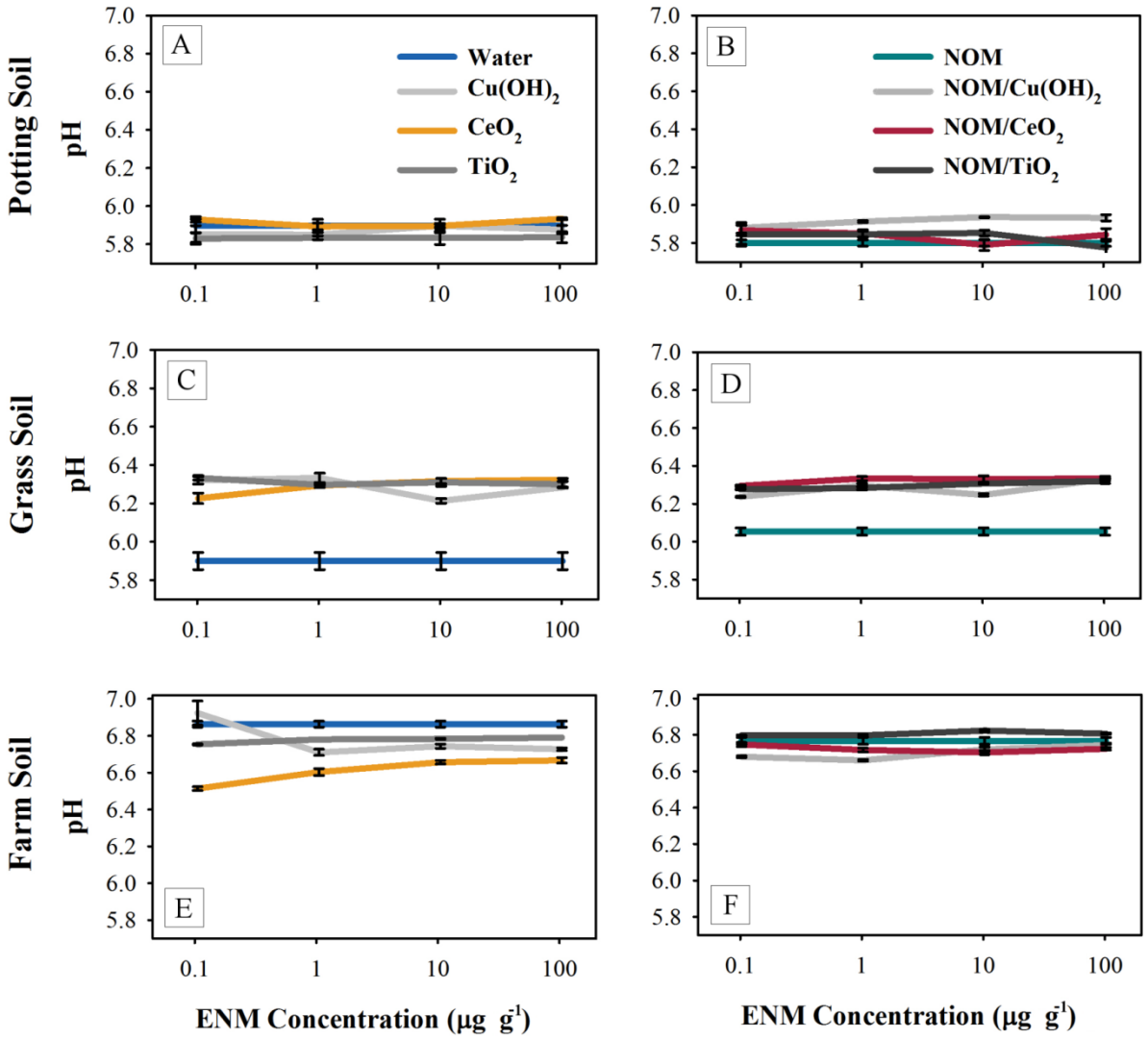

Figure 3.1. Changes in pH of potting, grass, and farm soil spiked with increasing concentrations of uncoated (A, C, E) and NOM-coated (B, D, F) TiO_2, CeO_2, and $Cu(OH)_2$ ENMs. Error bars are ± SE.

Evidence for this can be found in Figure 3.2, which reveals that, contrary to the second hypothesis, these ENMs in fact increase ion release from contaminated soils. However, the identity and amounts of ions released was dependent on soil type, with the total change in ion release for a given soil being roughly proportional to its CEC (Table 2.1). Fig. 3.2B shows that all three ENMs increase release of Mg^{2+} in grass soil, which may be the cause of the pH increases seen in grass soil (Fig. 3.1C) since Mg^{2+} is a basic cation. While no consistent corresponding changes in ion concentration were seen in farm soil, the decreases in pH may have been due to the release of H^{+} stored in the soil. The farm soil used here had relatively low amounts of basic Mg^{2+} and K^{+} and low cation exchange capacity (8.7 ± 0.1 meq 100 g^{-1}) and so has the lowest buffering capacity of the soils in this study. Potting soil had the highest concentrations of basic ions and CEC (69.2 ± 1.2 meq 100 g^{-1}) and correspondingly showed no changes in pH due to the presence of ENMs. $Cu(OH)_2$ consistently increased Na and S levels in the soil because both of these elements are major components of the soluble composite matrix the $Cu(OH)_2$ ENMs are embedded in and are released as the composite dissolves in water.

Similarly, it was found that these ENMs either had no effect or slightly increased the amount of water extractable or bioavailable P (Figure 3.3). This is likely due to the same mechanism described above, namely the replacement of PO_4^{3-} ions on soil surfaces by ENMs. Additionally, since these ENMs already possess or rapidly develop negative surface charges in soil solution (Fig. 2.3C) they will not attract negatively charged phosphate ions as readily and thus would not inhibit their mobility or bioavailability.

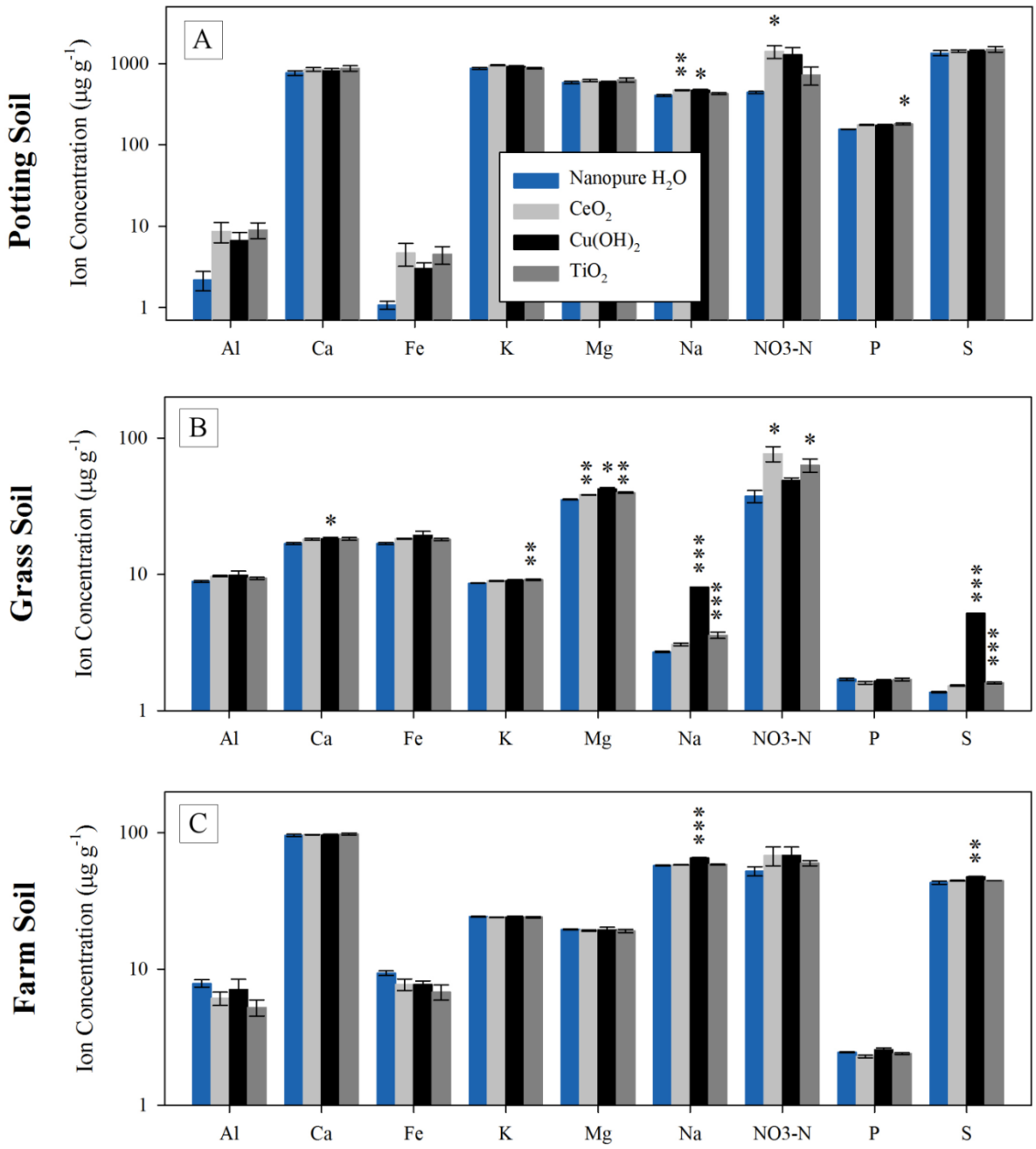

Figure 3.2. Changes in ion content of soil solutions extracted from potting, grass, and farm soil after contamination with 100 µg g^{-1} CeO_2, $Cu(OH)_2$, and TiO_2 ENMs. Asterisks represent significance differences between ion concentrations from contaminated and control soil solution extracts from Dunnett's tests. *$p < 0.05$, **$p < 0.01$, ***$p < 0.005$. Error bars are ± SE. Note variable y-axis.

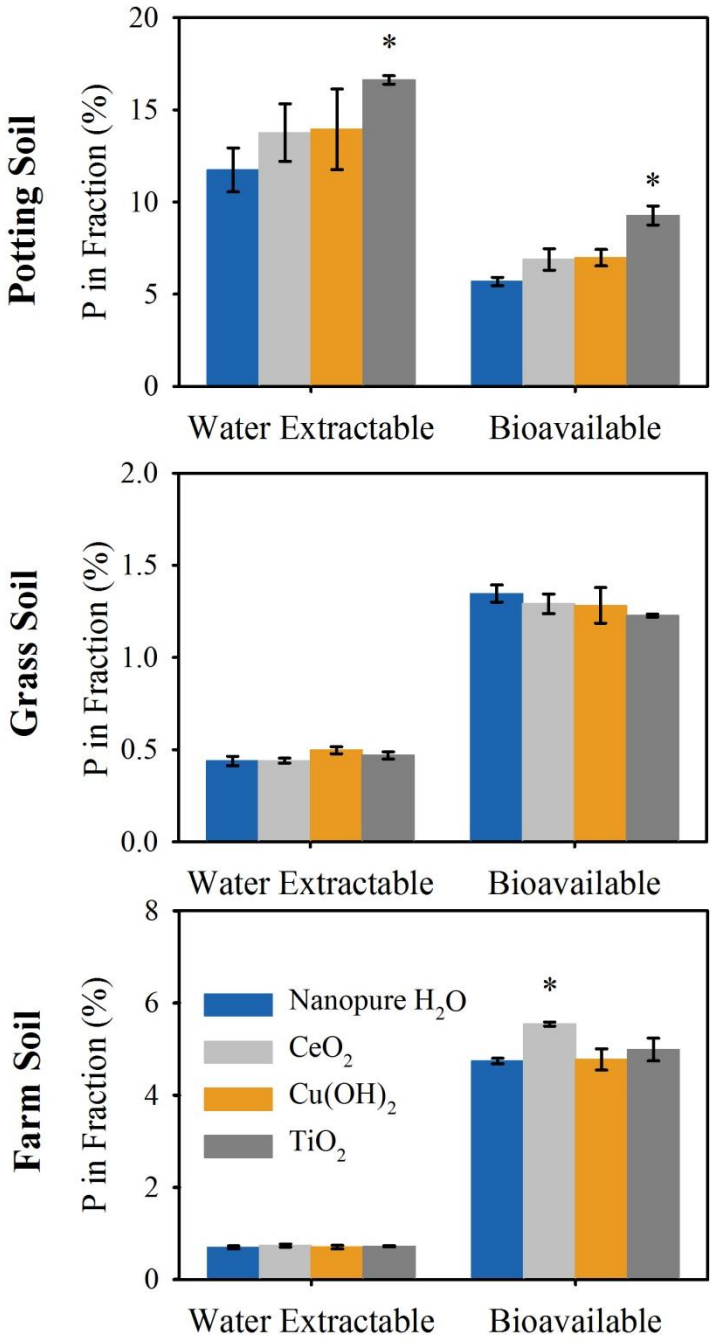

Figure 3.3. Changes in water extractable and bioavailable P fractions from potting soil, grass soil, and farm soil contaminated with CeO_2, $Cu(OH)_2$, and TiO_2. Asterisks represent significance differences between ENM treatments and Nanopure H_2O controls from Dunnett's tests. *$p < 0.05$. Error bars are ± SE. Note variable y-axis.

3.4. Conclusions

Here, I show that ENM contamination even at parts per billion concentrations could influence soil pH by enhancing ion release from the soil, although the effect was relatively minor and highly dependent on soil properties. However, this may have implications as both soil pH and nutrient availability are critical for many soil organisms. Soil pH is known to influence a wide range of soil properties, from mineral structure[13] to enzyme activity[14] to rhizobial bacterial communities,[15] and so ENM contamination may have any number of consequences for a given soil community. In addition to the implications for soil pH, enhancing the release of ions may have the effect of improving accessibility to these nutrients by organisms in the short term but may also increase the rate at which they are washed from the soil by rainfall or irrigation, resulting in increased nutrient loss and decreased productivity over time. This could eventually result in nutrient limitation, which in agricultural settings may have undesired economic impacts due to decreased crop yields or increased fertilizer demand.

3.5. References

1. Ben-Moshe, T.; Frenk, S.; Dror, I.; Minz, D.; Berkowitz, B., Effects of Metal Oxide Nanoparticles on Soil Properties. *Chemosphere* **2013,** *90*, (2), 640-646.
2. Cesco, S.; Mimmo, T.; Tonon, G.; Tomasi, N.; Pinton, R.; Terzano, R.; Neumann, G.; Weisskopf, L.; Renella, G.; Landi, L.; Nannipieri, P., Plant-Borne Flavonoids Released into the Rhizosphere: Impact on Soil Bio-Activities Related to Plant Nutrition. A Review. *Biology and Fertility of Soils* **2012,** *48*, (2), 123-149.
3. Ge, Y. G.; Schimel, J. P.; Holden, P. A., Evidence for Negative Effects of Tio2 and Zno Nanoparticles on Soil Bacterial Communities. *Environ. Sci. Technol.* **2011,** *45*, (4), 1659-1664.
4. Collins, D.; Luxton, T.; Kumar, N.; Shah, S.; Walker, V. K.; Shah, V., Assessing the Impact of Copper and Zinc Oxide Nanoparticles on Soil: A Field Study. *PLoS One* **2012,** *7*, (8).
5. VandeVoort, A. R.; Skipper, H.; Arai, Y., Macroscopic Assessment of Nanosilver Toxicity to Soil Denitrification Kinetics. *J. Environ. Qual.* **2014,** *43*, (4), 1424-1430.
6. Boehm, H. P., Acidic and Basic Properties of Hydroxylated Metal Oxide Surfaces. *Discussions of the Faraday Society* **1971,** *52*, (0), 264-275.
7. Horst, A. M.; Neal, A. C.; Mielke, R. E.; Sislian, P. R.; Suh, W. H.; Maedler, L.; Stucky, G. D.; Holden, P. A., Dispersion of Tio2 Nanoparticle Agglomerates by Pseudomonas Aeruginosa. *Appl. Environ. Microbiol.* **2010,** *76*, (21), 7292-7298.
8. Grand, S.; Lavkulich, L. M., Short-Range Order Mineral Phases Control the Distribution of Important Macronutrients in Coarse-Textured Forest Soils of Coastal British Columbia, Canada. *Plant Soil* **2015,** *390*, (1-2), 77-93.
9. Daou, T. J.; Begin-Colin, S.; Grenèche, J. M.; Thomas, F.; Derory, A.; Bernhardt, P.; Legaré, P.; Pourroy, G., Phosphate Adsorption Properties of Magnetite-Based Nanoparticles. *Chem. Mat.* **2007,** *19*, (18), 4494-4505.
10. Zhou, D.; Keller, A. A., Role of Morphology in the Aggregation Kinetics of Zno Nanoparticles. *Water Res.* **2010,** *44*, (9), 2948-2956.
11. Bray, R. H.; Kurtz, L. T., Determination of Total, Organic, and Available Forms of Phosphorous in Soils. *Soil Sci.* **1945,** *59*, (1), 39-45.
12. Rhoades, J., Soluble Salts. In *Methods of Soil Analysis: Part 2: Chemical and Microbiological Properties.*, 2nd ed.; Page, A., Ed. ASA: Madison, WI, 1982.
13. Brady, N. C.; Weil, R. R., *Elements of the Nature and Properties of Soils*. 13th ed.; Pearson Education Ltd.: Upper Saddle River, New Jersey, 2002.
14. Acosta-Martinez, V.; Tabatabai, M. A., Enzyme Activities in a Limed Agricultural Soil. *Biology and Fertility of Soils* **2000,** *31*, (1), 85-91.
15. Marschner, P.; Crowley, D.; Yang, C. H., Development of Specific Rhizosphere Bacterial Communities in Relation to Plant Species, Nutrition and Soil Type. *Plant Soil* **2004,** *261*, (1-2), 199-208.

4. Uptake and Translocation of Engineered Nanomaterials in Soil-Grown Plants

4.1. Introduction

Given the range of sizes, morphologies, and chemical properties they encompass, ENMs may be taken up into plant root tissues and transported through the vascular system in several ways. It has been known for some time that metal ions can be transported both apoplastically[1] and symplastically[2] in plants, but it has only been fairly recently that more definite mechanisms of ENM transport between different plant tissues have been put forth and tested (e.g., Larue, et al. (2012)[3]). One of the key barriers in plant roots that play a role in uptake is the Casparian strip (CS), a hydrophilic thickening of the primary cell wall and middle lamella of root cells in the endodermis that is composed primarily of lignin. The CS blocks apoplastic flow into the cortex and vascular bundle and so water and ions must either penetrate the cellular membranes of these endodermal cells or flow symplastically through plasmodesmata in order to reach the xylem and phloem and so be transported throughout the plant.[4] Another possible pathway for ENMs to penetrate into the vascular bundle is to enter through the root tip, which does not have a CS.

This has implications for the uptake of ENMs by plant roots, for if ENMs are bound in aggregates or complexes, or if their primary particle size is above a certain threshold, they will not be able to pass through endodermal cell pores (averaging 5-20 nm in diameter)[5, 6] or plasmodesmata (averaging 30-60 nm).[4] Reports of ENM uptake in both soil and hydroponic

systems vary[7-11] and likely depend on the interaction of several factors, including ENM composition, crystal structure, primary particle size, and coating, as well as plant type, soil composition, and solution chemistry. Under most conditions, ENMs in any solution rapidly aggregate to tens, hundreds, or even thousands times their primary particle size.[12, 13] However, there are three possible mechanisms by which ENMs could reach sizes small enough to pass through the barriers listed above.

Plant roots are known to release protons to free Ca^{2+} and Mg^{2+} ions from clays[4] and so may locally decrease the pH of the soil solution. This could potentially cause the release of primary particles from ENM aggregates by a similar mechanism. Alternately, free ENM primary particles likely exist in equilibrium with ENMs in aggregates[14] and so there may be a small fraction of particles that will be bioavailable at all times. A third possible mechanism is that ENMs will be coated and dispersed by natural organic matter (NOM) such as humic or fulvic acids[15] or inorganic substances like phosphate[16] and so be more bioavailable. However, Schwabe, et al. (2013)[17] found that coating CeO_2 ENMs with fulvic acid *decreased* their uptake into pumpkin shoots grown hydroponically, which may be due to increased aggregate size of NOM-coated particles (see Chapter 2).

Research on plant uptake of ENMs dates back less than a decade,[18] so as of yet these mechanisms are largely hypothetical. However, Sabo-Attwood, et al. (2012)[19] found Au ENMs above a size limit (18 nm) were excluded from vascular tissue in tobacco plants, which lends support to the hypothesis that particles must be small enough to pass through cell pores or plasmodesmata to enter the cortex. Similarly, Larue, et al. (2012)[3] found that TiO_2 ENMs above 140 nm did not accumulate in root tissues, those above 36 nm did not enter the cortex, but that ENMs 14 nm in diameter were able to pass through the CS, enter

the vascular tissue, and be translocated throughout the plant. Judy, et al. (2012)[20] found that uptake can be species-dependent, as citrate and tannate coated Au ENMs were taken up in tobacco but not wheat.

One aspect of plant/ENM interactions that has as yet received little attention is the influence of abiotic environmental conditions on plant uptake and translocation of ENMs. These include factors such as water and nutrient availability, temperature, soil salinity and pH, and light intensity. Plant performance depends heavily on environmental conditions, as physiological processes adapt to conditions that may be more or less favorable to growth. This has been shown for several non-nano pollutants. For example, high light intensities resulted in higher concentrations of As[21] and Cd[22] in sunflower and duckweed due to increased transpiration. Additionally, it was found in pea seedlings that nutrient stress (Fe depletion) increased the expression of transporter proteins that, in turn, increase cellular uptake of metals such as Cd.[23]

In these experiments I investigated the uptake and translocation of three metal oxide ENMs, CeO_2, TiO_2, and $Cu(OH)_2$, in soil-grown *Clarkia unguiculata* (Onagraceae), radish (*Raphanus sativus*), and wheat (*Triticum aestivum*) in different soils, illumination, and/or nutrient levels. In the first part of this study, *C. unguiculata* were grown in potting soil under different light and nutrient levels and exposed to a range of ENM concentrations in order to discern how uptake trends depend on soil ENM content. In the second part of this study *C. unguiculata* was again used as a model organism, but was grown in two natural soils under different light levels to gain insight into how soil properties influence ENM uptake. Finally, two crop plants were grown in natural soils to see how the trends seen in *C. unguiculata* vary with plant species.

Radishes and wheat were selected as model crop plants representing the two major groups of angiosperms, Dicots and Monocots. Additionally, they have edible parts arising from different tissue types, which may influence ENM accumulation; namely, the radish hypocotyl is derived from the stem while wheat grains arise from reproductive tissue. *C. unguiculata* is an annual wildflower often used in ecological and genetic studies, and was selected here for its ease of growth, distinct tissues, and moderate lifespan (10-12 weeks) that would allow for subchronic effects to be detected. I used *C. unguiculata* individuals from wild populations with greater genetic variability[24] than crop plants typically used in nanotoxicological studies,[3, 9, 10] which may mean results seen in this model organism are conservative with respect to detecting the effects of ENM exposure on plant uptake and performance.

Here, I hypothesized that ENM uptake and distribution would vary between plant and soil type due to differences in plant physiology and ENM behavior, but that ENMs would in general be found in highest concentrations in the roots as the point of uptake, followed by leaves as the endpoint of transpiration, then stems as an intermediary between the two. Second, I predicted that plants grown in high light would uptake and accumulate higher concentrations of ENMs in leaves due to higher rates of transpiration.[21] Third, I hypothesized that P would be positively correlated with ENM concentration in tissues due to sorption of phosphate from the soil. Natural metal oxides such as clays are known to strongly and preferentially sorb phosphate over other organic and inorganic ligands,[25] and research has shown that metal oxide ENMs can also sorb phosphorous and thereby potentially affect its bioavailability in soils and other environmental media.[26]

4.2. Methods

4.2.1. ENM Preparation

Stock suspensions of TiO_2, CeO_2, and $Cu(OH)_2$ ENMs (Table 1.1) were prepared for each application as 1 g L^{-1} and bath sonicated for 30 minutes. Stocks were then diluted to 1, 10, and 100 mg L^{-1}. Dilutions were not re-sonicated.

4.2.2. Plant Exposure and Growth Conditions

Clarkia unguiculata is an annual hermaphroditic flowering shrub native to oak/pine woodlands and disturbed slopes in central California. Additional details can be found in Dudley, et al. (2007)[27] and Vasek (1965)[24]. Seeds were collected from a field site in Kern County, CA (35° 41.453' N, 118° 43.911' W, elev. 2830 ft) in July 2008 and stored with desiccant in darkness at 4°C until use. Seeds were randomly sampled from ten maternal families, plated on agar in covered Petri dishes (8 g L^{-1}), vernalized in darkness for 5 days at 4°C, and then germinated under ambient light at room temperature for an additional 5 days. Seedlings were then transplanted into 2.5 cm diameter x 16.34 cm long cylindrical plastic growing tubes (Ray Leach Cone-tainers; Stuewe and Sons, Tangent, Oregon) (one seedling per tube) containing 17 ± 0.1 g of a 1:20 mixture of worm castings to a peat moss/perlite/dolomitic limestone potting soil (Sunshine Mix #4, Sun Gro Horticulture), 136 ± 1 g grass soil, or 167 ± 1 g farm soil. Soil properties other than Ce, Ti, and Cu content were measured at the UC Davis Analytical Lab (http://anlab.ucdavis.edu/) and are shown in Table 1.2. After transplantation, seedlings were kept moist and allowed to grow for 2.5 weeks before ENM exposure to allow them to become established, after which they were

grown for an additional 8 weeks until they had completed their life cycle. *C. unguiculata* plants were grown in growth chambers with a 14:10 hr 21:13°C day:night cycle under two light levels, 500 (high, H) or 50 (low, L) $\mu mol_{photon}\ m^{-2}\ s^{-1}$. These light conditions are roughly analogous to those on a partly cloudy day or a shaded understory.

In addition to being exposed to two light intensities, *C. unguiculata* grown in potting soil were also exposed to two different nutrient levels for a total of four distinct growth conditions: high light and excess nutrients (HE), high light and limited nutrients (HL), low light and excess nutrients (LE), and low light and limited nutrients (LL). Excess nutrient conditions were achieved through the addition of 140 ± 3 mg fertilizer pellets (19-6-12 Osmocote Smart Release Indoor & Outdoor Plant Food) prior to seedling transplantation, corresponding to 70.7 ± 1.5 mg NH_3 per L soil, 63.6 ± 1.5 mg L^{-1} NO_3, 42.4 ± 1.0 mg L^{-1} P_2O_5, and 84.8 ± 2.0 mg L^{-1} K_2O released over the course of the experiment. Plants grown with limited nutrient conditions did not receive fertilizer.

Starting in the second week of growth, 50 mL of 0, 1, 10, or 100 mg L^{-1} TiO_2, CeO_2, or $Cu(OH)_2$ suspensions were slowly poured onto the soil surface of each individual container to allow for absorption into the soil. This was repeated weekly for a total of 8 weeks to result in a soil contamination rate of 0, 0.25, 2.5, or 25 mg ENM per L soil per week, or 0, 2.9, 29, or 290 mg kg^{-1} wk^{-1}. Volumetric units are used here to describe soil ENM concentrations in order to provide comparable results for all three soils despite the large difference in density between potting soil and the two natural soils. *C. unguiculata* grown in natural (grass and farm) soils only received 50 mL of 0 or 100 mg L^{-1} TiO_2, CeO_2, or $Cu(OH)_2$ suspensions per week for soil contamination rates of 0 or 25 mg ENM L^{-1} wk^{-1}.

Cherry radish (*Raphanus sativum*) and Hard Red Spring wheat (*Triticum aestivum*) seeds were purchased from Seeds of Change (Rancho Dominuguez, CA, USA) and Salt Spring Seeds (Salt Spring Island, BC, Canada), respectively, and stored in darkness at 4°C until use. Radish seeds were planted in square, 4 inch Tech-Square pots (McConkey & Company) filled with 600 ± 1 g farm soil and wheat seeds were planted in cylindrical plastic growing tubes filled with 136 ± 1 g grass soil. Radish and wheat seeds were germinated under ambient light at room temperature for 3 days before being moved to growth chambers under 500 (high, H) or 50 (low, L) $\mu mol_{photon}\ m^{-2}\ s^{-1}$. After 1 week of growth radish and wheat individuals received 0 or 25 mg ENM $L^{-1}\ wk^{-1}$ as suspensions for the duration of their life cycles.

Four replicates were grown per plant species, ENM, light condition, soil type (for *C. unguiculata*), and concentration and nutrient level (for *C. unguiculata* in potting soil), and five control replicates were grown per species, light condition, nutrient level, or soil type that were not exposed to ENMs for a total of 300 individuals.

4.2.3. Elemental Analysis

C. unguiculata, wheat, and radish plants were sacrificed and tissue samples were collected after 10, 8, or 5 weeks of growth, respectively. For *C. unguiculata* and wheat, several leaves were collected at different heights and 5-6 cm segments of stem were taken from the middle of each plant and analyzed separately. All wheat grains were collected from each plant and analyzed together. For radishes, the largest leaf from each plant was collected and analyzed, along with a 1 cm thick cross-section of the hypocotyl. Roots from all three plants were thoroughly cleaned of any visible soil particles and were serially rinsed in clean

baths of deionized water and 2% HNO_3 before analysis to facilitate removal of adsorbed ENMs on the root surfaces. Plant and soil metal characterization samples were vacuum dried at 60°C for 3 days, weighed, and digested in aqua regia (1:3 HNO_3:HCl) in a microwave digestion system (Multiwave Eco, Anton Paar) at 200°C for 1.5 hours. Samples were then analyzed for Ti, Ce, Cu, and P via inductively coupled plasma atomic emission spectroscopy (ICP-AES, iCAP 6300 Thermo Scientific, Waltham, MA). Detection limits for all elements tested were approximately 5 µg L^{-1}. Standard solutions and blanks were measured every 15-20 samples for quality assurance.

Tissue metal concentrations for all three ENMs are reported as ionic, although neither CeO_2 nor TiO_2 were expected to dissolve to a significant degree under the conditions used in this experiment. TiO_2 is known to be highly insoluble in water and CeO_2 is similarly insoluble at pHs similar to those found in the soils used here.[28] Additionally, both ENMs have been found to be taken up into a variety of plant species in nanoparticulate form.[3, 29-31] However, the $Cu(OH)_2$ ENM used here is known to undergo partial dissolution under acidic conditions (up to 25-35% over 90 days)[13, 32] and will likely be at least partially present either as ionic Cu^{1+}/Cu^{2+} or as part of a complex with ions from the surrounding media.

4.2.4. Statistical Analysis

For *C. unguiculata* grown in potting soil, multiple regressions were used to model the effects of Soil ENM Concentration, Light Level, Nutrient Level, Tissue Type, and the interactions between these variables on Tissue Metal Concentrations for each ENM. For *C. unguiculata* grown in natural soils, 3-way ANOVA with interactions and post-hoc Tukey's tests were used to determine the effects of Soil Type, Light Level, and Soil ENM

Concentration on Tissue Metal Concentrations for each tissue and ENM. Two-way ANOVA with interactions and post-hoc Tukey's tests were used for radishes and wheat to determine the effects of Light Level and Soil ENM Concentration on Tissue Metal Concentration for each species, tissue, and ENM. Exceptions were made in the case of radish hypocotyls and wheat grains, where 1-way ANOVA were used because these tissues had not developed in the low light condition. Linear regressions were used to determine relationships between Tissue Metal Concentration and Tissue P Concentration for a given treatment. Levene's test was used to ensure homogeneity of variance. Statistical analyses were performed using Microsoft Excel 2007 and the statistical software R (v. 2.11.1).

4.3. Results and Discussion

4.3.1. ENM Uptake and Translocation in *Clarkia unguiculata*

4.3.1.1. *C. unguiculata* in Potting Soil

Metals from ENMs were taken up into all tissues in all treatments, although the amounts depended on ENM type, soil ENM concentrations, growth condition (high light and excess nutrient (HE), high light and limited nutrient (HL), low light and excess nutrient (LE), and low light and limited nutrient (LL)), and tissue type. Mean tissue metal concentrations of *C. unguiculata* grown in potting soil can be seen in Figure 4.1 and results from multiple regressions can be seen in Figures 4.2-4.4 and Table 4.1. In general, Ce and Ti were found in highest concentration in roots (Fig. 4.1C & 4.1F) while Cu was primarily found in leaves

(Fig. 4.1G), although relatively high concentrations of Ti were also seen in stems (Fig. 4.1E). Background concentrations of Ti and Cu were found in all three tissues, while background Ce was only found in roots. Among individuals in the Control group (those exposed to no supplemental nanoparticles), it is likely that Ce was not found in stems or leaves because it was not present in the soil at concentrations as high as Ti (Table 1.2), nor is it an essential micronutrient as is Cu.

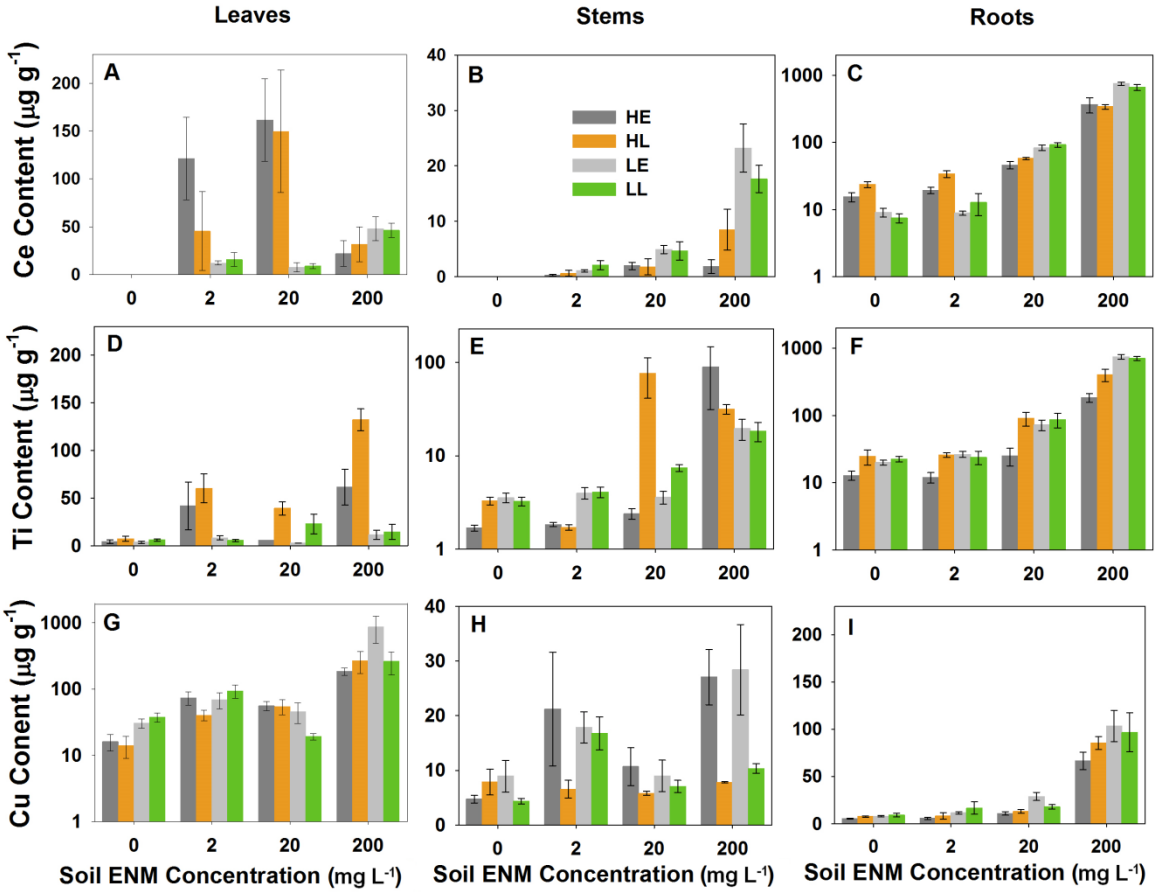

Figure 4.1. Tissue metal concentration of *C. unguiculata* grown in potting soil under high light excess nutrient (HE), high light limited nutrient (HL), low light excess nutrient (LE), and low light limited nutrient (LL) conditions. A-C show Ce content of leaves, stems, and roots from CeO_2 –exposed plants; D-F show Ti content of leaves, stems, and roots from TiO_2 –exposed plants; G-I show Cu content of leaves, stems, and roots from $Cu(OH)_2$ –exposed plants. Error bars are ±SE.

Of the three ENMs to which plants were exposed, those exposed to CeO_2 and TiO_2 followed the pattern of distribution described in my first hypothesis, with concentrations being consistently highest in the roots followed by leaves then stems (Fig. 4.1A-4.1F). In $Cu(OH)_2$-exposed plants, however, Cu concentrations were roughly an order of magnitude higher in leaves than in roots (Fig. 4.1G-4.1I). Plants from all groups showed statistically significant positive correlations between exposure concentration and metal concentration in roots (multiple regressions in Table 4.1, $p < 0.05$) and, with a few exceptions, tended to have

the highest metal concentrations at the highest exposure level in all tissues. The most notable exceptions to this trend are the variable Ce and Ti content of leaves from plants grown under high light, excess nutrient (HE) and high light, limited nutrient conditions (HL) (Fig. 4.1A & 4.1D). This reflects the high inter-leaf metal content variability for Ce and Ti and may be due to a randomized or patchy accumulation of these nanoparticles between leaves. There were no significant associations between leaf metal content and leaf node number, which is indicative of order of production (linear regressions, $p > 0.05$; data not shown). Since *C. unguiculata* leaves are produced in a temporal sequence along the height of the plant and are also larger lower on the plant, this indicates that ENM uptake into leaves was independent of both stage of growth and leaf size.

Table 4.1. Results of multiple regression for three models using Soil ENM Concentration (0, 2, 20, and 200 mg L^{-1}), Light Level (50 and 500 μmol_{photon} m^{-2} s^{-1}), Nutrient Level (Excess and Limited), Tissue Type (Leaf, Stem, and Root), and the interactions between these variable to predict Ce, Ti, or Cu concentrations in plants exposed to CeO_2, TiO_2, or $Cu(OH)_2$, respectively. Soil ENM Concentration and Light Level were modeled as continuous variable and Nutrient Level and Tissue Type were modeled as categorical variables. Values in parentheses indicate standard errors (SE) for regression correlation coefficients. Coefficient significance levels are indicated by asterisks: *$p < 0.05$, **$p < 0.01$, and ***$p < 0.001$. Interactions that did not significantly predict plant metal concentration in one or more models are omitted here.

	Ce (µg g^{-1})		Ti (µg g^{-1})		Cu (µg g^{-1})	
Regression Parameter	**Coefficient**	**(SE)**	**Coefficient**	**(SE)**	**Coefficient**	**(SE)**
Intercept	-0.8601	(6.286)	3.681	(4.888)	28.22	(36.54)
Soil ENM Concentration (mg L^{-1})	0.2538***	(0.0695)	0.01092	(0.04880)	4.579**	(0.416)
Light Level (μmol_{photon} m^{-2} s^{-1}) ($x10^{-2}$)	3.839*	(1.96)	0.842	(1.573)	-0.92	(12.09)
Nutrient Level (Limited)	-0.9946	(8.89)	2.854	(6.644)	12.84	(51.41)
Tissue Type (Root)	8.292	(10.33)	14.54	(7.88)	-18.03	(60.34)
Tissue Type (Stem)	5.021	(10.43)	0.030	(7.885)	-18.09	(60.97)
Conc. : Light ($x10^{-3}$)	-0.3822	(0.2576)	0.5153***	(0.1549)	-7.544***	(1.255)
Conc. : Nutrient (L)	-0.01270	(0.09320)	-0.03375	(0.07231)	-3.480***	(0.562)
Conc. : Tissue (R)	3.664***	(0.141)	3.947***	(0.104)	-4.087***	(0.829)
Conc. : Tissue (S)	-0.1474	(0.1411)	0.0291	(0.1156)	-4.489***	(0.830)
Conc. : Light : Nutrient (L) ($x10^{-3}$)	0.0498	(0.3596)	0.7436**	(0.2414)	7.861***	(1.939)
Conc. : Light : Tissue (R) ($x10^{-3}$)	-3.940***	(0.430)	-6.714***	(0.303)	7.171**	(2.376)
Conc. : Light : Tissue (S) ($x10^{-3}$)	0.1879	(0.4500)	0.2859	(0.3187)	7.563**	(2.380)
Conc. : Nutrient (L) : Tissue (R)	-0.4631*	(0.1965)	-0.3289*	(0.1492)	3.426**	(1.159)
Conc. : Nutrient (L) : Tissue (S)	-0.02006	(0.1969)	0.0627	(0.1573)	3.415**	(1.161)
Conc. : Light : Nutrient (L) : Tissue (R) ($x10^{-3}$)	0.5441	(0.6055)	2.065***	(0.440)	-7.586*	(3.451)
Conc. : Light : Nutrient (L) : Tissue (S) ($x10^{-3}$)	0.0813	(0.6201)	-1.421**	(0.451)	-7.963*	(3.540)
Model Parameters						
***p*-value**	< 2.2E-16		< 2.2E-16		< 2.2E-16	
R^2	0.85		0.9093		0.2386	
Degrees of Freedom	483		483		483	

Growth conditions also played a role in ENM uptake, with plants grown under high light accumulating more Ce and Ti in their leaves than those grown in low light (Fig. 4.2A, Fig. 4.3B, Table 4.1, multiple regressions, $p < 0.001$) and HL leaves accumulating more Ti than HE (Fig. 4.3A, Table 4.1, multiple regressions, $p < 0.01$). Along with the increased transpiration rates seen in plants grown under high light (discussed in Section 5), these findings validate my second hypothesis that plants exposed to high light would exhibit elevated uptake of ENMs to leaves due to increased transpiration. However, increased uptake of Cu into leaves and roots was found under low light conditions (Figure 4.4). These differences among ENM types in uptake and distribution are also likely to be due to differences in particle characteristics, particularly morphology and surface charge. The CeO_2 ENMs used here had a moderately high aspect ratio (Table 1.1) and thus had a smaller minimum dimension, which may allow them to pass through narrow vascular tissues in the stem more easily than the spherical TiO_2. Due to this physical size limitation, TiO_2 may also aggregate in the conductive tissues of the stems at higher concentrations, causing the buildup seen in Figure 4.1.

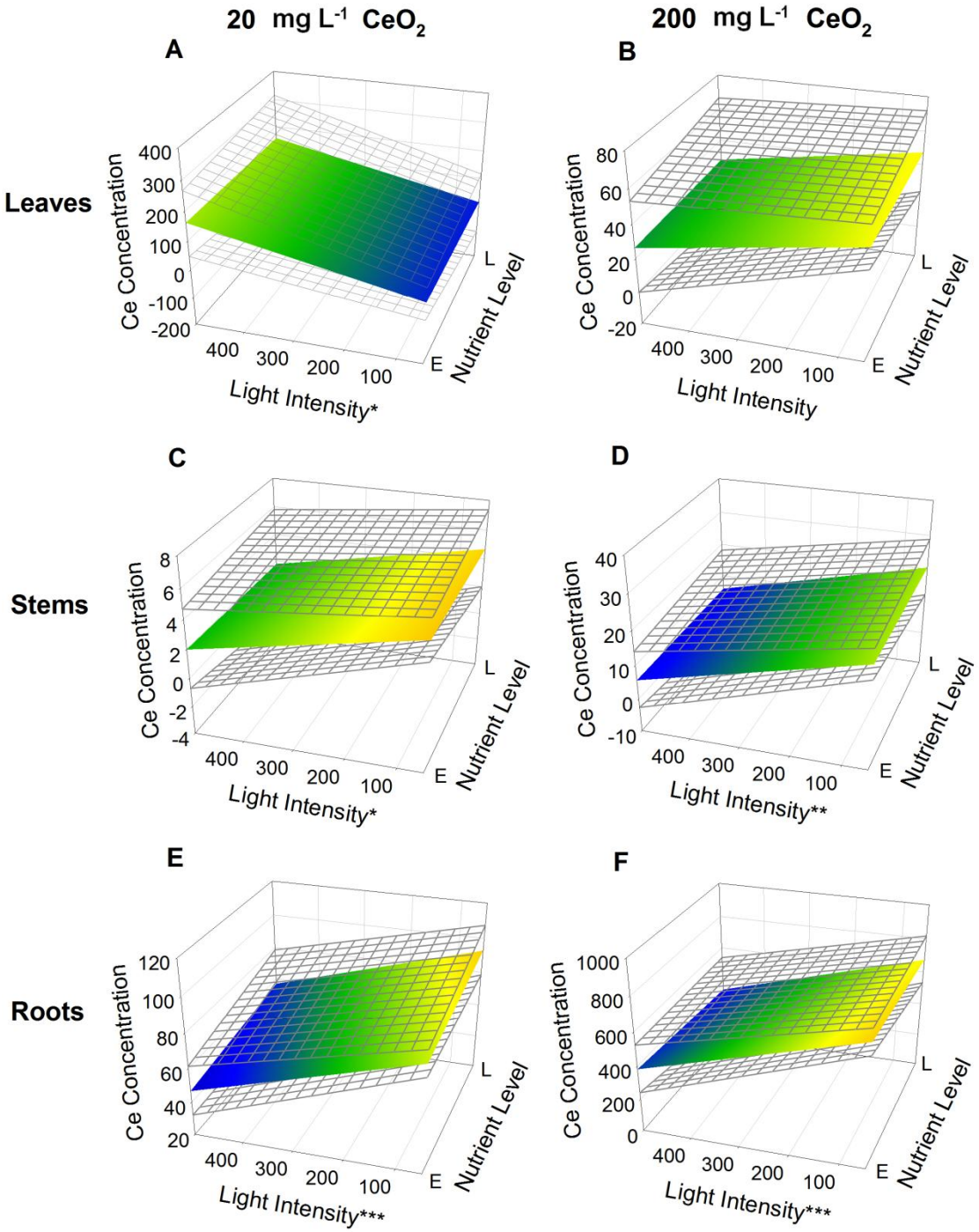

Figure 4.2. Predicted Ce concentrations (µg g^{-1}) in leaves, stems, and roots at 20 and 200 mg L^{-1} Soil CeO_2 Concentrations based on multiple regression results presented in Table 4.1. The lowest exposure concentrations were omitted for clarity. Cooler colors signify lower metal concentrations while warmer colors signify higher metal concentrations. Transparent planes represent ±1 SE. If Light Intensity (µmol_{photon} m^{-2} s^{-1}) or Nutrient Level (excess [E] or limited [L], defined in text) had a significant effect on tissue Ce Concentration, the corresponding axis label is marked with an asterisk. *$p < 0.05$, **$p < 0.01$, ***$p < 0.001$.

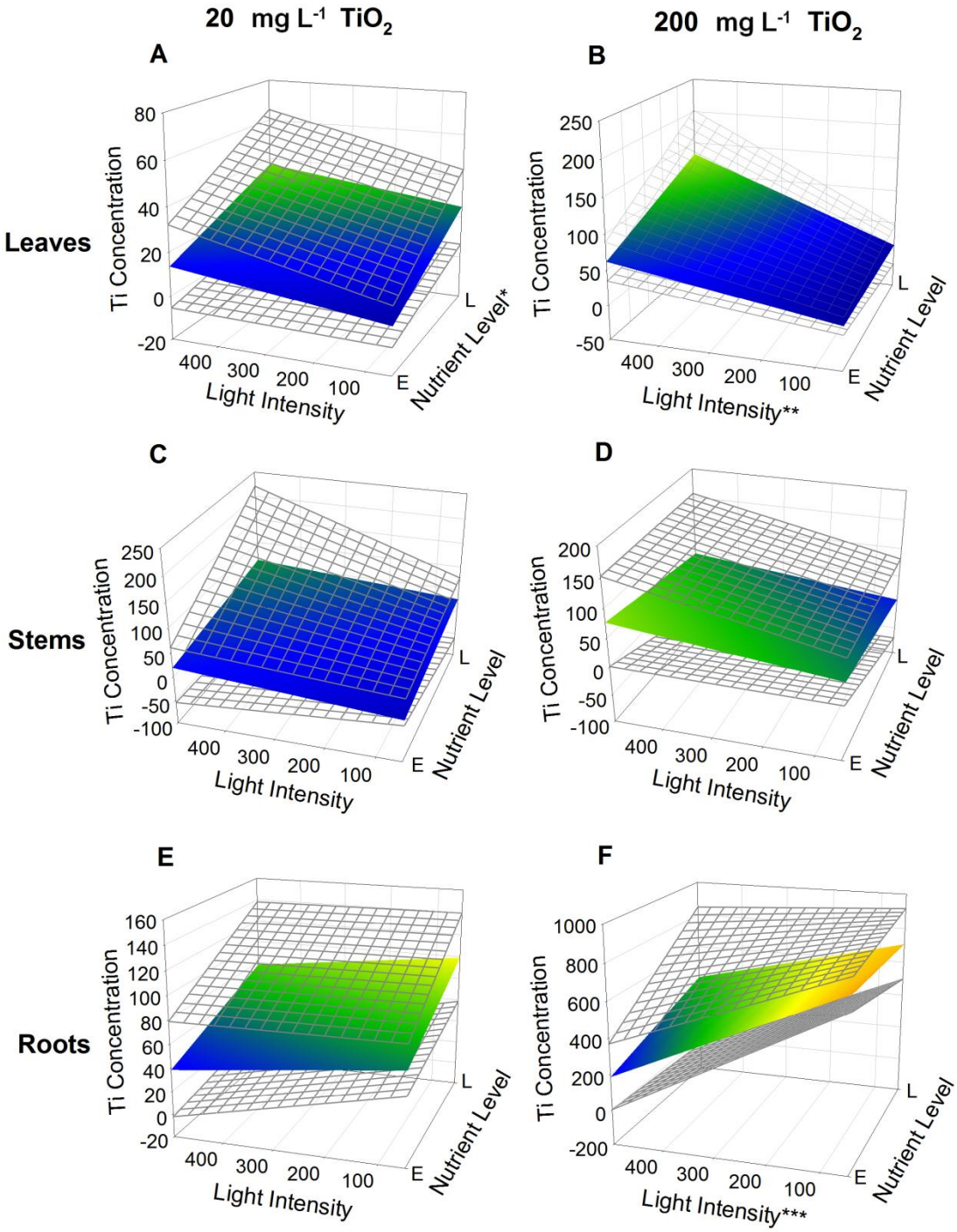

Figure 4.3. Predicted Ti concentrations (µg g^{-1}) in leaves, stems, and roots at 20 and 200 mg L^{-1} Soil TiO_2 Concentrations based on multiple regression results presented in Table 4.1. The lowest exposure concentrations were omitted for clarity. Cooler colors signify lower metal concentrations while warmer colors signify higher metal concentrations. Transparent planes represent ±1 SE. If Light Intensity (μmol_{photon} m^{-2} s^{-1}) or Nutrient Level (excess [E] or limited [L], defined in text) had a significant effect on tissue Ti Concentration, the corresponding axis label is marked with an asterisk. *$p < 0.05$, **$p < 0.01$, ***$p < 0.001$.

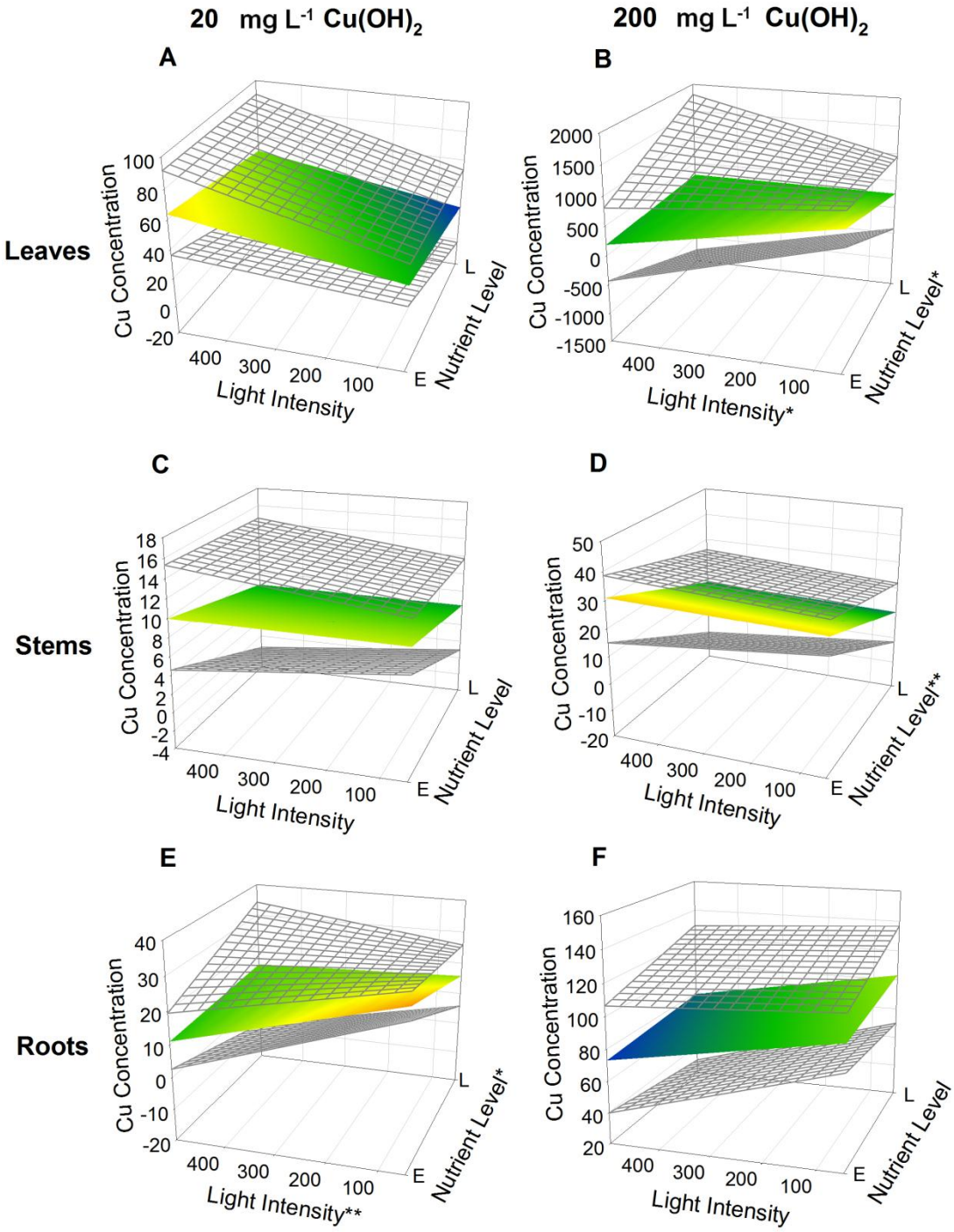

Figure 4.4. Predicted Cu concentrations (µg g^{-1}) in leaves, stems, and roots at 20 and 200 mg L^{-1} Soil $Cu(OH)_2$ Concentrations based on multiple regression results presented in Table 4.1. The lowest exposure concentrations were omitted for clarity. Cooler colors signify lower metal concentrations while warmer colors signify higher metal concentrations. Transparent planes represent ±1 SE. If Light Intensity (μmol_{photon} m^{-2} s^{-1}) or Nutrient Level (excess [E] or limited [L], defined in text) had a significant effect on tissue Cu Concentration, the corresponding axis label is marked with an asterisk. *$p < 0.05$, **$p < 0.01$.

Particle charge likely plays a large role in determining distribution as well. Figures 2.3C-D shows that all three ENMs used here had a weak negative charge in potting soil pore solution, although this was likely due to the high ionic strength and organic content of this soil shielding the particle surfaces and not a result of a direct alteration of the ENM crystal surface. Wang, et al. (2014)[33] and Zhu, et al. (2012)[34] found that under hydroponic conditions, well-dispersed particles coated with positively charged polymers (ζ-pot. ≈ +20 mV) are more readily taken up into plant roots compared to those coated with negatively charged polymers (ζ-pot. ≈ -20 mV), which had higher accumulation in leaves. The results seen here provide confirmation of the importance of surface charge in ENM uptake and distribution in plants under more environmentally relevant conditions, i.e., in soil and with polydisperse ENMs.

In addition to its surface charge, the tendency of $Cu(OH)_2$ to dissolve at low pH,[13, 32] such as is found in the soil used in this study (Table 1.2), likely also contributes to its uptake behavior. Rhizosphere pH tends to be more acidic than the surrounding soil due to the release of protons by roots to stimulate and counterbalance the uptake of ions from the soil;[35] one effect of this acidity may be to dissolve a portion of the $Cu(OH)_2$. Dissolved Cu would, in turn, encounter less size exclusion than ENMs and be retained less in the roots and stems in addition to being actively transported to the leaves. Although Cu is an essential component of several enzymes and other compounds in chloroplasts and mitochondria,[4] it can be toxic at higher concentrations.[36]

Lastly, although I predicted that P would be correlated with metal content in tissues due to physicochemical sorption of phosphate to the ENMs, it was only in root tissue of HL plants exposed to CeO_2 ENMs that a relationship was found. At root Ce concentrations

below 100 µg g^{-1}, P was positively associated with Ce (linear regression, $R^2 = 0.870$, $p < 0.005$), but this trend plateaued at higher concentrations. One possible explanation for this is that CeO_2 ENMs adsorbed P from the soil and were then sorbed into/onto the plant roots, but at higher exposure concentrations the soil was depleted of readily available P for the ENMs to adsorb. Previous studies using hydroponic systems have shown increased P uptake in maize exposed to ZnO ENMs[37] and in spinach exposed to nZVI,[38] although these results were due to the uptake of dissolved metal/phosphate complexes rather than ENM-sorbed P. Rui, et al. (2015)[39] observed the partial transformation of CeO_2 ENMs into particulate $CePO_4$ that were then taken up into hydroponically-grown cucumber seedlings, although the general lack of correlation between tissue Ce and P concentrations suggests this process was not occurring to a significant extent in this study.

4.3.1.2. *C. unguiculata* in Natural Soils

Tissue metal concentrations of *C. unguiculata* grown in farm and grass soil were found to vary with ENM, soil, light level, concentration, and tissue type (Figure 4.5 and Table 4.2). While some of the general trends seen in potting soil were also seen in natural soils (e.g., increased accumulation of CeO_2 and TiO_2 in roots), there was less total uptake in natural soils than in potting soil. In particular, ENMs in leaves were either present at very low concentrations or completely absent (Figs. 4.5A, 4.5D, & 4.5G), which resulted in fewer impacts on plant physiology (Chapter 5). All three ENMs used here have been shown to have greatly reduced mobility in farm and grass soil compared to potting soil (Chapter 2), which, in conjunction with an increase in aggregate size, is likely the cause of the decreased uptake seen here.

CeO_2 uptake was found to be limited almost exclusively to root tissue under all conditions, suggesting that only a very small fraction of CeO_2 aggregates were transported through the roots to the vascular tissue and upwards to the stems and leaves. Despite their compositional similarities TiO_2 was taken up in both roots and stems at much higher concentrations than CeO_2, possibly as a result of their different behaviors in grass and farm soil, or because background Ti concentrations in the soil were two orders of magnitude higher than background Ce concentrations. As discussed in Chapter 2, CeO_2 mean aggregate diameters in grass and farm soils (Fig. 2.2) and soil solutions (Fig. 2.3A) were larger than those of TiO_2 aggregates. Size exclusion has been implicated as one of the primary factors controlling plant uptake of ENMs[3, 19] and may be at least partially responsible for the results seen here.

Both farm soil and grass soil have roughly an order of magnitude less available phosphate than potting soil (even without fertilizer), which appears to have allowed for ENMs to influence P uptake by *C. unguiculata* grown in natural soils. In grass soil, root P concentrations were positively correlated with both Ce (linear regression, $R^2 = 0.88$, $p < 0.05$) and Cu (linear regression, $R^2 = 0.92$, $p < 0.05$) concentrations for individuals exposed to those ENMs, although this effect was only seen under low light conditions. Since neither of these ENMs increase P mobility or bioavailability in grass soil (Figure 3.3), this correlation may be due to sorption of phosphate from the soil by the ENMs, which are then taken up into the roots. This is similar to what was seen in unfertilized potting soil, and provides further evidence that that under nutrient limited conditions metal oxide ENMs, particularly CeO_2, are able to influence P bioavailability.

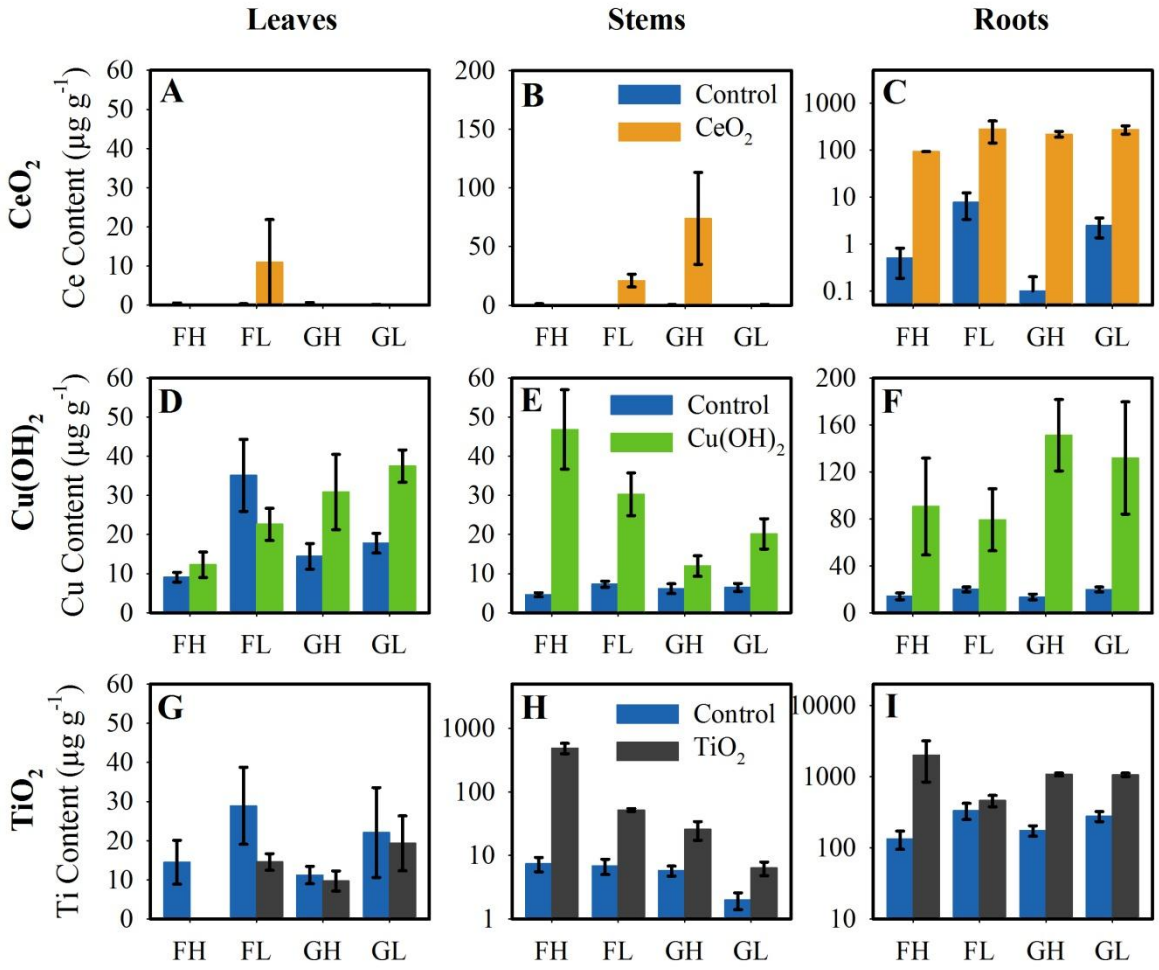

Figure 4.5. Tissue metal concentration of *C. unguiculata* grown in farm or grass soil under high light or low light conditions. FH: farm soil, high light; FL: farm soil, low light; GH: grass soil, high light; GL: grass soil, low light. A-C show Ce content of leaves, stems, and roots from CeO_2 –exposed plants; D-F show Ti content of leaves, stems, and roots from TiO_2 –exposed plants; G-I show Cu content of leaves, stems, and roots from $Cu(OH)_2$ – exposed plants. Error bars are ±SE. Note variable y-axes. Statistical analyses are displayed in Table 4.2.

Table 4.2. Results of 3-way ANOVA to determine the effects of Soil Type, Light Level, and Soil ENM Concentration on Tissue Metal Concentrations of *C. unguiculata* grown in farm soil or grass soil. Significance levels are indicated as follows: *$p < 0.05$, **$p < 0.01$, and ***$p < 0.001$. *Df* for all tests = 1.

Tissue	Parameter	CeO_2			$Cu(OH)_2$			TiO_2		
		f	*p*		*f*	*p*		*f*	*p*	
Leaf	Soil	1.27	0.26		0.56	0.45		0.20	0.66	
	Light	0.17	0.68		3.76	0.05	*	1.32	0.25	
	Concentration	3.97	0.05	*	1.19	0.28		0.66	0.42	
	Soil : Light	0.57	0.45		-	-		0.00	0.96	
	Soil : Conc	7.62	0.01	**	4.16	0.04	*	0.34	0.56	
	Light : Conc	1.98	0.16		-	-		0.00	0.97	
	Soil : Light : Conc	2.88	0.09		-	-		-	-	
Stem	Soil	1.54	0.22		15.37	0.00	***	65.4	0.0	***
	Light	3.59	0.06		0.03	0.86		34.3	0.0	***
	Concentration	21.94	0.00	***	135.01	0.00	***	130.0	0.0	***
	Soil : Light	3.09	0.09		1.84	0.18		43.3	0.0	***
	Soil : Conc	13.94	0.00	***	2.21	0.14		92.3	0.0	***
	Light : Conc	1.36	0.25		39.31	0.00	***	144.8	0.0	***
	Soil : Light : Conc	10.43	0.00	**	14.88	0.00	***	113.5	0.0	***
Root	Soil	7.21	0.01	**	1.88	0.18		1.06	0.31	
	Light	6.82	0.01	*	0.27	0.60		0.74	0.39	
	Concentration	265.61	0.00	***	81.77	0.00	***	25.44	0.00	***
	Soil : Light	0.20	0.66		0.39	0.54		2.10	0.15	
	Soil : Conc	7.98	0.01	**	3.88	0.05	*	6.30	0.02	*
	Light : Conc	2.46	0.12		3.99	0.05	*	0.32	0.58	
	Soil : Light : Conc	3.82	0.06		1.01	0.32		5.02	0.03	*

4.3.2. ENM Uptake and Translocation in Crop Plants

ENM uptake and translocation in crop plants was found to vary with both species and illumination intensity (Figures 4.6 and 4.7). In contrast to *C. unguiculata*, however, increased ENM accumulation was seen at low rather than high light intensities. This is especially evident in wheat, and is most likely due to decreases in transpiration rates of both wheat and radishes grown in high light later in their life cycle (Chapter 5). Additionally, some ENM accumulation was found in the edible radish hypocotyls and wheat grains, particularly Ti in radish hypocotyls.

Similar to *C. unguiculata* grown in farm soil, radishes accumulated very little to no metals in their leaves. However, radishes also had relatively low levels of ENMs in hypocotyl and root tissue although more root uptake occurred with CeO_2 and TiO_2 than $Cu(OH)_2$ under low light conditions, possibly as a consequence of ENM surface charge. Zhu, et al. (2012)[34] found increased uptake of positively charged Au ENMs over neutral or negatively charged particles in radish seedling root tissue grown hydroponically, so similar phenomena may be occurring here with the positively charged CeO_2 and TiO_2 and negatively charged $Cu(OH)_2$. The low overall uptake of ENMs may also be related to the short lifespan of radishes, which is roughly half of the other species tested here.

High concentrations of all three ENMs were found in wheat, particularly in individuals grown under low light conditions. On average, wheat had the highest concentrations of all three ENMs in all comparable tissues for all plant species, including *C. unguiculata* grown in potting soil. This last point is noteworthy for two reasons, namely, that all three ENMs have greatly decreased mobility in grass soil compared to potting soil and so the fraction of ENMs available for uptake is much smaller in grass soil, and that ENM uptake in wheat is

known to be subject to strict size limitations. Larue, et al. (2012)[3] found that TiO_2 ENMs above 140 nm did not accumulate in root tissues, those above 36 nm did not enter the cortex, but that ENMs 14 nm in diameter were able to pass through the CS, enter the vascular tissue, and be translocated throughout the plant. This aligns well with the distribution trends seen here (i.e., roughly ten times more CeO_2 and TiO_2 were found in roots than stems or leaves since larger aggregates are taken up into roots but do not pass into vascular tissue) and also shows that wheat plants are adept at taking up ENMs, even from soils where ENM mobility is highly limited.

The presence of Cu in all tissues at concentrations significantly higher than the background (Tables 4.3 and 4.4) provides further evidence that $Cu(OH)_2$ undergoes at least partial dissolution in soil, especially when its uptake and translocation patterns in these plants are compared to those of the relatively insoluble TiO_2 or CeO_2. Given that the $Cu(OH)_2$ ENM used in these studies is a commercial biocide designed to release Cu ions, it is not surprising that this is the case. However, Chapter 5 shows that this ENM has harmful effects on the plants it is meant to protect, as Cu ions can be toxic to many plants at high concentrations. Since $Cu(OH)_2$ is highly retained immediately at its point of entry to soil (Chapter 2) it may reach toxic concentrations in the soil even following application methods recommended by the manufacturer.

However, while no significant correlations between Ce, Cu, or Ti content and P content were found in radishes, P and Cu concentrations had a significant positive relationship in the leaves (linear regression, $R^2 = 0.89$, $p < 0.05$) and stems (linear regression, $R^2 = 0.98$, $p < 0.01$) of wheat grown under low light conditions. This suggests relatively high soil concentrations of $Cu(OH)_2$ may be able to enhance P uptake by certain plants.

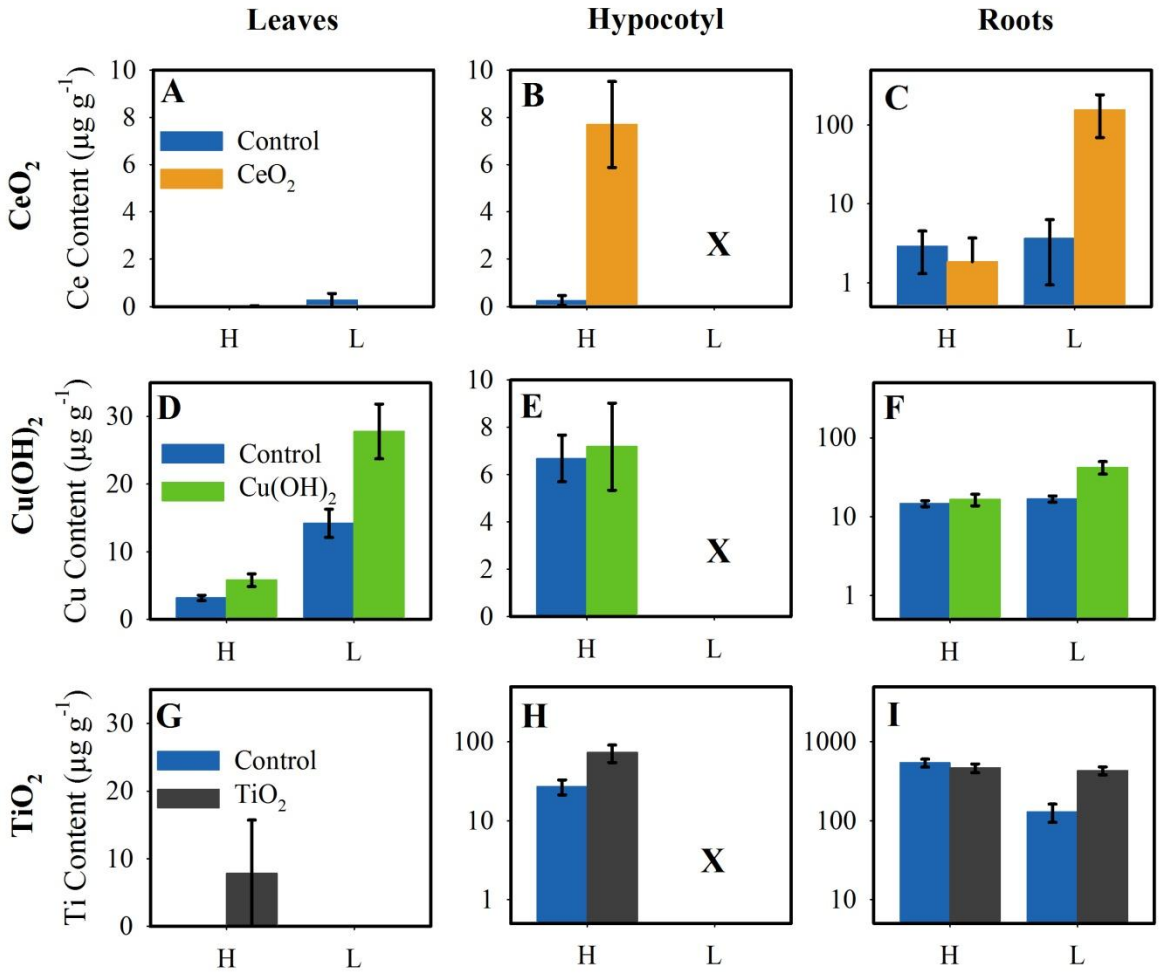

Figure 4.6. Tissue metal concentration of radishes grown in farm soil under high light (H) or low light (L) conditions. A-C show Ce content of leaves, hypocotyls, and roots from CeO_2 –exposed plants; D-F show Ti content of leaves, hypocotyls, and roots from TiO_2 – exposed plants; G-I show Cu content of leaves, hypocotyls, and roots from $Cu(OH)_2$ – exposed plants. Samples of all tissue types were tested from each growth conditions, although hypocotyls did not develop under low light conditions (marked with Xs) and so could not be tested. Error bars are ±SE. Note variable y-axes. Statistical analyses are displayed in Table 4.3.

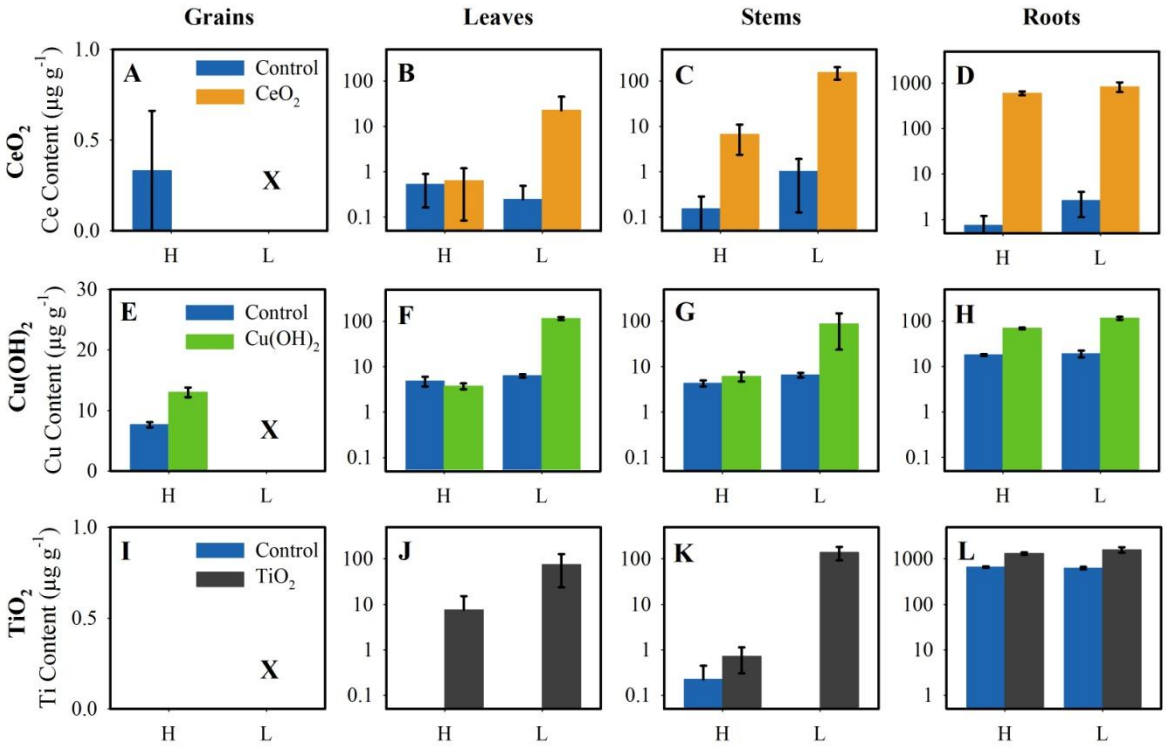

Figure 4.6. Tissue metal concentration of wheat grown in grass soil under high light (H) or low light (L) conditions. A-D show Ce content of grains, leaves, stems, and roots from CeO_2 –exposed plants; E-H show Ti content of grains, leaves, stems, and roots from TiO_2 – exposed plants; I-L show Cu content of grains, leaves, stems, and roots from $Cu(OH)_2$ – exposed plants. Samples of all tissue types were tested from each growth conditions, although grains did not develop under low light conditions (marked with Xs) and so could not be tested. Error bars are ±SE. Note variable y-axes. Statistical analyses are displayed in Table 4.4.

Table 4.3. Results of 1- and 2-way ANOVA to determine the effects of Light Level and Soil ENM Concentration on Tissue Metal Concentrations of radishes grown in farm soil. Hypo = hypocotyl. Significance levels are indicated as follows: *$p < 0.05$, **$p < 0.01$, and ***$p < 0.001$. *Df* for all tests = 1.

Tissue	Parameter	CeO_2			$Cu(OH)_2$			TiO_2		
		f	*p*		*f*	*p*		*f*	*p*	
Leaf	Light	0.92	0.35		51.98	0.00	***	1.18	0.29	
	Concentration	0.26	0.61		13.22	0.00	**	3.82	0.06	
	Light : Conc	0.33	0.57		6.06	0.02	*	3.82	0.06	
Hypo	Light	-	-		-	-		-	-	
	Concentration	48.69	0.00	***	0.17	0.68		11.5	0.00	**
	Light : Conc	-	-		-	-		-	-	
Root	Light	4.00	0.06		11.51	0.00	**	28.49	0.00	***
	Concentration	10.80	0.00	**	23.84	0.00	***	2.50	0.12	
	Light : Conc	11.33	0.00	**	18.11	0.00	***	7.39	0.01	*

Table 4.4. Results of 1- and 2-way ANOVA to determine the effects of Light Level and Soil ENM Concentration on Tissue Metal Concentrations of wheat grown in grass soil. Significance levels are indicated as follows: *$p < 0.05$, **$p < 0.01$, and ***$p < 0.001$. *Df* for all tests = 1.

Tissue	Parameter	CeO_2			$Cu(OH)_2$			TiO_2		
		f	*p*		*f*	*p*		*f*	*p*	
Grain	Light	-	-		-	-		-	-	
	Concentration	0.32	0.58		36.30	0.00	***	-	-	
	Light : Conc	-	-		-	-		-	-	
Leaf	Light	1.08	0.31		4.76	0.04	*	2.11	0.16	
	Concentration	3.53	0.07		9.47	0.00	**	9.01	0.01	**
	Light : Conc	3.53	0.07		10.79	0.00	**	6.13	0.02	*
Stem	Light	14.28	0.00	***	2.65	0.12		14.4	0.00	***
	Concentration	35.45	0.00	***	5.25	0.03	*	43.1	0.00	***
	Light : Conc	31.81	0.00	***	5.12	0.03	*	55.0	0.00	***
Root	Light	3.01	0.09		21.82	0.00	***	0.00	0.95	
	Concentration	163.17	0.00	***	397.29	0.00	***	152.58	0.00	***
	Light : Conc	4.53	0.04	*	37.71	0.00	***	5.96	0.02	*

4.4. Conclusions

Although uptake of ENMs by soil grown plants has been reported before,[9, 31, 40-42] here it is demonstrated that environmental conditions can influence the uptake and bioaccumulation of metals due to ENM exposure across a range of ENM types, plant species, and soils. Since plants are typically at the base of food webs, this trend has important implications for the possibility of cascading effects through trophic transfer. A limited number of studies have measured trophic transfer in terrestrial systems, but Hawthorne, et al. (2014)[43] recently observed transfer of CeO_2 ENMs in a terrestrial food chain from primary producer (zucchini) to primary consumer (cricket) to secondary consumer (spider), finding that ENMs were accumulated and transferred at higher concentrations than either bulk CeO_2 or ionic Ce. Judy, et al. (2011)[44] also found significant biomagnification of Au ENMs in hornworms that were fed tobacco leaves.

However, here it was found that TiO_2 and CeO_2 were highly concentrated in root tissue, which may result in high dietary exposure concentrations for root herbivores. This accumulation of ENMs in root tissue may also mean that decomposing plant roots could act as a hotspot for ENM release into the soil, impacting local fungal, microbial and animal communities. On the other hand, this provides insight into possible future phytoremediation of sites contaminated with specific types of ENMs. Little to no metal accumulation was seen in the edible tissues of radishes or wheat, which suggests there may be little transfer of ENMs to humans or livestock fed these crops. One exception was the relatively high concentrations of Ti found in radish hypocotyls, although because TiO_2 is approved for use

in a variety of personal care products and even foods[45] this may not present much risk to human or animal consumers.

4.5. References

1. Salt, D. E.; Pickering, I. J.; Prince, R. C.; Gleba, D.; Dushenkov, S.; Smith, R. D.; Raskin, I., Metal Accumulation by Aquacultured Seedlings of Indian Mustard. *Environ. Sci. Technol.* **1997,** *31*, (6), 1636-1644.
2. Vesk, P. A.; Nockolds, C. E.; Allaway, W. G., Metal Localization in Water Hyacinth Roots from an Urban Wetland. *Plant, Cell Environ.* **1999,** *22*, (2), 149-158.
3. Larue, C.; Laurette, J.; Herlin-Boime, N.; Khodja, H.; Fayard, B.; Flank, A. M.; Brisset, F.; Carriere, M., Accumulation, Translocation and Impact of Tio2 Nanoparticles in Wheat (Triticum Aestivum Spp.): Influence of Diameter and Crystal Phase. *Sci. Total Environ.* **2012,** *431*, 197-208.
4. Raven, P. H.; Evert, R. F.; Eichhorn, S. E., *Biology of Plants*. 7th ed.; W. H. Freeman and Company: 41 Madison Avenue, New York, NY, 2005.
5. Fleischer, A.; O'Neill, M. A.; Ehwald, R., The Pore Size of Non-Graminaceous Plant Cell Walls Is Rapidly Decreased by Borate Ester Cross-Linking of the Pectic Polysaccharide Rhamnogalacturonan Ii. *Plant Physiol.* **1999,** *121*, (3), 829-838.
6. Nair, R.; Varghese, S. H.; Nair, B. G.; Maekawa, T.; Yoshida, Y.; Kumar, D. S., Nanoparticulate Material Delivery to Plants. *Plant Sci.* **2010,** *179*, (3), 154-163.
7. Al-Salim, N.; Barraclough, E.; Burgess, E.; Clothier, B.; Deurer, M.; Green, S.; Malone, L.; Weir, G., Quantum Dot Transport in Soil, Plants, and Insects. *Sci. Total Environ.* **2011,** *409*, (17), 3237-3248.
8. Birbaum, K.; Brogioli, R.; Schellenberg, M.; Martinoia, E.; Stark, W. J.; Gunther, D.; Limbach, L. K., No Evidence for Cerium Dioxide Nanoparticle Translocation in Maize Plants. *Environ. Sci. Technol.* **2010,** *44*, (22), 8718-8723.
9. Priester, J. H.; Ge, Y.; Mielke, R. E.; Horst, A. M.; Moritz, S. C.; Espinosa, K.; Gelb, J.; Walker, S. L.; Nisbet, R. M.; An, Y.-J.; Schimel, J. P.; Palmer, R. G.; Hernandez-Viezcas, J. A.; Zhao, L.; Gardea-Torresdey, J. L.; Holden, P. A., Soybean Susceptibility to Manufactured Nanomaterials with Evidence for Food Quality and Soil Fertility Interruption. *Proc. Natl. Acad. Sci. U. S. A.* **2012**.
10. Wang, Z. Y.; Xie, X. Y.; Zhao, J.; Liu, X. Y.; Feng, W. Q.; White, J. C.; Xing, B. S., Xylem- and Phloem-Based Transport of Cuo Nanoparticles in Maize (Zea Mays L.). *Environ. Sci. Technol.* **2012,** *46*, (8), 4434-4441.
11. Batley, G. E.; Halliburton, B.; Kirby, J. K.; Doolette, C. L.; Navarro, D.; McLaughlin, M. J.; Veitch, C., Characterization and Ecological Risk Assessment of Nanoparticulate Ceo2 as a Diesel Fuel Catalyst. *Environ. Toxicol. Chem.* **2013,** *32*, (8), 1896-1905.
12. Keller, A. A.; Wang, H. T.; Zhou, D. X.; Lenihan, H. S.; Cherr, G.; Cardinale, B. J.; Miller, R.; Ji, Z. X., Stability and Aggregation of Metal Oxide Nanoparticles in Natural Aqueous Matrices. *Environ. Sci. Technol.* **2010,** *44*, (6), 1962-1967.
13. Conway, J. R.; Adeleye, A. S.; Gardea-Torresdey, J.; Keller, A. A., Aggregation, Dissolution, and Transformation of Copper Nanoparticles in Natural Waters. *Environ. Sci. Technol.* **2015,** *49*, (5), 2749-2756.
14. Zhou, D. X.; Bennett, S. W.; Keller, A. A., Increased Mobility of Metal Oxide Nanoparticles Due to Photo and Thermal Induced Disagglomeration. *PLoS One* **2012,** *7*, (5).

15. Thio, B. J. R.; Zhou, D. X.; Keller, A. A., Influence of Natural Organic Matter on the Aggregation and Deposition of Titanium Dioxide Nanoparticles. *J. Hazard. Mater.* **2011,** *189*, (1-2), 556-563.
16. Meyers, D. E.; Auchterlonie, G. J.; Webb, R. I.; Wood, B., Uptake and Localisation of Lead in the Root System of Brassica Juncea. *Environmental pollution (Barking, Essex : 1987)* **2008,** *153*, (2), 323-32.
17. Schwabe, F.; Schulin, R.; Limbach, L. K.; Stark, W.; Buerge, D.; Nowack, B., Influence of Two Types of Organic Matter on Interaction of Ceo2 Nanoparticles with Plants in Hydroponic Culture. *Chemosphere* **2013,** *91*, (4), 512-520.
18. Lin, D. H.; Xing, B. S., Phytotoxicity of Nanoparticles: Inhibition of Seed Germination and Root Growth. *Environ. Pollut.* **2007,** *150*, (2), 243-250.
19. Sabo-Attwood, T.; Unrine, J. M.; Stone, J. W.; Murphy, C. J.; Ghoshroy, S.; Blom, D.; Bertsch, P. M.; Newman, L. A., Uptake, Distribution and Toxicity of Gold Nanoparticles in Tobacco (Nicotiana Xanthi) Seedlings. *Nanotoxicology* **2012,** *6*, (4), 353-360.
20. Judy, J. D.; Unrine, J. M.; Rao, W.; Wirick, S.; Bertsch, P. M., Bioavailability of Gold Nanomaterials to Plants: Importance of Particle Size and Surface Coating. *Environ. Sci. Technol.* **2012,** *46*, (15), 8467-8474.
21. Yadav, G.; Srivastava, P. K.; Singh, V. P.; Prasad, S. M., Light Intensity Alters the Extent of Arsenic Toxicity in Helianthus Annuus L. Seedlings. *Biol. Trace Elem. Res.* **2014,** *158*, (3), 410-421.
22. Gaur, J. P.; Noraho, N., Role of Certain Environmental Factors on Cadmium Uptake and Toxicity in Spirodela Polyrhiza (L.) Schleid. And Azolla Pinnata R.Br. *Biomed. Environ. Sci.* **1995,** *8*, (3), 202-210.
23. Cohen, C. K.; Fox, T. C.; Garvin, D. F.; Kochian, L. V., The Role of Iron-Deficiency Stress Responses in Stimulating Heavy-Metal Transport in Plants. *Plant Physiol.* **1998,** *116*, (3), 1063-1072.
24. Vasek, F. C., Outcrossing in Natural Populations .2. Clarkia Unguiculata. *Evolution* **1965,** *19*, (2), 152-156.
25. Daou, T. J.; Begin-Colin, S.; Grenèche, J. M.; Thomas, F.; Derory, A.; Bernhardt, P.; Legaré, P.; Pourroy, G., Phosphate Adsorption Properties of Magnetite-Based Nanoparticles. *Chem. Mat.* **2007,** *19*, (18), 4494-4505.
26. Recillas, S.; Garcia, A.; Gonzalez, E.; Casals, E.; Puntes, V.; Sanchez, A.; Font, X., Preliminary Study of Phosphate Adsorption onto Cerium Oxide Nanoparticles for Use in Water Purification; Nanoparticles Synthesis and Characterization. *Water Sci. Technol.* **2012,** *66*, (3), 503-509.
27. Dudley, L. S.; Mazer, S. J.; Galusky, P., The Joint Evolution of Mating System, Floral Traits and Life History in Clarkia (Onagraceae): Genetic Constraints Vs. Independent Evolution. *J. Evol. Biol.* **2007,** *20*, (6), 2200-2218.
28. Cornelis, G.; Ryan, B.; McLaughlin, M. J.; Kirby, J. K.; Beak, D.; Chittleborough, D., Solubility and Batch Retention of Ceo2 Nanoparticles in Soils. *Environ. Sci. Technol.* **2011,** *45*, (7), 2777-2782.
29. Lopez-Moreno, M. L.; de la Rosa, G.; Hernandez-Viezcas, J. A.; Castillo-Michel, H.; Botez, C. E.; Peralta-Videa, J. R.; Gardea-Torresdey, J. L., Evidence of the Differential Biotransformation and Genotoxicity of Zno and Ceo2 Nanoparticles on Soybean (Glycine Max) Plants. *Environ. Sci. Technol.* **2010,** *44*, (19), 7315-7320.

30. Lopez-Moreno, M. L.; de la Rosa, G.; Hernandez-Viezcas, J. A.; Peralta-Videa, J. R.; Gardea-Torresdey, J. L., X-Ray Absorption Spectroscopy (Xas) Corroboration of the Uptake and Storage of Ceo2 Nanoparticles and Assessment of Their Differential Toxicity in Four Edible Plant Species. *J. Agric. Food Chem.* **2010,** *58*, (6), 3689-3693.
31. Du, W. C.; Sun, Y. Y.; Ji, R.; Zhu, J. G.; Wu, J. C.; Guo, H. Y., Tio2 and Zno Nanoparticles Negatively Affect Wheat Growth and Soil Enzyme Activities in Agricultural Soil. *J. Environ. Monit.* **2011,** *13*, (4), 822-828.
32. Adeleye, A. S.; Conway, J. R.; Perez, T.; Rutten, P.; Keller, A. A., Influence of Extracellular Polymeric Substances on the Long-Term Fate, Dissolution, and Speciation of Copper-Based Nanoparticles. *Environ. Sci. Technol.* **2014,** *48*, (21), 12561-12568.
33. Wang, J.; Yang, Y.; Zhu, H. G.; Braam, J.; Schnoor, J. L.; Alvarez, P. J. J., Uptake, Translocation, and Transformation of Quantum Dots with Cationic Versus Anionic Coatings by Populus Deltoides X Nigra Cuttings. *Environ. Sci. Technol.* **2014,** *48*, (12), 6754-6762.
34. Zhu, Z. J.; Wang, H. H.; Yan, B.; Zheng, H.; Jiang, Y.; Miranda, O. R.; Rotello, V. M.; Xing, B. S.; Vachet, R. W., Effect of Surface Charge on the Uptake and Distribution of Gold Nanoparticles in Four Plant Species. *Environ. Sci. Technol.* **2012,** *46*, (22), 12391-12398.
35. Brady, N. C.; Weil, R. R., *Elements of the Nature and Properties of Soils*. 2nd ed.; Pearson Education: Upper Saddle River, New Jersey, 2003.
36. Kupper, H.; Setlik, I.; Spiller, M.; Kupper, F. C.; Prasil, O., Heavy Metal-Induced Inhibition of Photosynthesis: Targets of in Vivo Heavy Metal Chlorophyll Formation. *J. Phycol.* **2002,** *38*, (3), 429-441.
37. Lv, J. T.; Zhang, S. Z.; Luo, L.; Zhang, J.; Yang, K.; Christie, P., Accumulation, Speciation and Uptake Pathway of Zno Nanoparticles in Maize. *Environ.-Sci. Nano* **2015,** *2*, (1), 68-77.
38. Almeelbi, T.; Bezbaruah, A., Nanoparticle-Sorbed Phosphate: Iron and Phosphate Bioavailability Studies with Spinacia Oleracea and Selenastrum Capricornutum. *ACS Sustain. Chem. Eng.* **2014,** *2*, (7), 1625-1632.
39. Rui, Y.; Zhang, P.; Zhang, Y.; Ma, Y.; He, X.; Gui, X.; Li, Y.; Zhang, J.; Zheng, L.; Chu, S.; Guo, Z.; Chai, Z.; Zhao, Y.; Zhang, Z., Transformation of Ceria Nanoparticles in Cucumber Plants Is Influenced by Phosphate. *Environ. Pollut.* **2015,** *198*, 8-14.
40. Josko, I.; Oleszczuk, P., Influence of Soil Type and Environmental Conditions on Zno, Tio2 and Ni Nanoparticles Phytotoxicity. *Chemosphere* **2013,** *92*, (1), 91-99.
41. Zhao, L. J.; Hernandez-Viezcas, J. A.; Peralta-Videa, J. R.; Bandyopadhyay, S.; Peng, B.; Munoz, B.; Keller, A. A.; Gardea-Torresdey, J. L., Zno Nanoparticle Fate in Soil and Zinc Bioaccumulation in Corn Plants (Zea Mays) Influenced by Alginate. *Environ. Sci.: Processes Impacts* **2013,** *15*, (1), 260-266.
42. Morales, M. I.; Rico, C. M.; Hernandez-Viezcas, J. A.; Nunez, J. E.; Barrios, A. C.; Tafoya, A.; Pedro Flores-Marges, J.; Peralta-Videa, J. R.; Gardea-Torresdey, J. L., Toxicity Assessment of Cerium Oxide Nanoparticles in Cilantro (Coriandrum Sativum L.) Plants Grown in Organic Soil. *J. Agric. Food Chem.* **2013,** *61*, (26), 6224-6230.
43. Hawthorne, J.; Roche, R. D.; Xing, B. S.; Newman, L. A.; Ma, X. M.; Majumdar, S.; Gardea-Torresdey, J.; White, J. C., Particle-Size Dependent Accumulation and Trophic Transfer of Cerium Oxide through a Terrestrial Food Chain. *Environ. Sci. Technol.* **2014,** *48*, (22), 13102-13109.

44. Judy, J. D.; Unrine, J. M.; Bertsch, P. M., Evidence for Biomagnification of Gold Nanoparticles within a Terrestrial Food Chain. *Environ. Sci. Technol.* **2011,** *45*, (2), 776-781.
45. Weir, A.; Westerhoff, P.; Fabricius, L.; Hristovski, K.; von Goetz, N., Titanium Dioxide Nanoparticles in Food and Personal Care Products. *Environ. Sci. Technol.* **2012,** *46*, (4), 2242-2250.

5. Physiological Impacts of Engineered Nanomaterials on Soil-Grown Plants

5.1. Introduction

Despite possible differences in the specific action of toxicity, plants exposed to engineered nanomaterials (ENMs), metal ions, and other pollutants often show several similar growth and physiological responses. These include decreased germination success, decreased shoot and/or root development, chlorosis, and oxidative stress, even for pollutants that are not redox-active.[1] These are generic toxic responses for plants that can be caused by several mechanisms, including the production of reactive oxygen species (ROS), genotoxicity through binding to DNA,[2] disturbance of the plant water balance,[1] altering membrane permeability and integrity, binding and inactivating key nutrients, disruption of antioxidant and other enzymatic activity, and displacing functional metal ions from biomolecules.[3]

Despite the short time in which their effects on plants have been studied,[4] ENMs have been shown to have all these effects. However, the effects reported thus far appear to depend on the type of ENM, any possible coatings the ENM may have, the medium of growth, and the model plant used. Consequently, there is a general lack of consensus in the literature regarding the action and extent of toxicity for most ENMs. For example, chlorophyll content was seen to diminish with exposure to CuO ENMs (but not ionic Cu) in duckweed[5] and corn seedlings[6] but TiO_2 had no effect in wheat seedlings[7] and had a *positive* effect on both

photosynthetic rates[8] and chloroplast viability[9] in spinach, although it is unclear how much of this variability is due to the model species tested, the properties of the specific nanomaterials used, and the method of exposure (root *vs.* foliar). ZnO ENMs have been shown to reduce germination and growth in a variety of plants in both hydroponic[10-15] and planted[16] systems, but much of their toxicity has been shown to be mostly from the release of Zn^{2+} ions.[11] Ag ENMs have similar effects and also dissolve at an environmentally-relevant rate, but their toxicity has been shown to be due to both the nanoparticles and released ions,[17] although in general soluble ENMs have been implicated in plant toxicity. Additionally, particle size has been shown to have large impacts on ENM uptake and distribution patterns in plants, with smaller particles typically being taken up in higher amounts and distributed throughout the plant.[7, 18-20] Smaller aggregate sizes achieved through surface coatings may be expected to show similar trends, but often the changes in surface charge and functionalization caused by these coatings are more important predictors of behavior than size alone.[14, 21]

Fewer studies have looked at effects of ENM toxicity not related to germination success or growth. Direct genotoxic effects were found with Ag ENMs in onions[22] and ZnO and CeO_2 in soybeans.[13] TiO_2 has been shown to be photoactive and produce ROS in the presence of light[23] and also to increase superoxide dismutase, catalase, and peroxidase activities in spinach.[9] However, it was shown to have no effect on wheat seedlings.[7] ZnO ENMs are also photoactive,[23] but had no effect on catalase or peroxidase activity (which typically provide evidence of ROS effects) in corn unless coated with alginate, a naturally produced polysaccharide.[16] Very few studies have looked at the effects of ENMs on any physiological traits relating to water use, but Priester, et al. (2012)[24] reported decreased

water content of roots and stems in soil-grown soybeans exposed to CeO_2 and ZnO. However, a study looking at ionic Cd, Zn, and Pb found that exposure in cardoon plants decreased stomatal conductance, water content, transpiration rate, and evapotranspiration,[25] which may be similar to the effects of some ENMs based on other shared toxicological effects.

Owing to the increased complexity associated with increasing the quantity of variables in a system, few studies have looked at the effects of ENMs on post-seedling plants[26] and fewer still have used soil-grown post-seedling plants.[24, 27] Results from these systems can be difficult to interpret compared to the well-controlled conditions of hydroponic or agar systems, but they are potentially more applicable to real systems. In addition, novel pathways may be uncovered that perhaps would not have been found otherwise. For example, Priester, et al. (2012)[24] found that soybeans grown in agricultural soil had decreased nitrogen fixation and consequent growth effects when exposed to CeO_2 ENM concentrations in the soil as low as 0.5 g kg^{-1}, which is similar to what has been found for soybeans grown in cadmium-contaminated soils.[28]

Plant physiology is heavily influenced by environmental conditions and may be more or less vulnerable to potential toxic effects under different growth scenarios. In one of the few previous studies specifically investigating the interactions between abiotic growth conditions and ENM phytotoxicity, Josko and Oleszczuk (2013)[29] found that the toxicity of metal oxide ENMs to cress (*L. sativum*) was enhanced under high light conditions and reduced at higher temperature. Building further understanding of how these factors affect the uptake and toxicity of ENMs in plants is key to accurate predictions of the overall impact of ENMs outside of the growth chamber or greenhouse and across both crop and wild species.

Similarly to the previous section, here I investigated the effects of three metal oxide ENMs, CeO_2, TiO_2, and $Cu(OH)_2$, on the growth and physiology of *Clarkia unguiculata* (Onagraceae), radish (*Raphanus sativus*), and wheat (*Triticum aestivum*) grown in different soils, illumination, and/or nutrient levels. In the first part of this study, *C. unguiculata* were grown in potting soil under different light and nutrient levels and exposed to a range of ENM concentrations in order to discern how ENM toxicity varies with increasing ENM concentration under these conditions. In the second part of this study *C. unguiculata* was again used as a model organism, but was grown in two natural soils under different light levels to gain insight into how soil properties influence ENM toxicity. Finally, two crop plants were grown in natural soils to see how the trends found in *C. unguiculata* vary across plant species.

I hypothesized that higher light and lower nutrient conditions, whether from lack of fertilizer or infertile soil, would be more physiologically stressful for plants and that highly stressed plants would be most vulnerable to ENM toxicity. Additionally, since TiO_2 and CeO_2 are photoactive and produce reactive oxygen species (ROS) when exposed to light[23, 30] I predicted that they would have the greatest effect in plants grown under high illumination by interfering with photosynthesis in leaves.

5.2. Methods

5.2.1. ENM Preparation

Stock suspensions of TiO_2, CeO_2, and $Cu(OH)_2$ ENMs (Table 1.1) were prepared for each application as 1 g L^{-1} and bath sonicated for 30 minutes. Stocks were then diluted to 1, 10, and 100 mg L^{-1}. Dilutions were not re-sonicated.

5.2.2. Plant Exposure and Growth Conditions

Clarkia unguiculata is an annual hermaphroditic flowering shrub native to oak/pine woodlands and disturbed slopes in central California. Additional details can be found in Dudley, et al. (2007)[31] and Vasek (1965)[32]. Seeds were collected from a field site in Kern County, CA (35° 41.453' N, 118° 43.911' W, elev. 2830 ft) in July 2008 and stored with desiccant in darkness at 4°C until use. Seeds were randomly sampled from ten maternal families, plated on agar in covered Petri dishes (8 g L^{-1}), vernalized in darkness for 5 days at 4°C, and then germinated under ambient light at room temperature for an additional 5 days. Seedlings were then transplanted into 2.5 cm diameter x 16.34 cm long cylindrical plastic growing tubes (Ray Leach Cone-tainers; Stuewe and Sons, Tangent, Oregon) (one seedling per tube) containing 17 ± 0.1 g of a 1:20 mixture of worm castings to a peat moss/perlite/dolomitic limestone potting soil (Sunshine Mix #4, Sun Gro Horticulture), 136 ± 1 g grass soil, or 167 ± 1 g farm soil. Soil properties other than Ce, Ti, and Cu content were measured at the UC Davis Analytical Lab (http://anlab.ucdavis.edu/) and are shown in Table 1.2. After transplantation, seedlings were kept moist and allowed to grow for 2.5 weeks before ENM exposure to allow them to become established, after which they were

grown for an additional 8 weeks until they had completed their life cycle. *C. unguiculata* plants were grown in growth chambers with a 14:10 hr 21:13°C day:night cycle under two light levels, 500 (high, H) or 50 (low, L) $\mu mol_{photon}\ m^{-2}\ s^{-1}$. These light conditions are roughly analogous to those on a partly cloudy day or a shaded understory.

In addition to being exposed to two light intensities, *C. unguiculata* grown in potting soil were also exposed to two different nutrient levels for a total of four distinct growth conditions: high light + excess nutrients (HE), high light + limited nutrients (HL), low light + excess nutrients (LE), and low light + limited nutrients (LL). Excess nutrient conditions were achieved through the addition of 140 ± 3 mg fertilizer pellets (19-6-12 Osmocote Smart Release Indoor & Outdoor Plant Food) prior to seedling transplantation, corresponding to 70.7 ± 1.5 mg NH_3 per L soil, 63.6 ± 1.5 mg L^{-1} NO_3, 42.4 ± 1.0 mg L^{-1} P_2O_5, and 84.8 ± 2.0 mg L^{-1} K_2O released over the course of the experiment. Plants grown with limited nutrients did not receive fertilizer.

Starting in the second week of growth, 50 mL of 0, 1, 10, or 100 mg L^{-1} TiO_2, CeO_2, or $Cu(OH)_2$ suspensions were slowly poured onto the soil surface of each individual container to allow for absorption into the soil. This was repeated weekly for a total of 8 weeks to result in a soil contamination rate of 0, 0.25, 2.5, or 25 mg ENM per L soil per week, or 0, 2.9, 29, or 290 mg kg^{-1} wk^{-1}. Volumetric units are used here to describe soil ENM concentrations in order to provide comparable results for all three soils despite the large difference in density between potting soil and the two natural soils. *C. unguiculata* grown in natural (grass and farm) soils only received 50 mL of 0 or 100 mg L^{-1} TiO_2, CeO_2, or $Cu(OH)_2$ suspensions per week for soil contamination rates of 0 or 25 mg ENM L^{-1} wk^{-1}.

Cherry radish (*Raphanus sativum*) and Hard Red Spring wheat (*Triticum aestivum*) seeds were purchased from Seeds of Change (Rancho Dominuguez, CA, USA) and Salt Spring Seeds (Salt Spring Island, BC, Canada), respectively, and stored in darkness at 4°C until use. Radish seeds were planted in square, 4 inch Tech-Square pots (McConkey & Company) filled with 600 ± 1 g farm soil and wheat seeds were planted in cylindrical plastic growing tubes filled with 136 ± 1 g grass soil. Radish and wheat seeds were germinated under ambient light at room temperature for 3 days before being moved to growth chambers under 500 (high, H) or 50 (low, L) $\mu mol_{photon}\ m^{-2}\ s^{-1}$. After 1 week of growth radish and wheat individuals received 0 or 25 mg ENM $L^{-1}\ wk^{-1}$ as suspensions for the duration of their life cycles.

Four replicates were grown per plant species, ENM, light condition, soil type (for *C. unguiculata*), and concentration and nutrient level (for *C. unguiculata* in potting soil), and five control replicates were grown per species, light condition, nutrient level, or soil type that were not exposed to ENMs for a total of 300 individuals.

5.2.3. Physiological and Growth Measurements

Physiological measurements follow methods outlined in Dudley, et al. (2012)[33]. Photosynthetic assimilation rate ($\mu mol_{CO2}\ m^{-2}{}_{leaf\ area}\ s^{-1}$, *A*), transpiration rate ($mol_{H2O}\ m^{-2}{}_{leaf\ area}\ s^{-1}$, *E*), photosystem II quantum yield efficiency (ΦPSII), quantum yield of CO_2 assimilation ($\mu mol_{CO2}\ \mu mol^{-1}{}_{photon}$, ΦCO_2), photochemical quenching (*qP*), electron transport rate ($\mu mol_{photon}\ m^{-2}{}_{leaf\ area}\ s^{-1}$, ETR), intercellular CO_2 concentration ($\mu mol_{CO2}\ mol^{-1}{}_{air}$, C_i), and various fluorescence parameters (F_o' and F_s) were measured from light-adapted leaves using a portable IR gas exchange analyzer (IRGA, LiCor 6400; Licor, Lincoln, Nebraska,

USA) with a LiCor 6400-40 fluorometer light source. The fraction of oxidized PSII reaction centers (*qL*) were calculated from Equation 1.[34]

$$q_L = q_P \cdot \frac{F_o'}{F_s} \qquad \text{Eq. 1}$$

Leaves were measured on plants sampled in random order between 0800 and 1200 hours using the following settings: PARi = 1500 ± 2, stomatal ratio = 0.5, flow = 500 µmol mol^{-1}, and reference CO_2 chamber concentration = 400 $\mu mol_{CO2}\, mol^{-1}$. Parameters were measured when photosynthetic, conductance, and fluorescence rates were stable (photo: slope < 1 for 10 s; conductance: slope < 0.05 for 10 s; fluorescence: dn/dt slope < 50 for 10 s). For *C. unguiculata* leaf node position on the stem relative to the cotyledons was recorded for each measurement. If sampled leaves were not large enough to fill the 2 cm^2 IRGA chamber, the surface of the gasket that seals the chamber (when closed) was covered with ink, thereby stamping an image of the chamber's boundary on the leaf surface. A photograph of the leaf was taken and analyzed using ImageJ (National Institute of Health, Bethesda, Maryland, USA; available at http://rsbweb.nih.gov/ij) to determine the leaf area that was exposed within the chamber, which was then used to recompute physiological parameters.

For *C. unguiculata*, plant heights and total leaf counts were recorded each week starting at the second week after seedling transplantation and physiological measurements were made every other week from the second week following the initiation of ENM exposure. For radishes, fluorescence and gas exchange measurements were taken every week starting with the second week of ENM exposure and leaf and hypocotyl biomass weights were recorded after five weeks of growth. For wheat, plant heights were measured each week, fluorescence and gas exchange measurements were taken every other week starting with the second week of ENM exposure, and grain mass was measured after eight weeks of growth.

5.2.4. Statistical Analysis

For *C. unguiculata* grown in potting soil, one-way linear regressions were used to determine the effects of Soil ENM Concentration or ENM Addition Rate on physiological (*A*, C_i, ΦCO_2, ΦPSII, and *qL*) and physical growth parameters (linear growth rates [cm wk^{-1}], maximum height, leaf production rate, leaf loss rate [as leaves desiccate and senesce], maximum number of leaves, and week of maximum leaf production). Separate regressions were performed for each growth condition, and for analyses of physiological and growth parameters Soil ENM Concentrations or ENM Addition Rates were log(x+1) transformed to improve. To determine the dependence of plant physiological rates on environmental conditions in the absence of ENM exposure, one-way ANOVA with posthoc Tukey's HSD tests or Kruskal-Wallis tests with multiple comparisons were used to detect the effects of growing conditions on photosynthetic rate (*A*), intracellular CO_2 (C_i), quantum yield of CO_2 assimilation (ΦCO_2), and transpiration rate (*E*) among plants that were not exposed to ENMs.

For plants grown in natural soils, Dunnett's tests were used to verify differences between individuals not exposed to ENMs and those that were. Separate tests were performed for each growth or physiological parameter and growth condition. Levene's test was used to ensure homogeneity of variance and if data were not homogenously distributed nonparametric tests were used. Statistical analyses were performed using Microsoft Excel 2007 and the statistical software R (v. 2.11.1).

5.3. Results and Discussion

5.3.1. Physiological and Growth Impacts on *Clarkia unguiculata* in Potting Soil

I found that the physiological effects of ENM exposure on *C. unguiculata* grown in potting soil were strongly dependent on the environmental conditions under which plants were grown, namely, high light excess nutrient (HE), high light limited nutrient (HL), low light excess nutrient (LE), and low light limited nutrient (LL). By comparing photosynthetic rates (*A*) and other physiological parameters of the zero concentration groups across growth conditions baseline levels of stress[35] can be established for each condition, which can be used to explain the trends seen in ENM-exposed plants.

Figure 5.1 shows that photosynthesis (*A*) and quantum yield of CO_2 assimilation (ΦCO_2) decline rapidly in *C. unguiculata* grown under high light conditions, resulting in the high intracellular CO_2 content (C_i) shown in Fig. 5.1B. These effects are likely due to negative correlation between light intensity and photosynthetic efficiency plants typically display.[36] Transpiration rate (*E*, Fig. 5.1D) was also elevated in plants grown under high light conditions due to increased leaf temperatures (data not shown) from the increased light intensity. Exposure to higher light conditions also caused plants to reach maturity faster than those grown under low light conditions. Based on these results, the relative rankings from most to least stressful growth condition appear to be HL > HE > LL ≈ LE. This ranking aligns with the hypothesis that higher light and lower nutrient conditions are the most stressful conditions imposed in this experiment.

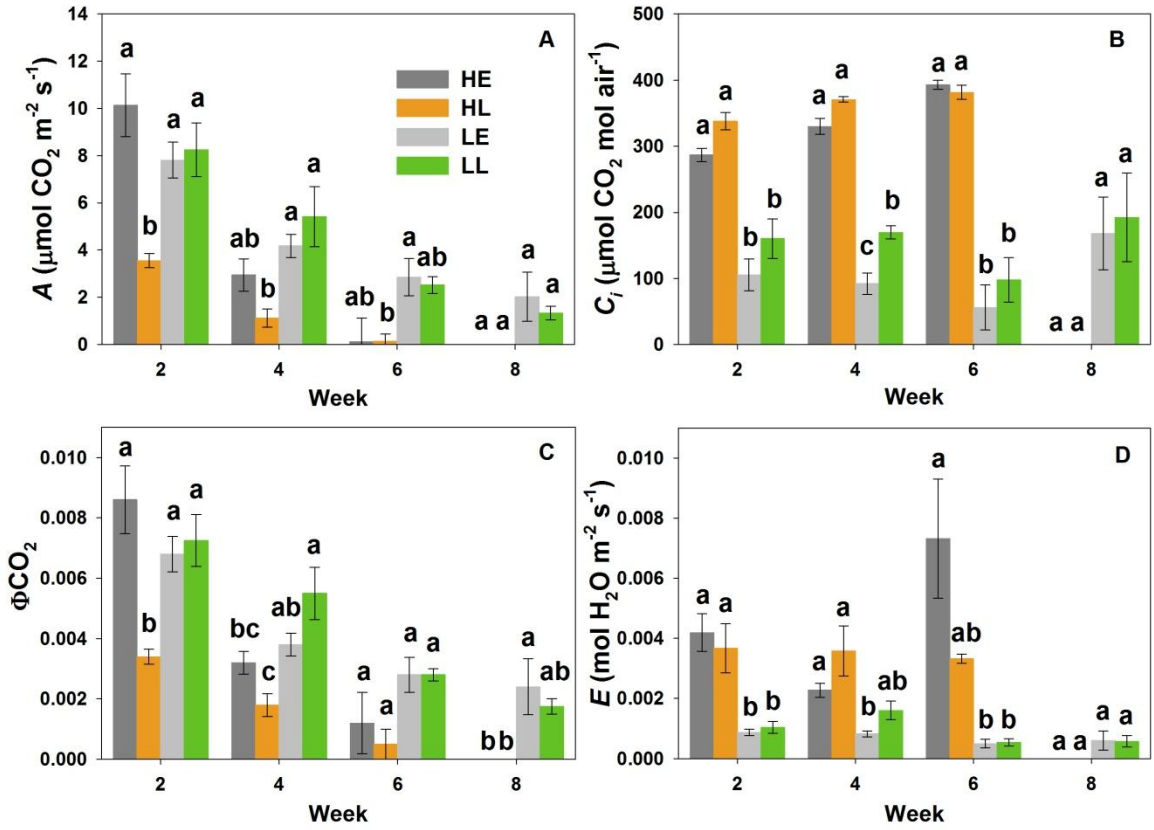

Figure 5.1. Physiological parameters of *C. unguiculata* not exposed to ENMs (zero concentration groups) grown under high light excess nutrient (HE), high light limited nutrient (HL), low light excess nutrient (LE), and low light limited nutrient (LL) conditions. Panel A shows photosynthetic rate (*A*), B shows intracellular CO_2 content (C_i), C shows quantum yield of CO_2 assimilation (ΦCO_2), and D shows transpiration rate (*E*). Error bars are ±SE. HE = high light + excess nutrients, HL = high light + limited nutrients, LE = low light + excess nutrients, and LL = low light + limited nutrients. Within each week, mean values represented by distinct letters indicate significant differences detected by one-way ANOVA followed by posthoc Tukey's test or Kruskal-Wallis tests with multiple comparisons.

For plants exposed to these ENMs, few significant correlations between the physiological parameters measured and ENM exposure concentration were seen at the second or sixth week of exposure, and by the eighth week all high light plants, including the control plants, had reached the end of their life cycle and ceased photosynthesizing. However, at the fourth week of exposure *A* and ΦCO_2 decreased significantly with

increasing exposure concentrations and C_i increased significantly with increasing exposure concentration (linear regressions, $p < 0.05$, Figure 5.2, Table 5.1) for HE plants exposed to CeO_2 and TiO_2. This supports my final hypothesis and indicates that these two photoactive ENMs reduce photosynthetic rate by interfering with the assimilation of CO_2 required for photosynthesis, which results in a build-up of CO_2 within leaf cells. Additionally, there were no changes in ΦPSII in these plants, and this lack of correlation between ΦPSII and ΦCO_2 could indicate that energy transfer from photosystem II (PSII) or photosystem I (PSI) to the Calvin cycle is being disrupted by the ENMs since the conversion of photons to electrons by PSII (ΦPSII) was unaffected while the conversion of energy from PSII/PSI to carbohydrates using CO_2 (ΦCO_2) decreased.[35]

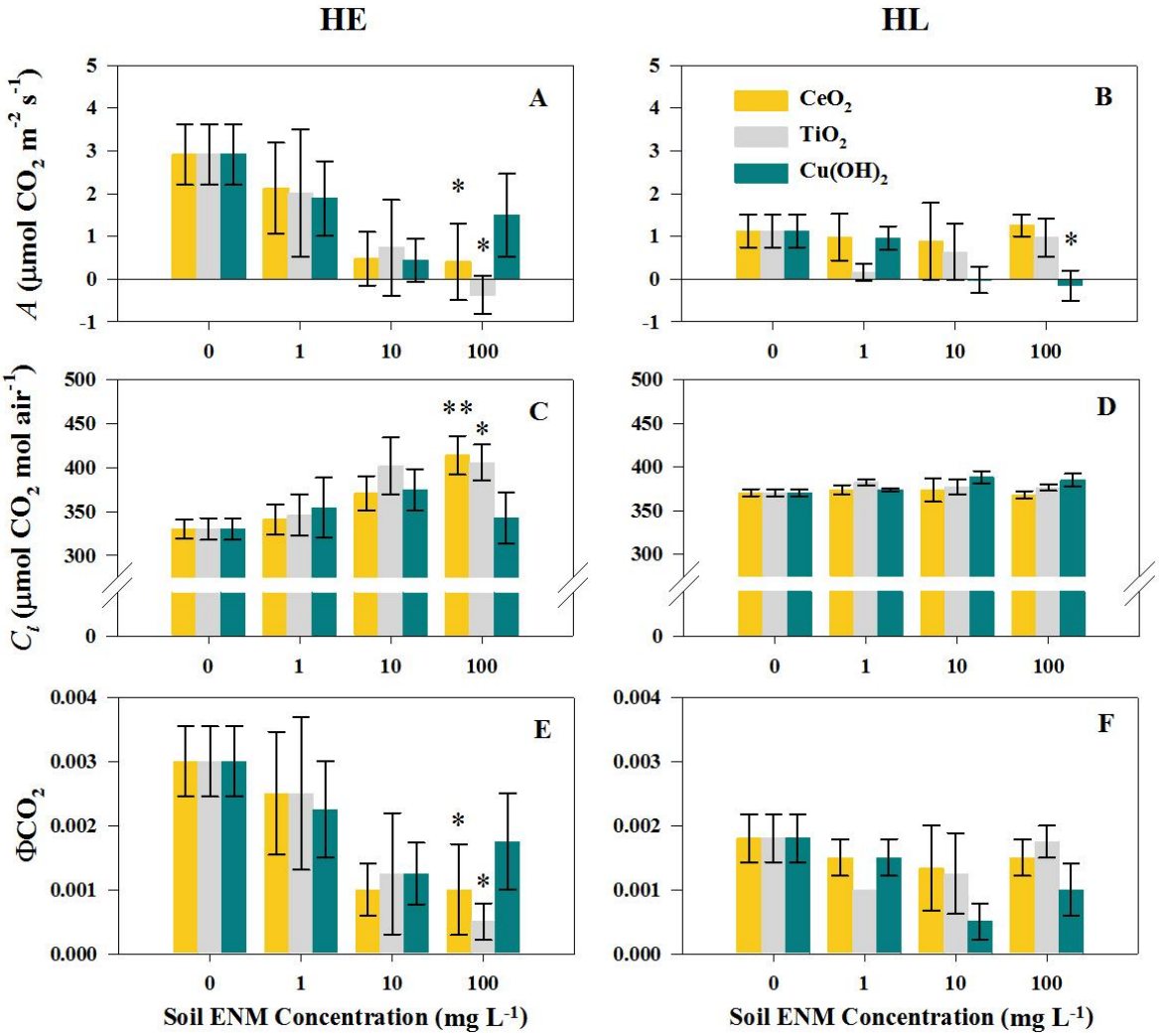

Figure 5.2. Physiological parameters of ENM-exposed groups during the fourth week of exposure. A-B show photosynthetic rate (*A*) of HE (A) and HL plants (B), C-D show intracellular CO_2 content (C_i) of HE (C) and HL plants (D), and E-F shows quantum yield of CO_2 assimilation (ΦCO_2) of HE (E) and HL plants (F). Error bars are ±SE. Treatments marked with asterisks at the highest concentrations are those that exhibit statistically significant correlation coefficients between soil ENM concentration and *A*, C_i, or ΦCO_2 based on linear regressions among individual plant values, as reported in Table 3. *$p < 0.05$, **$p < 0.01$.

Table 5.1. Slopes (± SE), R^2 values, and significance levels from linear regressions among individual plants of physiological parameters (*A*, C_i, ΦCO_2 , ΦPSII, and *qL*) on Soil ENM Concentrations during the fourth week of exposure. N = 17 for each treatment. Abbreviations are defined in text. **p* < 0.05, ***p* <0.01. Bivariate relationships in low light conditions are not shown because none were statistically significant.

	HE			**HL**		
	CeO_2	**TiO_2**	**$Cu(OH)_2$**	**CeO_2**	**TiO_2**	**$Cu(OH)_2$**
A	-1.7±0.8*	-1.6±0.6*	-0.8±0.8	0.1±0.2	0.2±0.4	-1.0±0.3*
R^2	0.24	0.32	0.07	0.01	0.01	0.35
C_i	62±17**	55±22*	3.4±20	-2.8±5.6	1.0±5.1	11±5
R^2	0.47	0.30	0.00	0.02	0.00	0.20
ΦCO_2 ($x10^{-3}$)	-1.4±0.7*	-1.8±0.7*	0.7±0.6	-0.2±0.3	0.2±0.4	-0.6±0.4
R^2	0.24	0.29	0.09	0.01	0.02	0.13
ΦPSII ($x10^{-3}$)	-2.8±7.9	-4.0±7.6	-3.0±7.8	-1.7±3.8	-1.7±3.2	12±6
R^2	0.01	0.02	0.01	0.01	0.02	0.21
qL ($x10^{-2}$)	1.5±2.5	3.3±2.3	-1.1±1.2	0.9±1.4	-1.1±1.0	3.5±1.5*
R^2	0.02	0.12	0.05	0.026	0.08	0.25

This effect appears to be light-driven since no changes in any physiological parameter relative to control plants were seen in individuals grown under low light conditions. High light conditions had the two-fold impact of increasing particle uptake to leaves (Fig. 4.1A & 4.1D), by increasing transpiration rates (Fig. 5.1D) and possibly stimulating greater photoactivity of TiO_2 and CeO_2. The disruption of energy transfer observed may be due to the absorption of electrons from photosystem II (PSII) by the ENM upon the creation of an e^-/h^+ pair after excitation by a photon, or alternately through reactions with ROS produced by the ENM. Exposure to CeO_2 had slightly weaker effects on physiological parameters than TiO_2, and if the latter scenario is correct this could be due to the lower relative ROS production rate of CeO_2 compared to TiO_2.[23] Barhoumi, et al. (2015)[37] saw an inhibition of PSII and a corresponding increase in ROS in *L. gibba* exposed to iron oxide ENMs, so similar phenomena may be occurring here. ROS production by TiO_2 and CeO_2 ENMs may also explain why no physiological effects were seen in HL plants, since plants upregulate antioxidant production at higher stress levels[38] that may counteract ROS produced by these ENMs.

Additionally, interference with photosynthetic mechanisms suggests that CeO_2 and TiO_2 ENMs are able to penetrate or be actively transported not only into the leaf cells but into the chloroplasts as well, and are able to intercalate themselves between thylakoid stacks to intercept electrons from PSII. Given that inter-thylakoid gaps can be on the order of 50-250 nm,[36] individual particles or small aggregates would not necessarily be excluded based on size alone. Whiteside, et al. (2009)[39] found uptake of NH_2-coated quantum dots < 15 nm in diameter into bluegrass chloroplasts and Larue, et al. (2012)[7] found 14 nm TiO_2 ENMs in wheat chloroplasts, so it is plausible that at least primary particles of TiO_2 and CeO_2 were

able to enter the chloroplasts of this model plant. Both of these ENMs have very limited dissolution and have been shown to be taken up into plant tissues as nanoparticles,[7, 24, 40] making it unlikely that any effects on photosynthesis are due to ionic Ti or Ce.

A similar decrease in *A* was seen in HL plants after four weeks of exposure to $Cu(OH)_2$, but without a corresponding change in ΦCO_2 or C_i (Figure 5.2). By further decreasing the already low photosynthetic rate of HL plants, $Cu(OH)_2$ had a larger relative impact than in HE, LE, or LL plants. This suggests that $Cu(OH)_2$ may affect photosynthesis through a different mechanism than TiO_2 and CeO_2. Additionally, I found that the fraction of oxidized PSII reaction centers (*qL*) increased significantly with increasing exposure concentration (linear regression, $p < 0.05$, Table 5.1). In healthy plants *qL* is typically positively associated with photosynthetic production,[35] but since a negative correlation between $Cu(OH)_2$ exposure and photosynthesis was found (Table 5.1), the increases in *qL* observed were likely due to interference with the oxidation of the primary PSII quinine acceptor (Q_A) by light rather than increased photosynthetic efficiency. See Figure 5.3 for a diagram of the mechanisms postulated here.

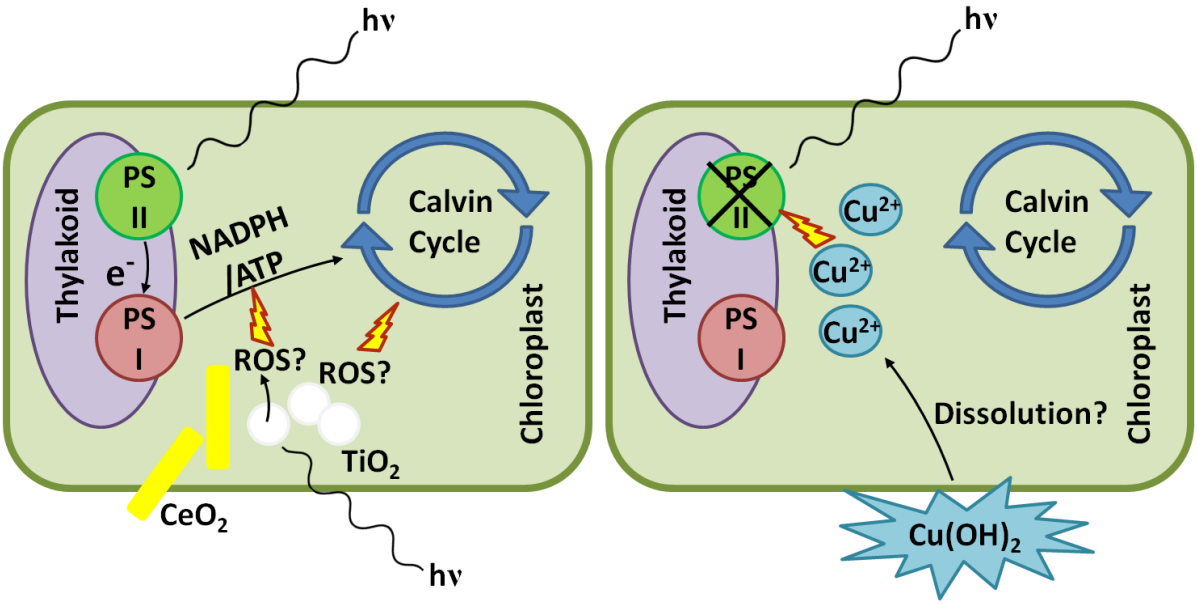

Figure 5.3. Conceptual model of hypothesized mechanisms by which CeO_2, TiO_2, and $Cu(OH)_2$ ENMs affect photosynthesis.

Others have found similar oxidation of PSII reaction centers in plants exposed to ionic copper due to interference with the photon antennae of PSII,[41-43] which may indicate $Cu(OH)_2$ toxicity seen in this study is due to Cu ions released from the $Cu(OH)_2$ ENMs. In this system, $Cu(OH)_2$ could be dissolved either in the rhizosphere and taken up as ionic Cu or be taken up into the plant in particle form and dissolved within the plant tissues. However, since these $Cu(OH)_2$ particles has been shown to have increased dissolution at acidic pH and lower dissolution at basic pH,[44] the majority of dissolution probably occurs in the soil (pH 5.7) rather than in the neutral or slightly basic conditions of cell or chloroplast interiors.[45, 46]

Linear growth rates (cm wk^{-1}), maximum height, leaf production rate, leaf loss rate (as leaves desiccate and senesce), maximum number of leaves, and week of maximum leaf production were calculated from physical measurements and are shown in Figures 5.4-5.10.

Few effects due to ENM exposure were seen under any growth condition, although LE plants exposed to $Cu(OH)_2$ had reduced growth rates, leaf production rates, and maximum number of leaves with increasing exposure concentrations (linear regressions, $p < 0.05$). Cu is an essential plant micronutrient but at high concentrations such as those observed in this experiment, Cu can decrease the uptake of other nutrients from the soil[47-49] and disrupt nitrogen metabolism.[41] Nutrient limitation caused by the presence of $Cu(OH)_2$ may have been responsible for limiting the growth of LE plants. The lack of a growth response in HE plants exposed to CeO_2 and TiO_2 may be because, under high light conditions, reductions in CO_2 assimilation have been shown to have minimal impacts on C gain.[42]

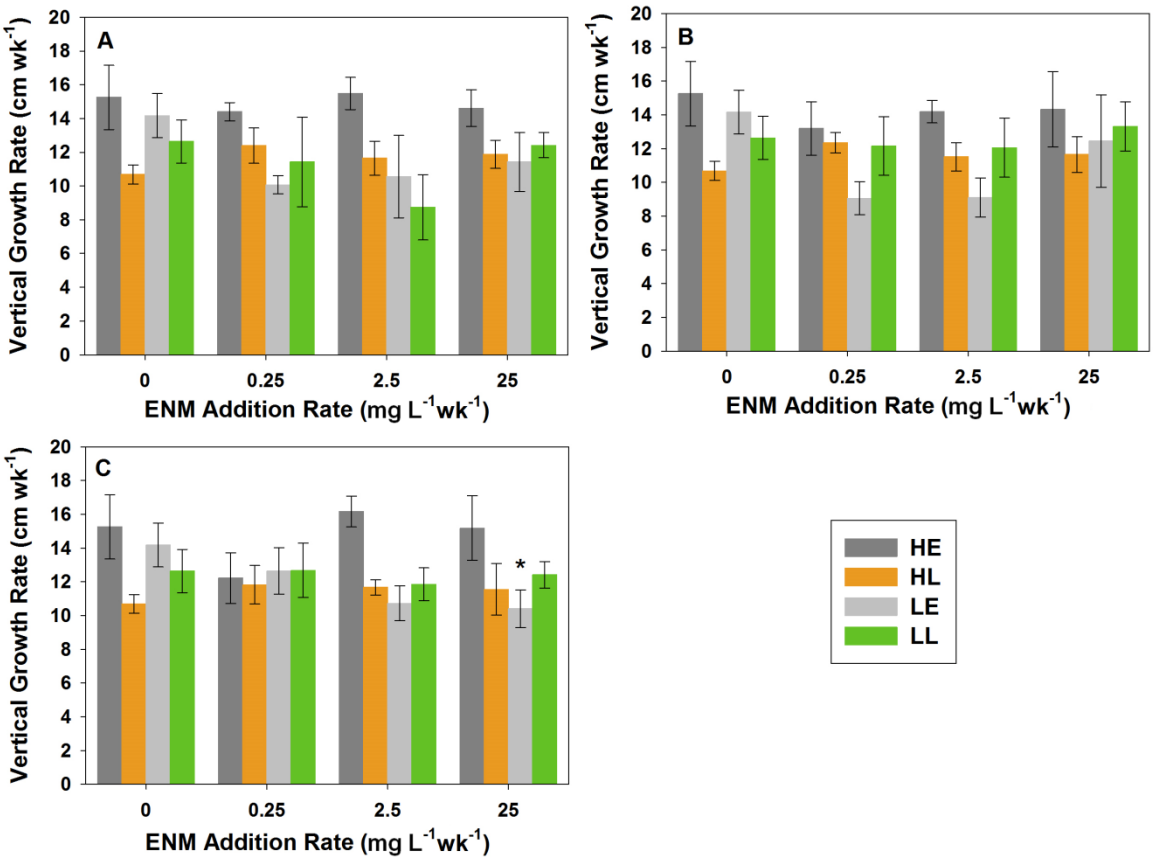

Figure 5.4. Vertical growth rate of plants exposed to (A) CeO_2, (B) TiO_2, and (C) $Cu(OH)_2$ ENMs and grown under high light excess nutrient (HE), high light limited nutrient (HL), low light excess nutrient (LE), and low light limited nutrient (LL) conditions. Error bars are ±SE. Growth conditions marked with asterisks at the highest ENM Addition Rate exhibit statistically significant correlation coefficients between ENM Addition Rate and Vertical Growth Rate based on linear regressions among individual plant values (analyses not shown). *$p < 0.05$.

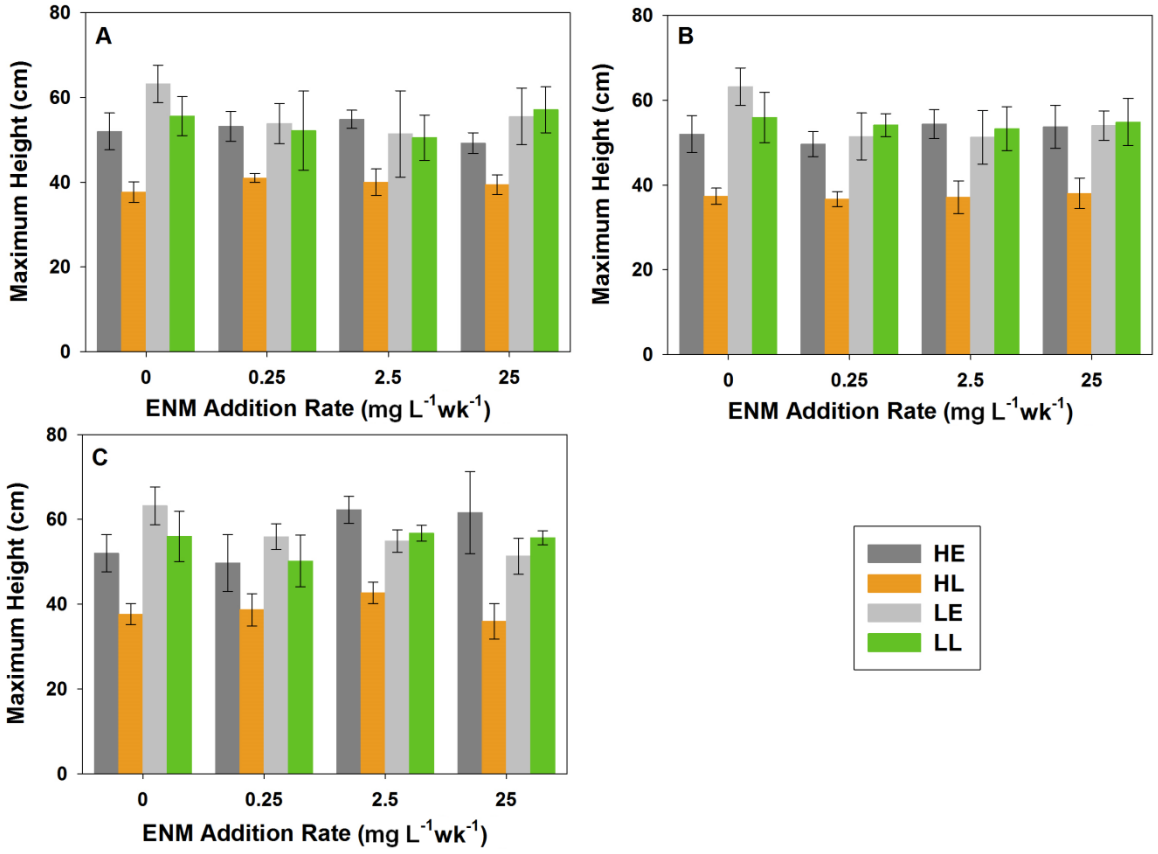

Figure 5.5. Maximum height of plants exposed to (A) CeO_2, (B) TiO_2, and (C) $Cu(OH)_2$ ENMs and grown under high light excess nutrient (HE), high light limited nutrient (HL), low light excess nutrient (LE), and low light limited nutrient (LL) conditions. Error bars are ±SE.

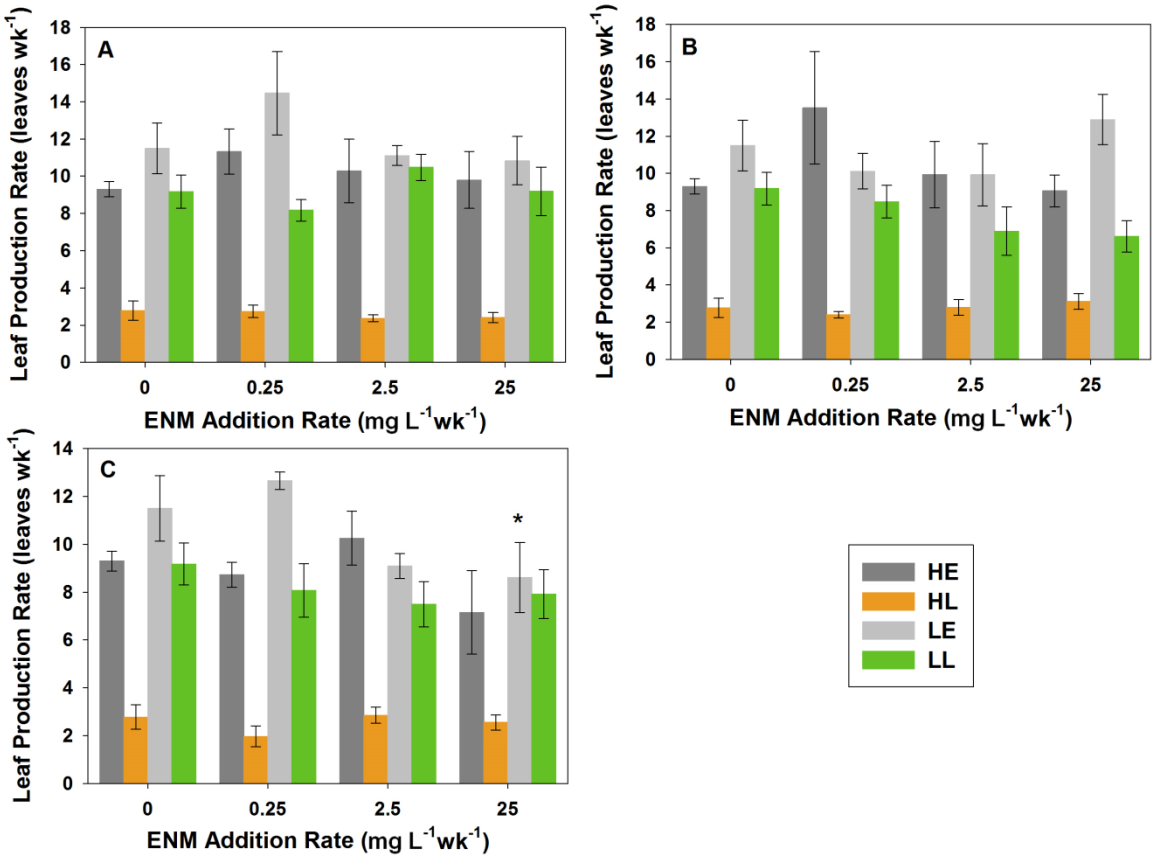

Figure 5.7. Leaf production rate of plants exposed to (A) CeO_2, (B) TiO_2, and (C) $Cu(OH)_2$ ENMs and grown under high light excess nutrient (HE), high light limited nutrient (HL), low light excess nutrient (LE), and low light limited nutrient (LL) conditions. Error bars are ±SE. Growth conditions marked with asterisks have statistically significant correlations between ENM Addition Rate and Leaf Production Rate based on linear regressions. *p < 0.05.

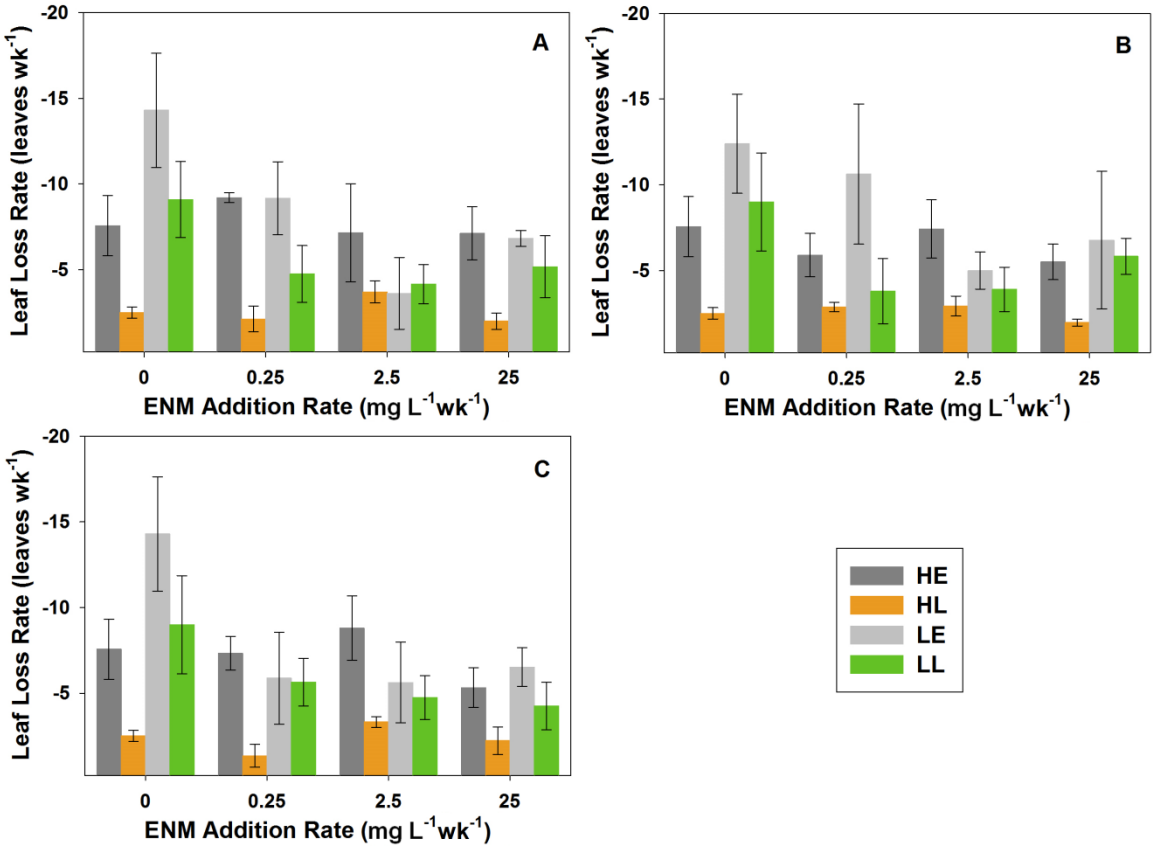

Figure 5.8. Rate of leaf senescence of plants exposed to (A) CeO_2, (B) TiO_2, and (C) $Cu(OH)_2$ ENMs and grown under high light excess nutrient (HE), high light limited nutrient (HL), low light excess nutrient (LE), and low light limited nutrient (LL) conditions. Error bars are ±SE.

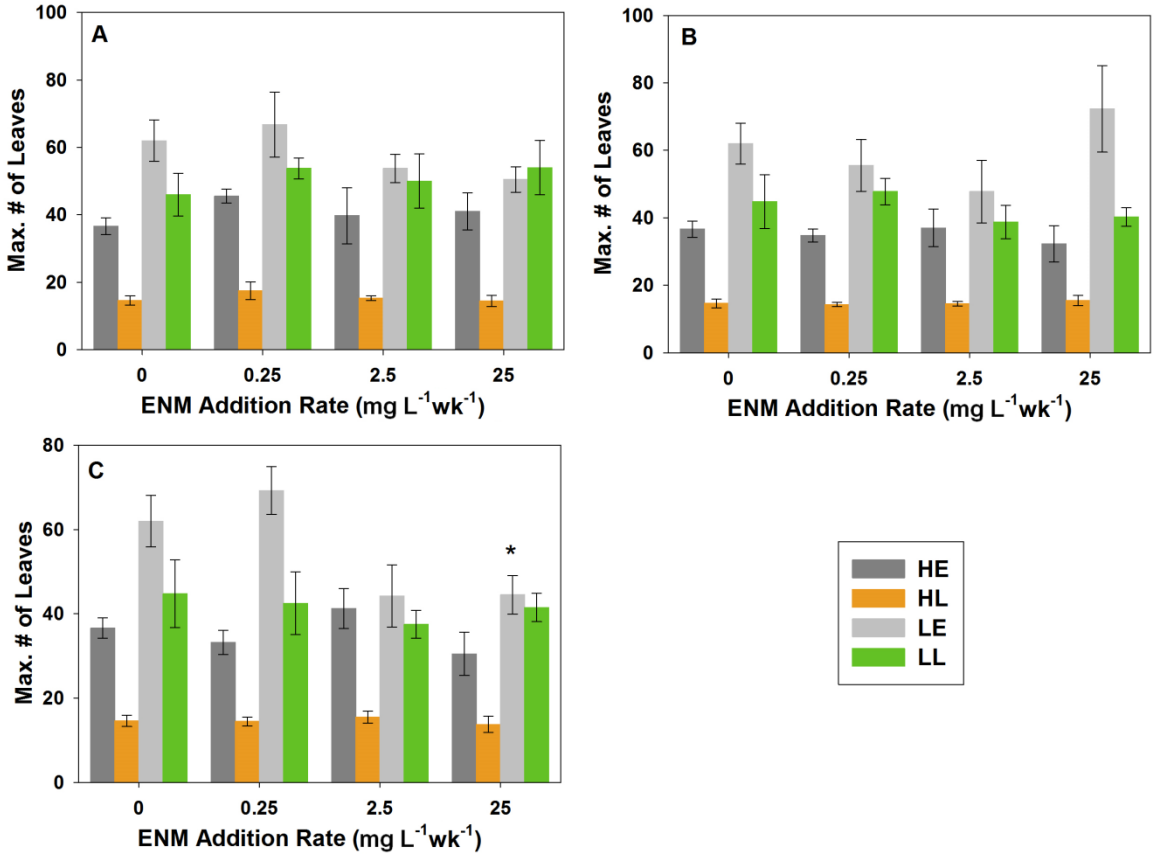

Figure 5.9. Peak number of leaves of plants exposed to (A) CeO_2, (B) TiO_2, and (C) $Cu(OH)_2$ ENMs and grown under high light excess nutrient (HE), high light limited nutrient (HL), low light excess nutrient (LE), and low light limited nutrient (LL) conditions. Error bars are ±SE. Growth conditions marked with asterisks have statistically significant correlations between ENM Addition Rate and Maximum Leaf Count based on linear regressions. *$p < 0.05$.

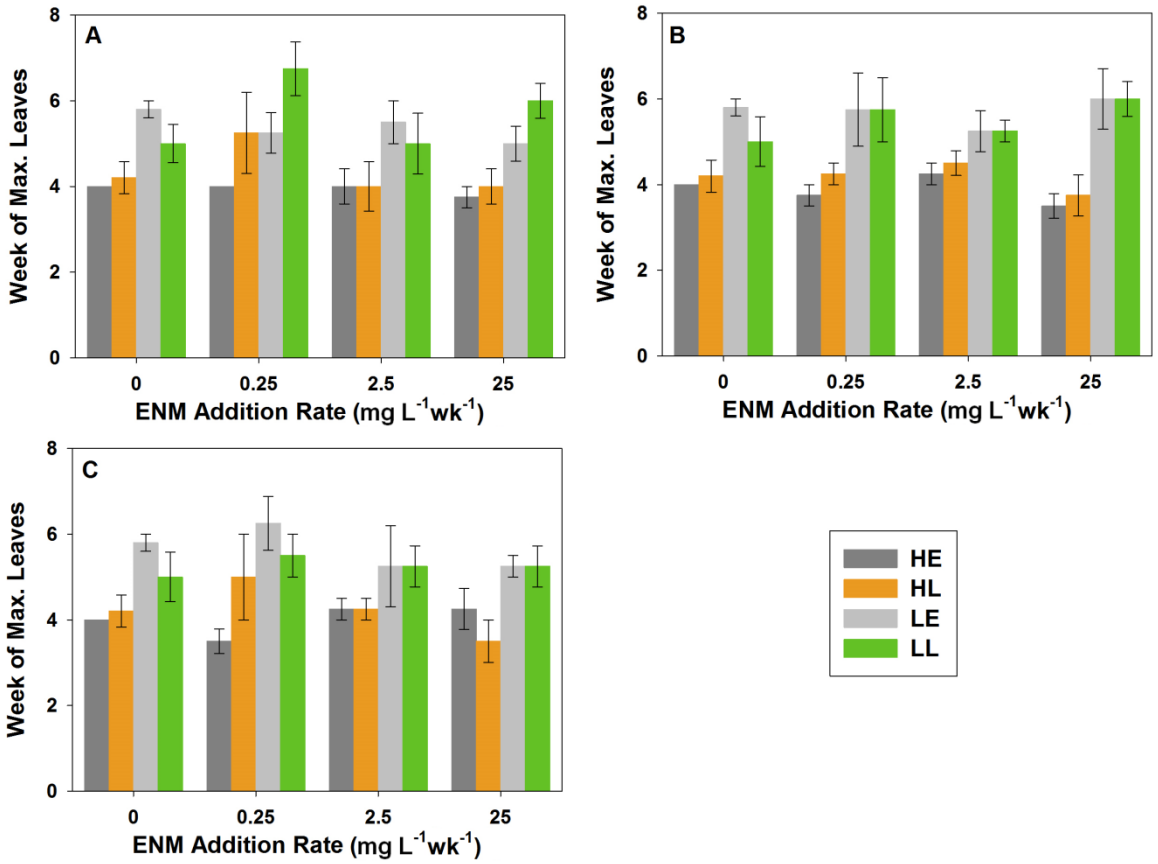

Figure 5.10. Week of peak number of leaves of plants exposed to (A) CeO_2, (B) TiO_2, and (C) $Cu(OH)_2$ ENMs and grown under high light excess nutrient (HE), high light limited nutrient (HL), low light excess nutrient (LE), and low light limited nutrient (LL) conditions. Error bars are ±SE.

5.3.2. Physiological and Growth Impacts on Plants in Natural Soils

Clarkia unguiculata displayed markedly different trends in growth and physiology when grown in natural soils than when grown in potting soil, likely as a result of the different soil/ENM interactions between potting soil and natural soils (Chapters 2 & 3) as well as the loss of measurable leaves in the high light treatments (Figure 5.11). No changes in photosynthesis due to ENM exposure were seen in any condition during any week of growth, nor were there any effects on CO_2 assimilation. However, individuals grown in grass soil under high light conditions had significantly stunted vertical growth with exposure to all three ENMs (Fig. 5.11E). Additionally, several physiological parameters were impacted in individuals exposed to CeO_2 and $Cu(OH)_2$ ENMs, but only in plants grown in grass soil (Figures 5.12-5.13).

Specifically, in the second week of ENM exposure, *C. unguiculata* grown in grass soil under low light conditions that were exposed to CeO_2 had significantly greater PSII operating efficiency (*qP*, Dunnet's test, $p < 0.05$) as well as significantly higher proportions of oxidized PSII reaction centers (*qL*, Dunnet's test, $p < 0.05$, Figure 5.12). Together, these indicate that these plants were able to harvest light more efficiently, although the relatively modest increases in *qP* and *qL* along with the absence of changes in photosynthetic rate or growth show that this increased efficiency had negligible impacts on the overall health of the plant. Additionally, in the eighth week of ENM exposure, these plants had a slight but significant increase in water use efficiency (WUE, Dunnett's test, $p < 0.05$, Figure 5.13). Given that no CeO_2 was detected in the leaves of individuals grown in grass soil (Figure 4.5A) it is unlikely these minor effects on physiology were due to direct action of CeO_2 ENMs within the plant, but may instead have been related to increased nutrient release from

the soil. CeO_2 caused additional NO_3^- to be released in grass soil (Figure 3.2), which is a key plant nutrient and has been implicated in influencing photosynthetic efficiency[50] and WUE.[51]

In contrast to the short-term increases in photosynthetic efficiency seen with CeO_2, *C. unguiculata* grown in grass soil under low light conditions that were exposed to $Cu(OH)_2$ showed an eventual decrease in several aspects of photosynthetic efficiency. As Figure 5.13 shows, in the eighth week of exposure significant decreases were seen in both *qP* and *qL* (Dunnet's tests, $p < 0.001$) as well as ΦPSII (photosystem II quantum yield efficiency, Dunnett's test, $p < 0.01$) and electron transport rate through PSII (ETR, Dunnett's test, $p < 0.01$). While it is known that Cu ions can interfere with PSII, [41-43] these findings also contrast to the effects of $Cu(OH)_2$ exposure seen in *C. unguiculata* grown in potting soil (Table 5.1), which had decreased photosynthetic rate but increased *qL* during the period of peak growth rates. It would therefore appear that soil type changes the interactions between plants and $Cu(OH)_2$, although the exact mechanism(s) by which $Cu(OH)_2$ influences photosynthetic efficiency in individuals grown in grass soil is unclear. Finally, in the second week of ENM exposure, *C. unguiculata* grown in grass soil under high light conditions that were exposed to $Cu(OH)_2$ had significantly increased transpiration rates (*E*, Dunnett's test, $p < 0.05$). This may have been due to a combination of the stress-inducing high light condition along with exposure to high concentrations of copper. Exposure to high levels of metals has been linked to increased transpiration rates, possibly as a result of loss of stomatal control.[52]

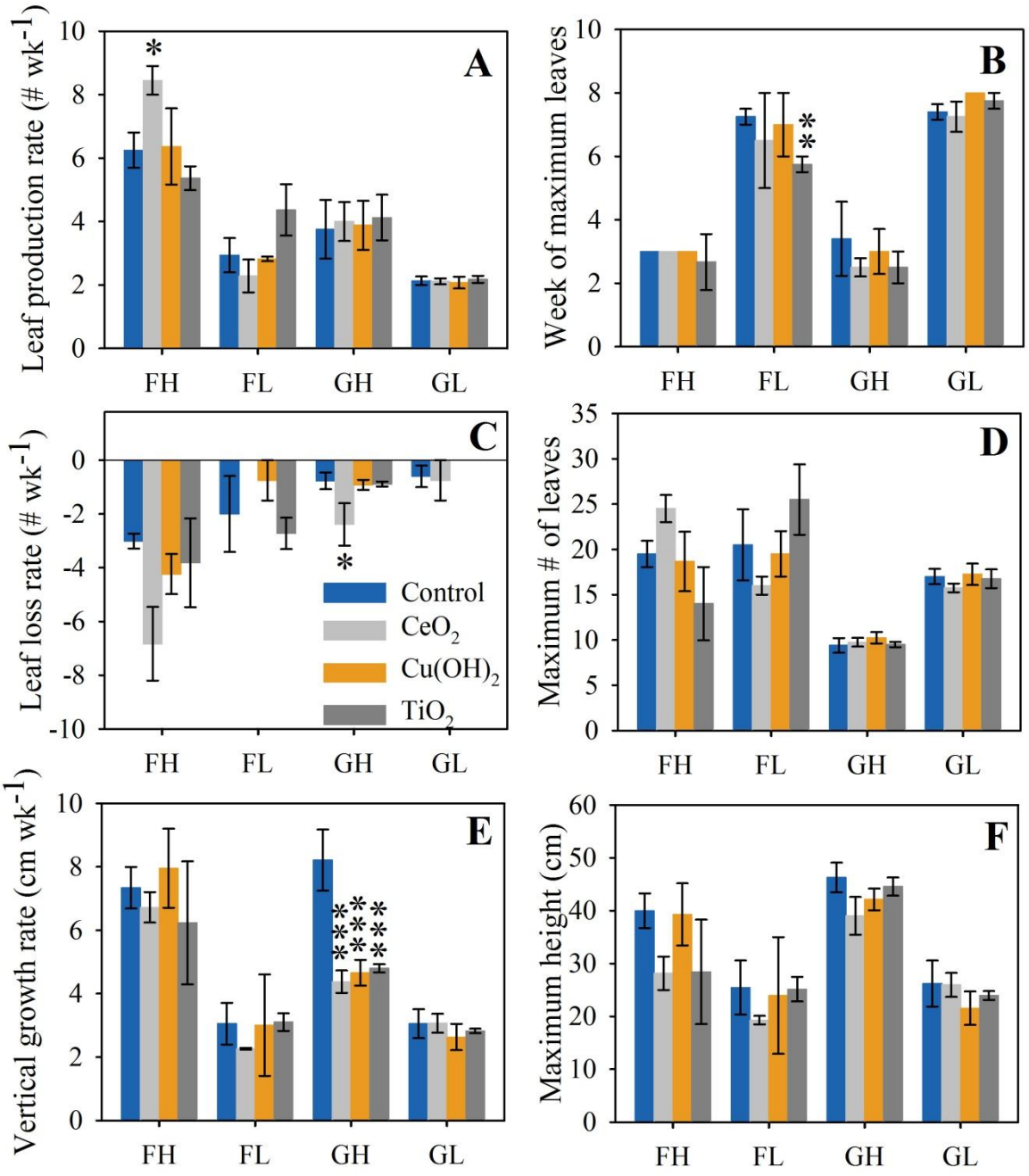

Figure 5.11. Leaf production rate (A), Week of maximum leaves (B), Leaf loss rate (C), Maximum # of leaves (D), Vertical growth rate (E), and Maximum height (F) of *C. unguiculata* exposed to 0 or 25 mg L^{-1} wk^{-1} CeO_2, $Cu(OH)_2$, or TiO_2 ENM and grown in farm or grass soil under high light or low light conditions. FH: farm soil, high light; FL: farm soil, low light; GH: grass soil, high light; GL: grass soil, low light. Asterisks represent significant differences from Control groups based on Dunnett's tests. Error bars are ±SE. **p* < 0.05, ***p* <0.01, ****p* <0.001.

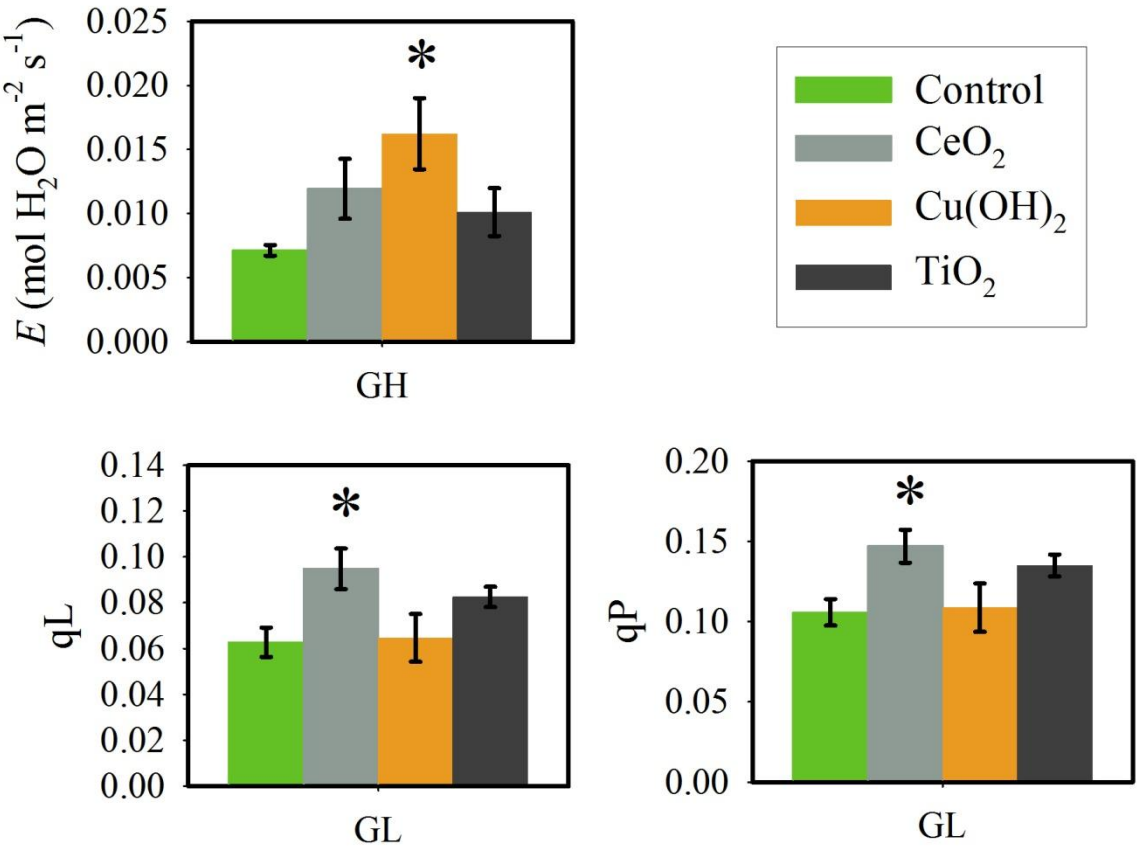

Figure 5.12. Transpiration (*E*), fraction of oxidized PSII reaction centers (*qL*), and photochemical quenching (*qP*) of *C. unguiculata* grown in grass soil under high (GH) or low (GL) light conditions during the second week of exposure. Asterisks represent significant differences from Control groups based on Dunnett's tests. Error bars are ±SE. *$p < 0.05$.

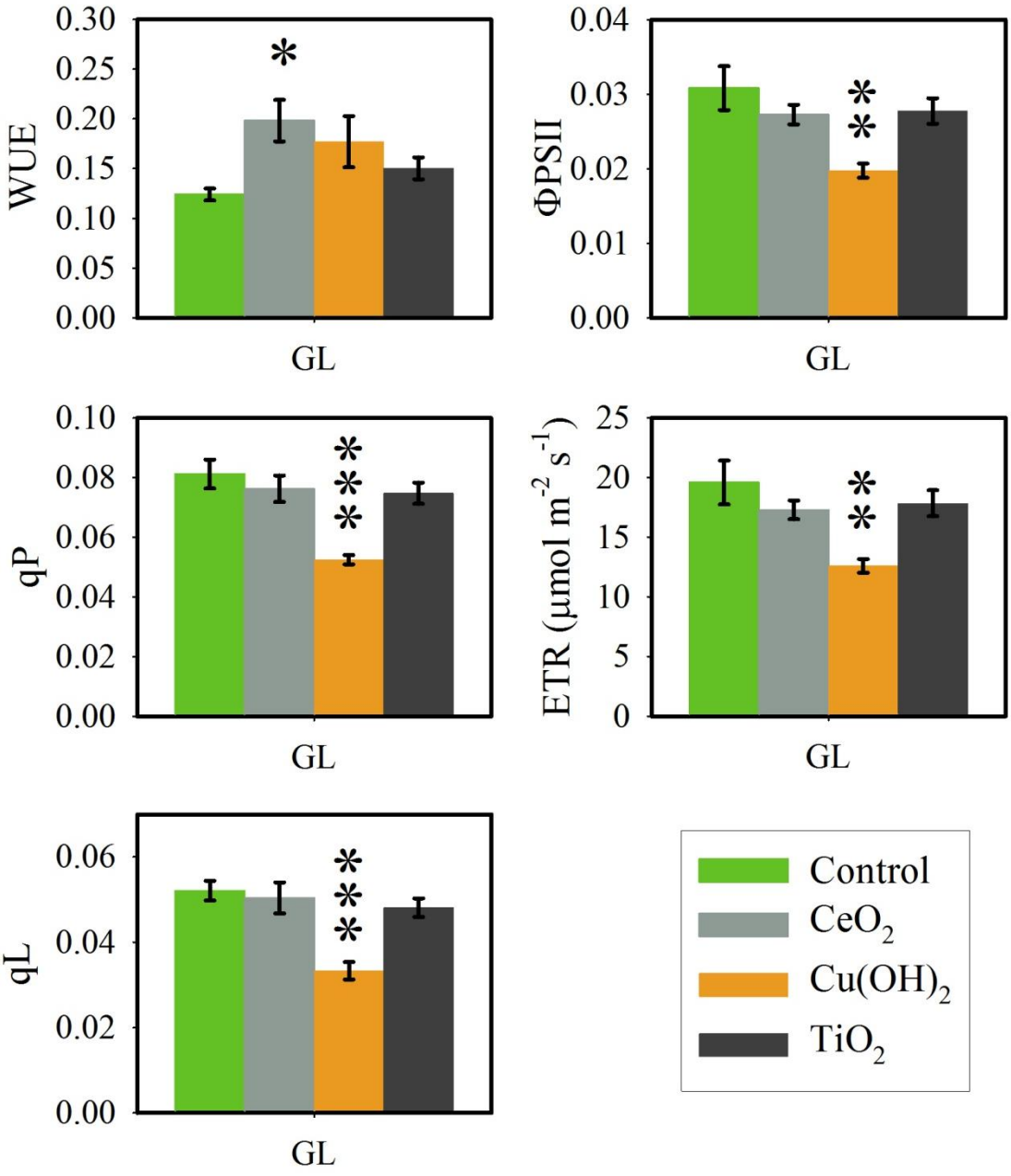

Figure 5.13. Water use efficiency (WUE), photosystem II quantum yield efficiency (ΦPSII), photochemical quenching (*qP*), electron transport rate (ETR), and fraction of oxidized PSII reaction centers (*qL*) of *C. unguiculata* grown in grass soil under low (GL) light conditions during the eighth week of exposure. Asterisks represent significant differences from Control groups based on Dunnett's tests. Error bars are ±SE. *$p < 0.05$, **$p < 0.01$, ***$p < 0.001$.

No significant changes in any physiological parameter due to ENM exposure were found in either radishes or wheat. Despite this, significant effects on growth were seen in both species under high light conditions, as shown in Figures 5.14 and 5.15. Specifically, radishes exposed to all three ENMs were found to have significantly larger hypocotyls (up to nearly twice the mass of control hypocotyls, Fig. 5.14B), while wheat exposed to $Cu(OH)_2$ had significantly decreased grain yield (Fig. 5.15C). That these impacts on growth were not reflected in some way in the physiological parameters measured is somewhat surprising, and may be related to physiological changes not detected here such as the plant changing the duration of its daily active photosynthetic period.

Transpiration rates of control groups of *C. unguiculata* grown in grass and farm soil and of radish and wheat can be seen in Figure 5.16. These results help explain many of the trends seen in ENM uptake from the previous chapter, specifically the increased uptake of radishes and particularly wheat grown under low light conditions as the transpiration rates of these plants grown under high light conditions were found to drop below those grown under low light conditions. This suggests that transpiration rates may be one of the major factors determining plant ENM uptake from soils irrespective of plant species or environmental condition, apart from how those variables influence transpiration.

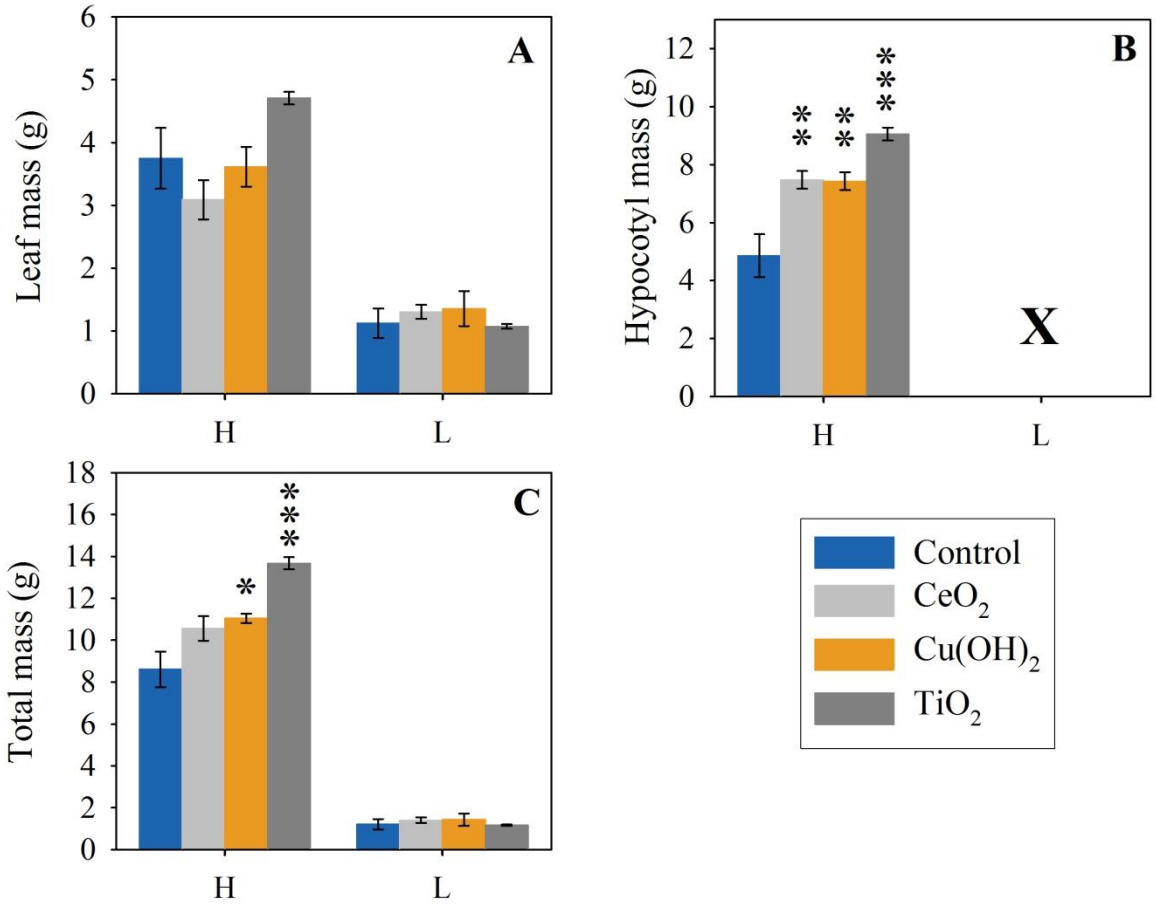

Figure 5.14. Leaf mass (A), Hypocotyl mass (B), and Total mass of radishes exposed to 0 or 25 mg L^{-1} wk^{-1} CeO_2, $Cu(OH)_2$, or TiO_2 ENM and grown in farm soil under high light (H) or low light (L) conditions. Hypocotyls did not develop in the low light condition and are marked with an X. Asterisks represent significant differences from Control groups based on Dunnett's tests. Error bars are ±SE. *p < 0.05, **p <0.01, ***p <0.001.

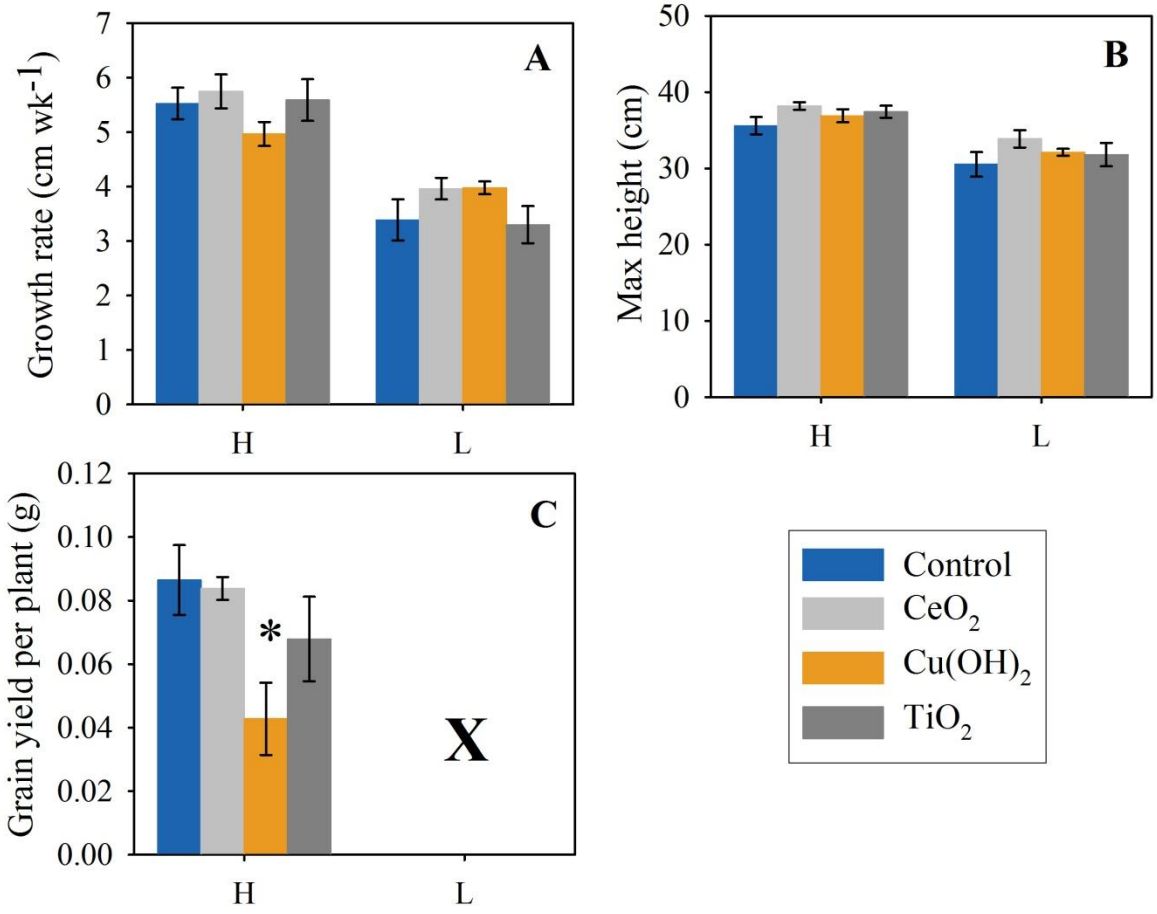

Figure 5.16. Vertical growth rate (A), Maximum height (B), and Grain yield per plant (C) of wheat exposed to 0 or 25 mg L^{-1} wk^{-1} CeO_2, $Cu(OH)_2$, or TiO_2 ENM and grown in grass soil under high light (H) or low light (L) conditions. Grains did not develop in the low light condition and are marked with an X. Asterisks represent significant differences from control groups based on Dunnett's tests. Error bars are ±SE. *$p < 0.05$.

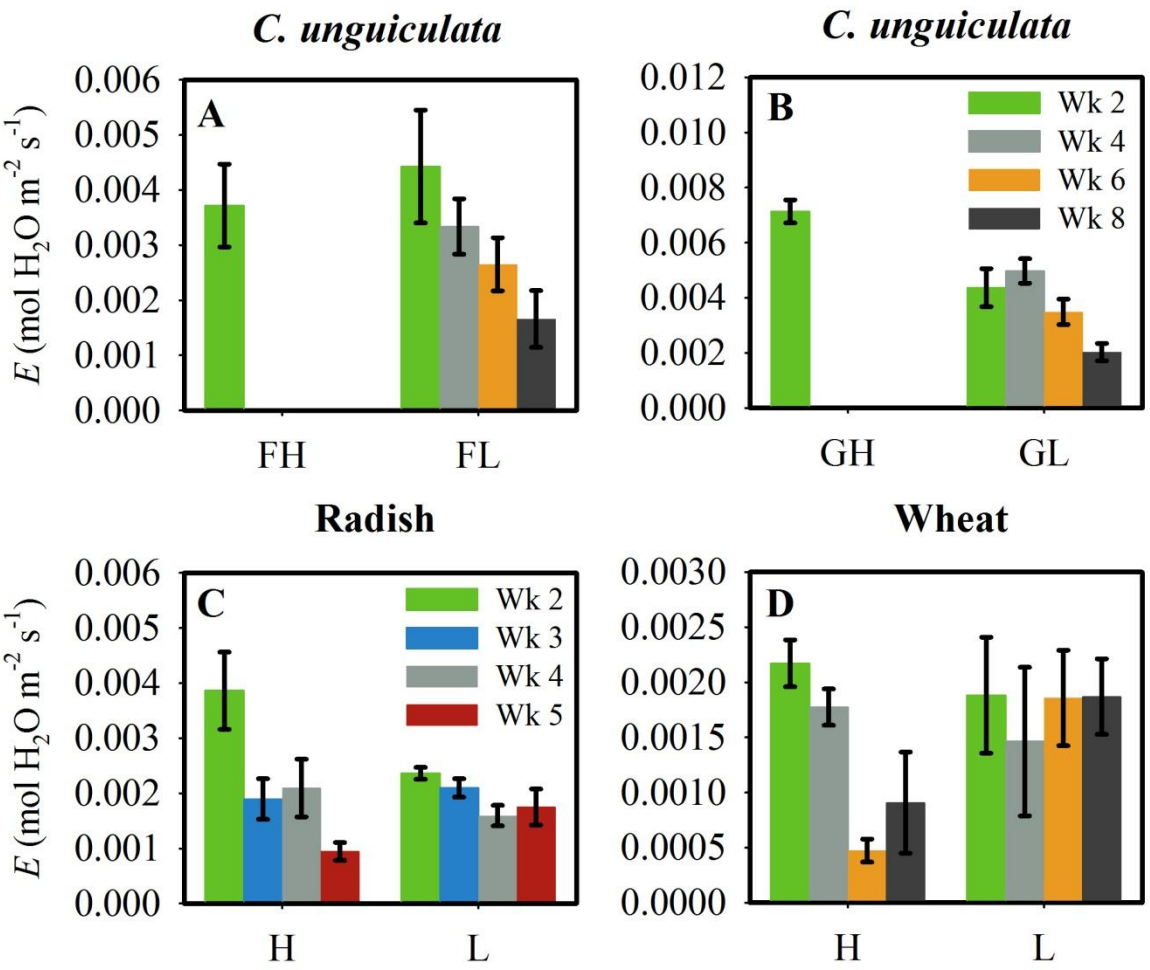

Figure 5.16. Transpiration rates of *C. unguiculata*, radish, and wheat not exposed to ENMs (control groups) grown in farm soil (F), grass soil (G) under high (H) or low (L) light conditions. *C. unguiculata* in high light conditions lost all measurable leaves after the second week of exposure so transpiration rates were not able to be collected. Note variable y-axes. Error bars are ±SE.

5.4. Conclusions

The results presented here show the importance of two factors that have not received much attention when predicting the characteristics of plant/ENM interactions in environmentally relevant scenarios: illumination intensity and soil characteristics. Based on the effects of these factors on plant transpiration rates, and consequently ENM accumulation and toxicity, one can hypothesize plant populations that may be vulnerable to certain ENMs. Due to the high light and nutrient conditions of agricultural fields, crop plants may be vulnerable to decreases in photosynthesis (and potentially yield) by photoactive ENMs such as TiO_2 and CeO_2, while plants grown in nutrient limited soils may be more vulnerable to nanoparticles with high dissolution rates such as $Cu(OH)_2$.

However, since the model plants used in these studies utilize the C_3 photosynthetic pathway (as do 85% of plant species),[53] these results should not be used to make predictions regarding how C_4 plants such as maize, sugarcane, or sorghum may be affected by ENM exposure. Since the C_4 pathway is more efficient in CO_2 assimilation and nutrient usage, C_4 plants may be able to compensate for reductions in photosynthesis caused by ENMs. Additionally, few effects of ENM exposure on plant performance were seen in the early or late stages of growth, when growth and total carbon fixation were low. This suggests that these plants are most vulnerable to photosynthesis disruption by ENMs during the period of highest metabolic activity (i.e., at later growth stages).

5.5. References

1. Clemens, S., Toxic Metal Accumulation, Responses to Exposure and Mechanisms of Tolerance in Plants. *Biochimie* **2006,** *88*, (11), 1707-1719.
2. Briat, J. F.; Lebrun, M., Plant Responses to Metal Toxicity. *Comptes Rendus De L Academie Des Sciences Serie Iii-Sciences De La Vie-Life Sciences* **1999,** *322*, (1), 43-54.
3. Patra, M.; Sharma, A., Mercury Toxicity in Plants. *Bot. Rev.* **2000,** *66*, (3), 379-422.
4. Zheng, L.; Hong, F. S.; Lu, S. P.; Liu, C., Effect of Nano-Tio2 on Strength of Naturally and Growth Aged Seeds of Spinach. *Biol. Trace Elem. Res.* **2005,** *104*, (1), 83-91.
5. Shi, J.; Abid, A. D.; Kennedy, I. M.; Hristova, K. R.; Silk, W. K., To Duckweeds (Landoltia Punctata), Nanoparticulate Copper Oxide Is More Inhibitory Than the Soluble Copper in the Bulk Solution. *Environ. Pollut.* **2011,** *159*, (5), 1277-1282.
6. Wang, Z. Y.; Xie, X. Y.; Zhao, J.; Liu, X. Y.; Feng, W. Q.; White, J. C.; Xing, B. S., Xylem- and Phloem-Based Transport of Cuo Nanoparticles in Maize (Zea Mays L.). *Environ. Sci. Technol.* **2012,** *46*, (8), 4434-4441.
7. Larue, C.; Laurette, J.; Herlin-Boime, N.; Khodja, H.; Fayard, B.; Flank, A. M.; Brisset, F.; Carriere, M., Accumulation, Translocation and Impact of Tio2 Nanoparticles in Wheat (Triticum Aestivum Spp.): Influence of Diameter and Crystal Phase. *Sci. Total Environ.* **2012,** *431*, 197-208.
8. Hong, F. H.; Zhou, J.; Liu, C.; Yang, F.; Wu, C.; Zheng, L.; Yang, P., Effect of Nano-Tio2 on Photochemical Reaction of Chloroplasts of Spinach. *Biol. Trace Elem. Res.* **2005,** *105*, (1-3), 269-279.
9. Hong, F. H.; Yang, F.; Liu, C.; Gao, Q.; Wan, Z. G.; Gu, F. G.; Wu, C.; Ma, Z. N.; Zhou, J.; Yang, P., Influences of Nano-Tio2 on the Chloroplast Aging of Spinach under Light. *Biol. Trace Elem. Res.* **2005,** *104*, (3), 249-260.
10. Lin, D. H.; Xing, B. S., Phytotoxicity of Nanoparticles: Inhibition of Seed Germination and Root Growth. *Environ. Pollut.* **2007,** *150*, (2), 243-250.
11. Lin, D. H.; Xing, B. S., Root Uptake and Phytotoxicity of Zno Nanoparticles. *Environ. Sci. Technol.* **2008,** *42*, (15), 5580-5585.
12. Lee, C. W.; Mahendra, S.; Zodrow, K.; Li, D.; Tsai, Y. C.; Braam, J.; Alvarez, P. J. J., Developmental Phytotoxicity of Metal Oxide Nanoparticles to Arabidopsis Thaliana. *Environ. Toxicol. Chem.* **2010,** *29*, (3), 669-675.
13. Lopez-Moreno, M. L.; de la Rosa, G.; Hernandez-Viezcas, J. A.; Castillo-Michel, H.; Botez, C. E.; Peralta-Videa, J. R.; Gardea-Torresdey, J. L., Evidence of the Differential Biotransformation and Genotoxicity of Zno and Ceo2 Nanoparticles on Soybean (Glycine Max) Plants. *Environ. Sci. Technol.* **2010,** *44*, (19), 7315-7320.
14. Parsons, J. G.; Lopez, M. L.; Gonzalez, C. M.; Peralta-Videa, J. R.; Gardea-Torresdey, J. L., Toxicity and Biotransformation of Unocated and Coated Nickel Hydroxide Nanoparticles on Mesquite Plants. *Environ. Toxicol. Chem.* **2010,** *29*, (5), 1146-1154.
15. Ghodake, G.; Seo, Y. D.; Lee, D. S., Hazardous Phytotoxic Nature of Cobalt and Zinc Oxide Nanoparticles Assessed Using Allium Cepa. *J. Hazard. Mater.* **2011,** *186*, (1), 952-955.
16. Zhao, L. J.; Hernandez-Viezcas, J. A.; Peralta-Videa, J. R.; Bandyopadhyay, S.; Peng, B.; Munoz, B.; Keller, A. A.; Gardea-Torresdey, J. L., Zno Nanoparticle Fate in Soil

and Zinc Bioaccumulation in Corn Plants (Zea Mays) Influenced by Alginate. *Environ. Sci.: Processes Impacts* **2013,** *15*, (1), 260-266.
17. Yin, L.; Cheng, Y.; Espinasse, B.; Colman, B. P.; Auffan, M.; Wiesner, M.; Rose, J.; Liu, J.; Bernhardt, E. S., More Than the Ions: The Effects of Silver Nanoparticles on Lolium Multiflorum. *Environ. Sci. Technol.* **2011,** *45*, (6), 2360-2367.
18. Hawthorne, J.; Roche, R. D.; Xing, B. S.; Newman, L. A.; Ma, X. M.; Majumdar, S.; Gardea-Torresdey, J.; White, J. C., Particle-Size Dependent Accumulation and Trophic Transfer of Cerium Oxide through a Terrestrial Food Chain. *Environ. Sci. Technol.* **2014,** *48*, (22), 13102-13109.
19. Gui, X.; He, X.; Ma, Y. H.; Zhang, P.; Li, Y. Y.; Ding, Y. Y.; Yang, K.; Li, H. F.; Rui, Y. K.; Chai, Z. F.; Zhao, Y. L.; Zhang, Z. Y., Quantifying the Distribution of Ceria Nanoparticles in Cucumber Roots: The Influence of Labeling. *RSC Adv.* **2015,** *5*, (6), 4554-4560.
20. Zhang, W.; Ebbs, S. D.; Musante, C.; White, J. C.; Gao, C.; Ma, X., Uptake and Accumulation of Bulk and Nanosized Cerium Oxide Particles and Ionic Cerium by Radish (Raphanus Sativus L.). *J. Agric. Food Chem.* **2015,** *63*, (2), 382-390.
21. Schwabe, F.; Schulin, R.; Limbach, L. K.; Stark, W.; Buerge, D.; Nowack, B., Influence of Two Types of Organic Matter on Interaction of Ceo2 Nanoparticles with Plants in Hydroponic Culture. *Chemosphere* **2013,** *91*, (4), 512-520.
22. Kumari, M.; Mukherjee, A.; Chandrasekaran, N., Genotoxicity of Silver Nanoparticles in Allium Cepa. *Sci. Total Environ.* **2009,** *407*, (19), 5243-5246.
23. Bennett, S. W.; Keller, A. A., Comparative Photoactivity of Ceo2, Gamma-Fe2o3, Tio2 and Zno in Various Aqueous Systems. *Appl. Catal. B-Environ.* **2011,** *102*, (3-4), 600-607.
24. Priester, J. H.; Ge, Y.; Mielke, R. E.; Horst, A. M.; Moritz, S. C.; Espinosa, K.; Gelb, J.; Walker, S. L.; Nisbet, R. M.; An, Y.-J.; Schimel, J. P.; Palmer, R. G.; Hernandez-Viezcas, J. A.; Zhao, L.; Gardea-Torresdey, J. L.; Holden, P. A., Soybean Susceptibility to Manufactured Nanomaterials with Evidence for Food Quality and Soil Fertility Interruption. *Proc. Natl. Acad. Sci. U. S. A.* **2012**.
25. Hernandez-Allica, J.; Garbisu, C.; Barrutia, O.; Becerril, J. M., Edta-Induced Heavy Metal Accumulation and Phytotoxicity in Cardoon Plants. *Environ. Exp. Bot.* **2007,** *60*, (1), 26-32.
26. Judy, J. D.; Unrine, J. M.; Bertsch, P. M., Evidence for Biomagnification of Gold Nanoparticles within a Terrestrial Food Chain. *Environ. Sci. Technol.* **2011,** *45*, (2), 776-781.
27. Du, W. C.; Sun, Y. Y.; Ji, R.; Zhu, J. G.; Wu, J. C.; Guo, H. Y., Tio2 and Zno Nanoparticles Negatively Affect Wheat Growth and Soil Enzyme Activities in Agricultural Soil. *J. Environ. Monit.* **2011,** *13*, (4), 822-828.
28. Chen, Y. X.; He, Y. F.; Yang, Y.; Yu, Y. L.; Zheng, S. J.; Tian, G. M.; Luo, Y. M.; Wong, M. H., Effect of Cadmium on Nodulation and N-2-Fixation of Soybean in Contaminated Soils. *Chemosphere* **2003,** *50*, (6), 781-787.
29. Josko, I.; Oleszczuk, P., Influence of Soil Type and Environmental Conditions on Zno, Tio2 and Ni Nanoparticles Phytotoxicity. *Chemosphere* **2013,** *92*, (1), 91-99.
30. Collin, B.; Auffan, M.; Johnson, A. C.; Kaur, I.; Keller, A. A.; Lazareva, A.; Lead, J. R.; Ma, X. M.; Merrifield, R. C.; Svendsen, C.; White, J. C.; Unrine, J. M., Environmental

Release, Fate and Ecotoxicological Effects of Manufactured Ceria Nanomaterials. *Environ.-Sci. Nano* **2014,** *1*, (6), 533-548.
31. Dudley, L. S.; Mazer, S. J.; Galusky, P., The Joint Evolution of Mating System, Floral Traits and Life History in Clarkia (Onagraceae): Genetic Constraints Vs. Independent Evolution. *J. Evol. Biol.* **2007,** *20*, (6), 2200-2218.
32. Vasek, F. C., Outcrossing in Natural Populations .2. Clarkia Unguiculata. *Evolution* **1965,** *19*, (2), 152-156.
33. Dudley, L. S.; Hove, A. A.; Mazer, S. J., Physiological Performance and Mating System in Clarkia (Onagraceae): Does Phenotypic Selection Predict Divergence between Sister Species? *Am. J. Bot.* **2012,** *99*, (3), 488-507.
34. Kramer, D. M.; Johnson, G.; Kiirats, O.; Edwards, G. E., New Fluorescence Parameters for the Determination of Q(a) Redox State and Excitation Energy Fluxes. *Photosynth. Res.* **2004,** *79*, (2), 209-218.
35. Baker, N. R., Chlorophyll Fluorescence: A Probe of Photosynthesis in Vivo. In *Annual Review of Plant Biology*, 2008; Vol. 59, pp 89-113.
36. Raven, P. H.; Evert, R. F.; Eichhorn, S. E., *Biology of Plants*. 7th ed.; W. H. Freeman and Company: 41 Madison Avenue, New York, NY, 2005.
37. Barhoumi, L.; Oukarroum, A.; Taher, L. B.; Smiri, L. S.; Abdelmelek, H.; Dewez, D., Effects of Superparamagnetic Iron Oxide Nanoparticles on Photosynthesis and Growth of the Aquatic Plant Lemna Gibba. *Arch. Environ. Contam. Toxicol.* **2015,** *68*, (3), 510-20.
38. Hasanuzzaman, M.; Hossain, M. A.; da Silva, J. A. T.; Fujita, M., *Plant Response and Tolerance to Abiotic Oxidative Stress: Antioxidant Defense Is a Key Factor*. 2012; p 261-315.
39. Whiteside, M. D.; Treseder, K. K.; Atsatt, P. R., The Brighter Side of Soils: Quantum Dots Track Organic Nitrogen through Fungi and Plants. *Ecology* **2009,** *90*, (1), 100-108.
40. Lopez-Moreno, M. L.; de la Rosa, G.; Hernandez-Viezcas, J. A.; Peralta-Videa, J. R.; Gardea-Torresdey, J. L., X-Ray Absorption Spectroscopy (Xas) Corroboration of the Uptake and Storage of Ceo2 Nanoparticles and Assessment of Their Differential Toxicity in Four Edible Plant Species. *J. Agric. Food Chem.* **2010,** *58*, (6), 3689-3693.
41. Xiong, Z. T.; Liu, C.; Geng, B., Phytotoxic Effects of Copper on Nitrogen Metabolism and Plant Growth in Brassica Pekinensis Rupr. *Ecotoxicol. Environ. Saf.* **2006,** *64*, (3), 273-280.
42. Peng, H. Y.; Kroneck, P. M. H.; Kupper, H., Toxicity and Deficiency of Copper in Elsholtzia Splendens Affect Photosynthesis Biophysics, Pigments and Metal Accumulation. *Environ. Sci. Technol.* **2013,** *47*, (12), 6120-6128.
43. Janik, E.; Maksymiec, W.; Gruszecki, W. I., The Photoprotective Mechanisms in Secale Cereale Leaves under Cu and High Light Stress Condition. *J. Photochem. Photobiol. B-Biol.* **2010,** *101*, (1), 47-52.
44. Adeleye, A. S.; Conway, J. R.; Perez, T.; Rutten, P.; Keller, A. A., Influence of Extracellular Polymeric Substances on the Long-Term Fate, Dissolution, and Speciation of Copper-Based Nanoparticles. *Environ. Sci. Technol.* **2014,** *48*, (21), 12561-12568.
45. Werdan, K.; Heldt, H. W.; Milovancev, M., Role of Ph in Regulation of Carbon Fixation in Chloroplast Stroma - Studies on Co2 Fixation in Light and Dark. *Biochim. Biophys. Acta* **1975,** *396*, (2), 276-292.

46. Heldt, H. W.; Werdan, K.; Milovanc, M.; Geller, G., Alkalization of Chloroplast Stroma Caused by Light-Dependent Proton Flux into Thylakoid Space. *Biochim. Biophys. Acta* **1973,** *314*, (2), 224-241.
47. Puig, S.; Andres-Colas, N.; Garcia-Molina, A.; Penarrubia, L., Copper and Iron Homeostasis in Arabidopsis: Responses to Metal Deficiencies, Interactions and Biotechnological Applications. *Plant, Cell Environ.* **2007,** *30*, (3), 271-290.
48. Bouazizi, H.; Jouili, H.; Geitmann, A.; El Ferjani, E., Copper Toxicity in Expanding Leaves of Phaseolus Vulgaris L.: Antioxidant Enzyme Response and Nutrient Element Uptake. *Ecotoxicol. Environ. Saf.* **2010,** *73*, (6), 1304-1308.
49. Alaoui-Sosse, B.; Genet, P.; Vinit-Dunand, F.; Toussaint, M. L.; Epron, D.; Badot, P. M., Effect of Copper on Growth in Cucumber Plants (Cucumis Sativus) and Its Relationships with Carbohydrate Accumulation and Changes in Ion Contents. *Plant Sci.* **2004,** *166*, (5), 1213-1218.
50. Sherameti, I.; Sopory, S. K.; Trebicka, A.; Pfannschmidt, T.; Oelmüller, R., Photosynthetic Electron Transport Determines Nitrate Reductase Gene Expression and Activity in Higher Plants. *Journal of Biological Chemistry* **2002,** *277*, (48), 46594-46600.
51. Claussen, W., Growth, Water Use Efficiency, and Proline Content of Hydroponically Grown Tomato Plants as Affected by Nitrogen Source and Nutrient Concentration. *Plant Soil* **2002,** *247*, (2), 199-209.
52. Poschenrieder, C.; Barcelo, J., Heavy Metal Stress in Plants; from Molecules to Ecosystems. In Prasad, M. N. V.; Hagemeyer, J., Eds. Springer: 1999.
53. Moore, R.; Clark, W. D.; Stern, K. R.; Vodopich, D., *Botany*. William C Brown Pub: 1995.